



Thesis for Master of Science degree in Aerospace Engineering

**Conceptual Design of a Reusable TSTO: Guess Data
estimation and Matching Analysis**

Author:

Alberto Za

Tutor:

Prof.ssa Nicole Viola

Co-tutor:

Prof.ssa Roberta Fusaro

Prof. Davide Ferretto

April 2021

This page has been intentionally left blank

Index

<i>Abstract</i>	8
<i>Chapter 1</i>	
1.1 The concept of TST	10
1.2 Staging alternatives	11
1.3 Propulsive technologies	15
1.3.1 Turbojet	16
1.3.2 Turbofan.	21
1.3.3 Afterburner	26
1.3.4 Ramjet & Scramjet	28
1.3.5 Rocket	31
<i>Chapter 2</i>	
2.1 Statistical analysis	34
2.1.1 Subsonic first stage Database	35
2.1.2 Supersonic first stage Database	43
2.1.3 Rocket first stage Database	54
2.2 Implementation of the Matlab GUI	60
2.3 Example of GUI's use	68
<i>Chapter 3</i>	
3.1 Iteration logic	72
3.2 Matching chart analysis	72
3.3 TSTO mission profile	73
3.4 Weight Analysis and sizing	76
3.4.1 Subsonic first stage weight estimation	76
3.4.2 Supersonic first and second stage weight estimation	79
<i>Chapter 4</i>	
4.1 First stage requirements	83
4.2 Take-off requirement	83
4.3 Second segment requirement	87
4.4 Climb and cruise requirement	90
4.5 Landing requirement	98
<i>Chapter 5</i>	
5.1 Second stage requirements.	102
5.2 Orbit-achievement requirement	102
5.3 Payload requirement	114
5.4 Re-entry requirement	117
5.5 Matlab GUI implementation	120
<i>Conclusion.</i>	124
<i>Bibliography</i>	126

This page has been intentionally left blank

List of figures

1.1 Different stage combinations for TSTO	11
1.2 Different propulsive combination for TSTO	13
1.3 Specific impulse in function of Mach for different propulsive typologies	14
1.4 Ideal Joule-Brayton cycle.	15
1.5 Cycle work in function of and T_3/T_1 and β	16
1.6 Real Joule-Brayton cycle	16
1.7 Turbojet engine scheme	17
1.8 Turbojet Joule-Brayton cycle	18
1.9 Turbofan engine scheme	22
1.10 Turbofan Joule-Brayton cycle	23
1.11 Mixed flow turbofan scheme	23
1.12 Mixed flow turbofan Joule-Brayton cycle	24
1.13 Effect of β in the performance	25
1.14 Effect of OPR on the performance	25
1.15 Engine with afterburner scheme	26
1.16 Engine with afterburner Joule-Brayton cycle	27
1.17 Ramjet and Scramjet scheme	29
1.18 Ramjet and Scramjet Joule-Brayton cycle	30
1.19 Liquid propellant rocket section	31
1.20 Solid propellant rocket section	32
1.21 Rocket effective exhaust velocity in function of acceleration	33
2.1 Statistical analysis logic	34
2.2 Subsonic first stage database $MTOW=f(\text{payload})$	40
2.3 Subsonic first stage database $\text{Thrust}=f(MTOW)$	41
2.4 Subsonic first stage database $PMF=f(MTOW)$	41
2.5 Subsonic first stage database $\text{Wing Surface}=f(MTOW)$	42
2.6 Subsonic first stage database $Isp=(MTOW)$	42
2.7 Supersonic first stage database $MTOW=f(\text{payload})$	51
2.8 Supersonic first stage database $\text{Thrust}=f(MTOW)$	52
2.9 Supersonic first stage database $PMF=f(MTOW)$	52
2.10 Supersonic first stage database $\text{Wing Surface}=f(MTOW)$	53
2.11 Supersonic first stage database $Isp=(MTOW)$	53
2.12 Rocket first stage database $MTOW=f(\text{payload})$	57
2.13 Rocket first stage database $\text{Thrust}=f(MTOW)$	57
2.14 Rocket first stage database $PMF=f(MTOW)$	58
2.15 Rocket first stage database $\text{Wing Surface}=f(MTOW)$	58
2.16 Rocket first stage database $Isp=(MTOW)$	59
3.1 Matching chart analysis logic.	73
3.2 TSTO mission profile.	74
3.3 Subsonic first stage weight breakdown	78

3.4 Geometry options.	82
4.1 Take off distance.	83
4.2 Take off distance in function of TOP	84
4.3 Cl max take off evaluation	85
4.4 Take off req.	86
4.5 Take off req. with the variation of Cl max	86
4.6 Take off req. with the variation of airport height	87
4.7 Segmented climb	88
4.8 Second segment req.	89
4.9 Second segment req. with the variation of Cd	89
4.10 Second segment req. with the variation of Cl	90
4.11 Aircraft equilibrium during climb	90
4.12 Aircraft equilibrium during cruise.	91
4.13 Drag polar	92
4.14 Drag in function of speed	93
4.15 Cruise req.	96
4.16 Cruise req. with the variation of Mach.	96
4.17 Cruise req. with the variation of Cd0.	97
4.18 Climb req.	97
4.19 Landing distance.	98
4.20 Cd max take off evaluation.	99
4.21 Landing req.	100
4.22 Landing req. with the variation of Cl max landing	100
4.23 Landing req. with the variation of landing weight ratio	101
5.1 Standard air table.	104
5.2 Necessary thrust in function of speed at different altitude	105
5.3 Available thrust in function of speed at different altitudes	106
5.4 Mutual behaviour of necessary and available thrust.	106
5.5 Graphical calculation of the ceiling.	108
5.6 Orbit-achievement req.	109
5.7 Payload weight variation in function of second stage weight, rocket thrust and target orbit	110
5.8 Payload weight variation in function of second stage weight, rocket thrust and Mach	111
5.9 Variation of the ceiling altitude in function of first stage weight and static thrust at $z=0$ of the first stage.	111
5.10 Variation of the ceiling altitude in function of first stage weight and static thrust at $z=0$ of the first stage and Mach	114
5.11 Re-entry req.	116
5.12 Re-entry req. with the variation of descent angle.	117
5.13 Re-entry req. with the variation of deorbit height	117
5.14 Payload req.	118
5.15 Payload req. at the variation of payload weight.	119

Abstract

Nowadays space access is guaranteed by expandable launchers which, once the mission has ended, can't be reuse for the successive mission. This involves a big waste of resources and necessarily high costs. One solution to reduce the costs and gain flexibility in space missions is the use of reusable or partially reusable vehicle.

Reusable launch vehicles are facing a great evolution in the last years, and in particular reusable two-stage-to-orbit have been identified from many studies as the vehicle of the future in the aerospace field because they have the capability of delivering a wide range of payload in orbit at low cost, with a greater flexibility using conventional airports and infrastructures even gaining many operative and legal advantages.

This thesis has a twofold target: the first is to find a useful method to define the most important data, called guess data, which are used to start the conceptual design of a TSTO vehicle and the second is to adapt the matching chart analysis to this type of vehicles; for both the points it has been developed a Graphical User Interface in Matlab environment using App Designer.

In chapter 1 the concept of the two-stage-to-orbit and its historical evolution will be introduced, the most important state of art typologies of staging and a brief explanation of the types of engine.

In chapter 2 statistical analysis will be developed, a database of vehicle will be created on the basis of the type of propulsion of the first and the second stage, and then a methodology generated for the calculation of guess data is presented, at the end of the chapter the GUI is shown with an example of its use.

In chapter 3 the method to execute the matching chart analysis is explained and all the requirements that both the first stage and the second stage must fulfil are introduced, in particular, for the first stage will be analysed the take-off req., second segment req., climb req., cruise req. and landing req.; on the other hand, for the second stage the requirements analysed will be the orbit-achievement req., the re-entry req., the payload req., and lastly the landing req.

Finally, in chapter 4 a method for the weight estimation will be submitted and a Graphical User Interface to calculate the matching charts is shown to the reader with an example of its use.

This page has been intentionally left blank

Chapter 1

1.1 The concept of TSTO

As definition a two-stage-to-orbit vehicle is a spacecraft in which two different stages provide to the propulsion in order to reach the orbital altitude and the orbital speed. The conventional architecture of a TSTO is made of a booster stage and an orbiter mounted on the top of it, the latter, after the separation from the booster stage, has the scope to deliver the payload into the orbit.

Through the years a lot of TSTO vehicles have been developed, the first concept was the two stage rocket which has the defect to be expandable so that it doesn't represent an advantageous solution in economic terms but also in terms of flexibility due to the fact it needs a specific launch site to operate. In the last years thanks to SpaceX a new concept of semi reusable two stage to orbit has been developed with the falcon 9, which has the capability to reuse the first stage with the consequence of a big decrease of the costs per flight.

Another concept of TSTO uses an aircraft, called carrier vehicle, generally propelled by an airbreathing engine and not by a rocket, as first stage to reach an altitude and a speed to which the second stage can work in optimal conditions and reach the orbit. One of the first examples from this typology was the Sanger and then many other vehicles have been developed following this model; moreover among all the past and under-development projects, even military and civil aircrafts are used as carrier vehicle, which is a choice oriented to minimize all the effort and costs needed to develop a first stage from the beginning.

1.2 Staging alternatives

In the TSTO vehicle different propulsive system can be adopted and they can be resume in the figure below:

		First Stage			
		Propulsive System only	Propulsive Sys and Propellant Sys(existing carrier)	Propulsive Sys and Propellant Sys (To be developed)	Propellant System only
Second Stage	Propulsive System only	Unfeasible	Unfeasible	Unfeasible	Conf. 3.1
	Propulsive Sys and Propellant Sys	Conf. 1.2	Conf. 2.2 (a)	Conf. 2.2 (b)	Conf. 3.2
	Propellant System only	Unfeasible	Unfeasible	Unfeasible	Unfeasible
	No Propulsive and No Propellant systems	Unfeasible	Conf. 2.4 (a)	Conf. 2.4 (b)	Unfeasible

Figure 1.1

Different combinations of first and second stage are shown. For the first stage the choice is made between a vehicle with a propulsive system only, with a propulsive system and propellant system (existing or not), with propellant system only; on the other hand for the second stage the possible alternatives are a vehicle with no propellant and propulsive system, with only propellant system, with both propellant and propulsive system and lastly with propulsive system only.

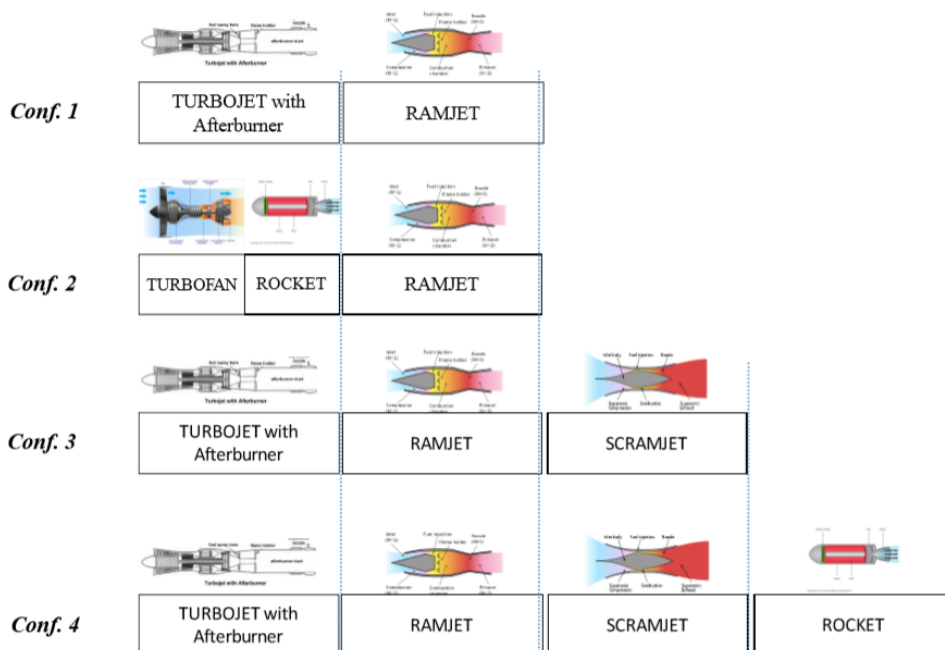
As it can be seen from the table not all the staging combinations are feasible, moreover configuration 1.2 and 3.1 don't represent good alternatives, in fact conf. 1.2 which consists in a first stage with propulsive system only and a complete second stage that should contain all the amount of propellant required to feed both stages with the consequence to have an exaggerated increase in the second stage mass; similarly the conf. 3.1 isn't a reasonable alternative because the propulsive system which is hosted

only in the second stage can be fed only until the two stages are attached since the propellant system is present just in the first stage.

Excluded these configurations all the others can be feasible and represent promising solutions for a TSTO vehicle, conf. 2.2 is defined by a design where both the stages have a propulsive system, here the first stage is used to accelerate the second stage and let him to meet the optimal working conditions in the atmosphere to save costs and improve its operability; conf. 2.4 consists in a complete first stage which should guarantee to the second stage that has no operative capabilities to reach the target altitude.

The last configuration feasible is conf. 3.2, in this case the first stage act like a tank while the second stage is powered by a propulsive system and accelerate the whole vehicle.

On the base of these different staging alternatives an analysis of the engine combinations for a TSTO can be defined.



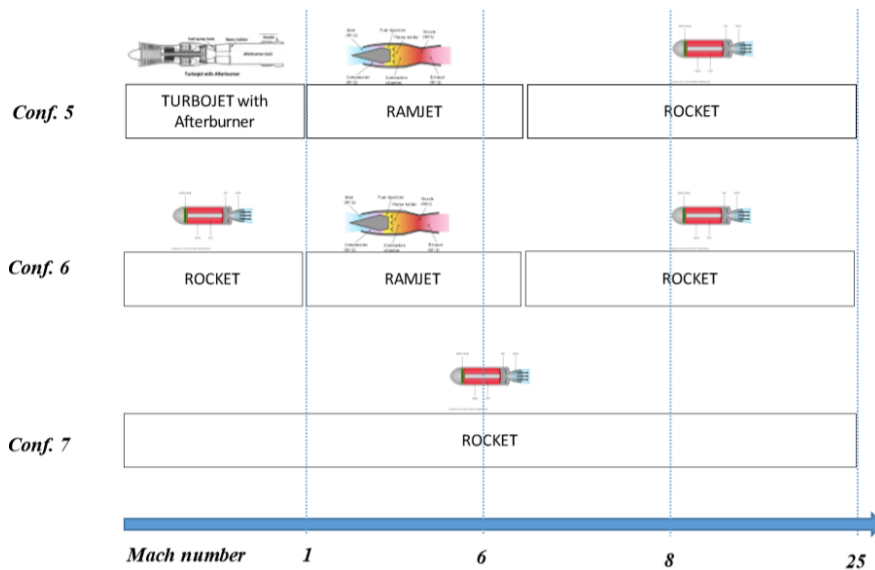


Figure 1.2

The choice between one configuration or another strongly depends on the mission that the vehicle should perform because from it will derive the maximum Mach to be achieved and the altitude that each stage must reach.

The propulsive technologies that currently exist let us to choose among two main different alternatives: air-breathing engines and rockets.

Using the air-breathing propulsion has many advantages respect to the rocket, for example in terms of launch, that could be horizontal, or operability, and the most important the ability to use atmospheric oxygen for combustion reducing the mass of propellant that must be carried; on the other hand rockets are essential for missions where orbital altitude must be reached since above a certain height the air is so thin that the air-breathing engine can't work efficiently and don't provide the adequate thrust, as a consequence turbojet and turbofan can be exploited at the beginning of the mission profile, then a transition to rocket propulsion should be adopted to reach the desired Mach and altitude.

A good solution to reach high velocities is the adoption of ramjet and scramjet, which are typically used in high speed aircraft and could be employed in the first stage of the TSTO too, the only drawback is that they need to be accelerated at a certain velocity to start to work, that's why they are generally used in combination with a turbofan or a turbojet with afterburner as it can be seen from the figure above.

It is worth noting that in addition to the technologies mentioned above, it is a common target of current research activities to develop engines where within a single subsystem are integrated different propulsive technologies, examples are:

- > Air Turbo Ramjet (ATR) which works as a turbojet at low speed and as a rocket engine at higher speeds, the speed regime is between 0 and Mach about 6 and in general the ATR offers high thrust to weight ratio at low speeds and good performances at high Mach numbers. It exists in two version the Gas Generator Cycle ATR and the Expander Cycle ATR.
- > Dual Mode Ramjet (DMR) which is a ramjet engine that operate in both subsonic and supersonic combustion mode thanks to a geometric variation of the inlet or the combustion chamber.
- > Rocket Based Combined Cycle (RBCC).
- > Turbine Based Combined Cycle (TBCC), in its typical use the turbine engine powers the craft from take-off up to ramjet engine speed, when it switches to ramjet, the latter function until the vehicle reaches scramjet speeds, when the scramjets ignite. This allows the three different air-breathing propulsion types to be used over their functional area of the flight profile into the atmosphere.

In the figure below there is a resume on the achievable performance with the principle types of engine:

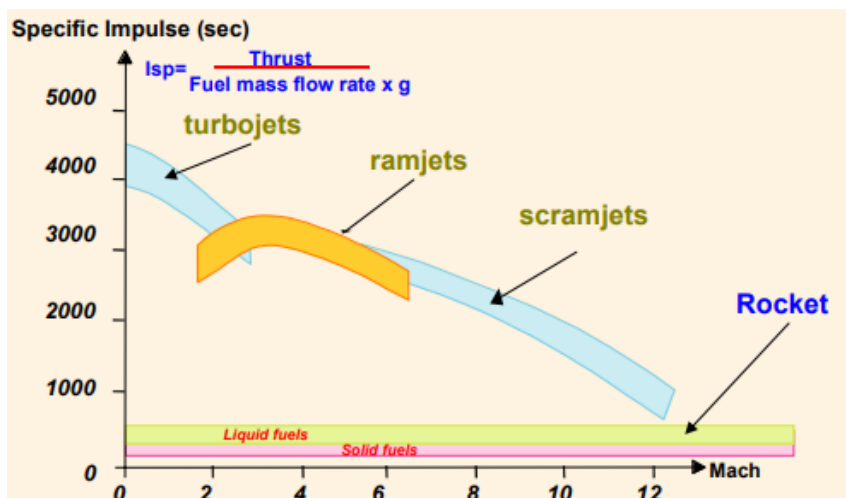


Figure 1.3

In the next section the main propulsive technologies are analysed since the engine type will be the base of the statistical analysis

1.3 Propulsive technologies

One of the first steps in the definition of a vehicle is the choice of the engine, it sets (with the definition of the aerodynamic) the most important parameters such as those that influence the kilometric consumption and maximum thrust required and available, parameters directly related with the cost of the entire mission and with the weight and the volume of the engine.

Among all the types of propulsive technologies, those that will be analysed in this thesis are turbojet, turbofan, ramjet, scramjet and lastly the rocket because they represent basically the most important alternatives for a TSTO vehicle.

The base of the functioning of all airbreathing engines is the Joule-Brayton cycle, it is characterized by four thermodynamic transformations (two isentropic with a non-zero internal work and two isobaric transformations with heat transfer) in this order to define a close-loop cycle: isentropic compression, isobaric combustion, isentropic expansion, isobaric cooling.

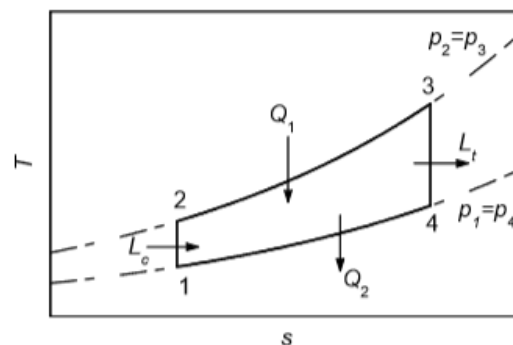


Figure 1.4

In the Joule-Brayton cycle an important parameter is the cycle efficiency defined by the following equation:

$$\eta_{id} = 1 - \frac{T_1}{T_2} = 1 - \frac{1}{\beta^{\frac{\gamma-1}{\gamma}}}$$

Where β is the compression rate defined by ratio between $\beta = \frac{p_2}{p_1} = \frac{p_3}{p_4}$

It is interesting investigate the trend of the cycle work in function of the ratio between T_3 and T_1 and β , and even the trend of the efficiency in function of β

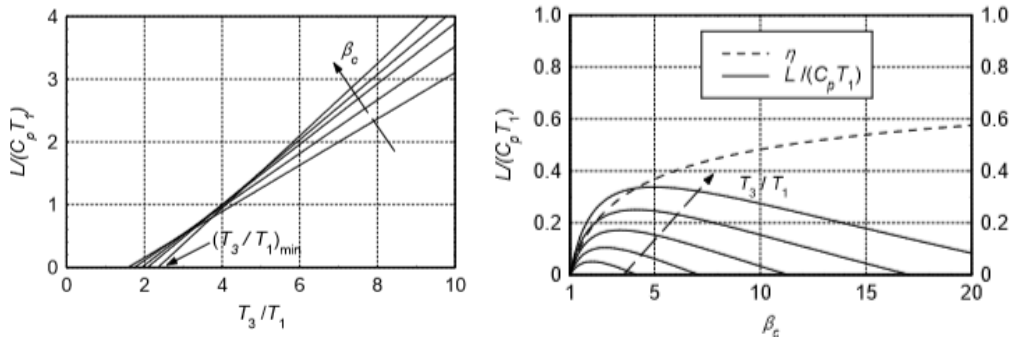


Figure 1.5

In air-breathing engine application the cycle's behaviour is influenced by real effects of dissipation that bring it to not execute a isentropic transformation but an adiabatic transformation so that the entropy is no longer constant but there is not heat exchange with the external environment.

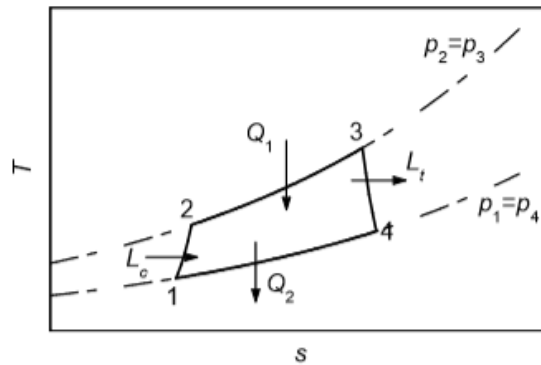


Figure 1.6

In the real case the curves which represent the cycle work and the efficiency in function of β and $\frac{T_3}{T_1}$ have the same evolution presented in the ideal case with the variation of these parameters.

1.3.1 Turbojet

The Turbojet engine is a type of reaction engine which, thanks to the third principle of the dynamic, it is able to produce thrust while working into the atmosphere as a consequence of the air acceleration through the propulsor. This engine is excellent for subsonic flights but is not the better choice for supersonic mission, in this case is

generally used methods to augment the performances such as the intercooling, the regeneration and the mostly used afterburning which will be analysed subsequently.

Turbojet engine is schematized in the figure below:

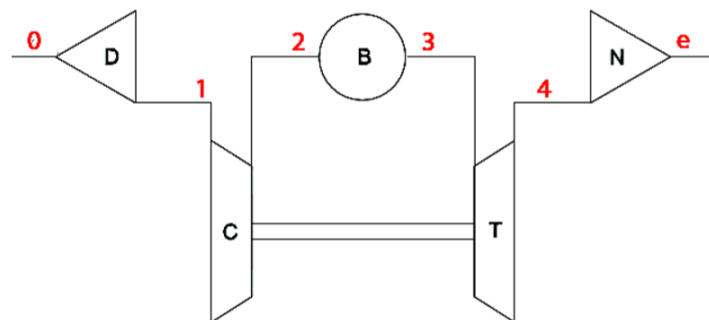
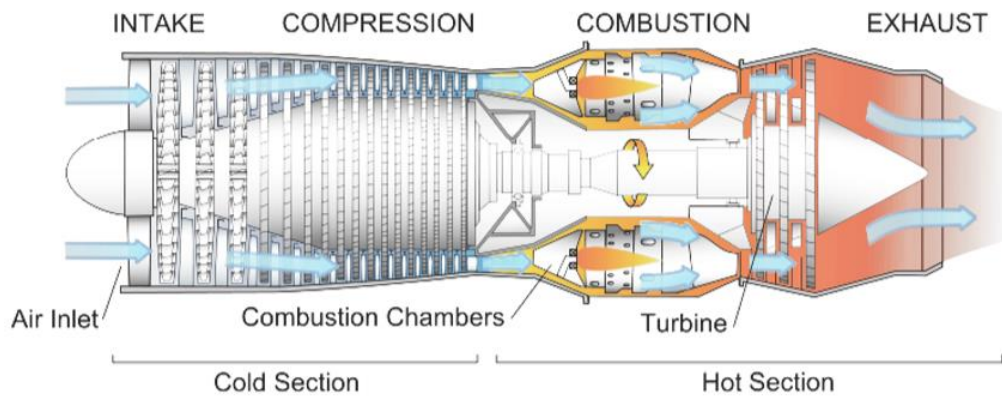


Figure 1.7

As it can be noticed from the figure above the most important parts with which turbojet engine is made are an intake (D), a compressor (C), a combustor (B), a turbine (T) and a nozzle (N), the compressor is driven by the turbine which extracts the power from the exhaust gases outcoming from the combustor.

In a turbojet the air is conveyed by the air intake, which starts a first compression and has also the scope to decelerate the flow, then it is sent to the compressor which continues the compression, from here it is sent to the combustion chamber, where it mixes with the atomised fuel from the injectors and ignited, and then it is allowed to expand through the turbine, finally the turbine exhaust is then expanded in the

propelling nozzle where it is accelerated to high speed to provide thrust. The geometry of the engine is the same both in the subsonic and in the supersonic version except for the intake and the nozzle that are divergent or convergent-divergent respectively for subsonic and supersonic.

The air flow evolution is described by a Joule-Brayton Cycle and follows the trend in the figure below:

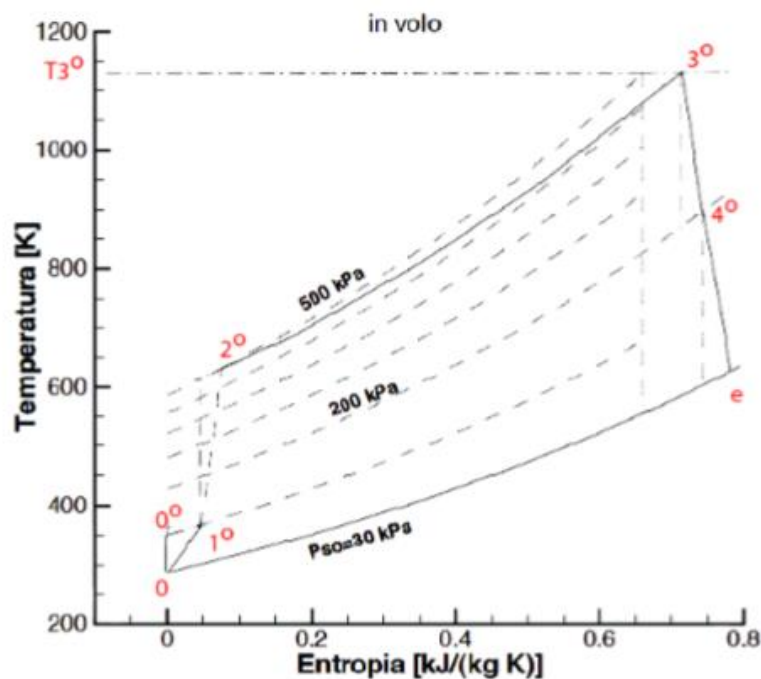


Figure 1.8

To define turbojet's performances means calculate the specific thrust I_a and the thrust specific fuel consumption $TSFC$ or q_s , but in order to do that flight conditions must be known, it means the altitude z from which external temperature and pressure are defined (the latter doesn't enter in the calculations for the performances but is useful to find engine's dimensions for a required power) and the Mach. The flight parameters are the OPR (Overall Pressure Ratio) which define the compression ratio inside of the compressor and the TIT (Turbine Inlet Temperature) which is the temperature of the gases that fall out of the combustor and enter in the turbine, this represent also a limit in the engine design since the adequate material should be chosen to face high temperature at the entrance in the turbine trying to not make the engine excessively heavy.

To derive the value of the two performance parameters previously defined it is necessary calculate the thermodynamics quantities that describe the transformations for the Joule-Brayton cycle.

0→1: the conditions after the air flow passage from the air intake are calculated, not as 'static' quantities but as 'total'.

$$T_0^\circ = T_0 \left(1 + \frac{\gamma - 1}{2} M_0^2 \right) = T_1^\circ$$

$$p_0^\circ = p_0 \left(1 + \frac{\gamma - 1}{2} M_0^2 \right)^{\frac{\gamma}{\gamma - 1}}$$

$$p_1^\circ = \varepsilon_d p_0^\circ$$

1→2: the air flow suffers an adiabatic compression, from the formula of the transformation efficiency the total temperature in point 2 can be calculated, while the pressure is defined by the *OPR* that is known.

$$p_2^\circ = \beta_c p_1^\circ$$

$$\eta_c = \frac{L_{c_{is}}}{L_c} = \frac{c_p (T_{2_{is}}^\circ - T_1^\circ)}{c_p (T_2^\circ - T_1^\circ)}$$

$$T_{2_{is}}^\circ = T_1^\circ \beta_c^{\frac{\gamma}{\gamma - 1}}$$

$$T_2^\circ = T_1^\circ + \frac{T_1^\circ}{\eta_c} \left[\left(\frac{T_{2_{is}}^\circ}{T_1^\circ} \right) - 1 \right] = T_1^\circ \left[1 + \frac{1}{\eta_c} \left(\beta_c^{\frac{\gamma}{\gamma - 1}} - 1 \right) \right]$$

$$L_c = h_2^\circ - h_1^\circ = c_p (T_2^\circ - T_1^\circ)$$

2→3: here the combustion takes place, the value of T3 is a project data while the pressure at the exit is calculated through the combustor efficiency.

$$T_3^\circ = \text{project data}$$

$$p_3^\circ = \varepsilon_b p_2^\circ$$

3→4: in this transformation an adiabatic expansion is executed, the main variables are found by a balance of power at the shaft.

$$T_4^\circ = T_3^\circ - \frac{L_t}{c_p'}$$

$$p_4^\circ = \frac{1}{\beta_t} p_3^\circ$$

4→e: the expansion continues in the nozzle that can be adapted, non-adapted or a generic non-adapted nozzle. From the first principle of the thermodynamic the exit velocity can be calculated and in the case of an adapted nozzle it is equal to

$$w_e = \sqrt{2c_p' T_4^\circ \left[1 - \frac{1}{(\varepsilon_n \beta_n)^{\frac{\gamma'-1}{\gamma'}}} \right]}$$

Once discussed all the transformation in the turbojet air flow cycle it is possible to calculate the performances parameters equal to:

$$I_a = \frac{S}{\dot{m}} = \left(\frac{\alpha + 1}{\alpha} \right) w_e - u$$

$$q_s = \frac{\dot{m}_b}{S} = \frac{1}{\alpha I_a}$$

As it has been said previously turbojet is a good alternative as propulsion system for the first stage of a TSTO but it has some limitations: at low and subsonic Mach the increasing of the weight is the main constrain that set a maximum on the size of the

engine, on the other hand for high Mach value the limit is represented by its volume which can bring to exaggerated values of drag and to its increase.

1.3.2 Turbofan

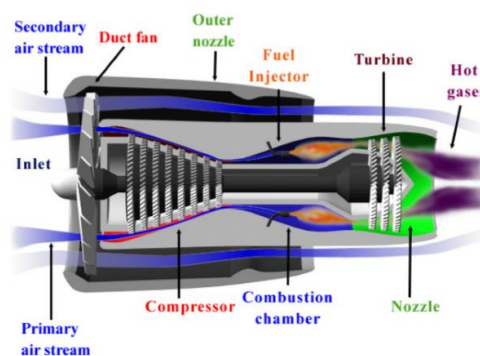
Turbofan is another type of reaction engine and its functioning is similar to the turbojet but in the turbofan the air flux is divided in two ways: the hot flux and the cold flux, and the ratio between the mass flow of the cold flow and the hot flow is called bypass ratio (BPR), that with the β_{cf} are the two new project parameters together with those already present in the turbojet (OPR and TIT).

This engine can be seen as a turbojet with an additional duct, the ‘bypass duct’ from which passes the cold flow that doesn’t enter in the turbofan as it is represented in the figure below.

This engine is based on the concept that it is more efficient generating thrust by accelerating a great mass flow with small acceleration than a small flow with great acceleration, for this reason the turbofan is designed with the thermodynamic of the turbojet but an increase in the flow, and the higher the value of BPR , the higher the efficiency of the engine will be.

On the base on the value of the BPR two types of turbofan can be identified:

- › Separated flows turbofan: characterized by an high BPR and conventionally used in the subsonic flight (with this solution there are low consumption but big overall dimension).
- › Mixed flows turbofan: characterized by a limited BPR typically used in the supersonic flight (smaller front dimension at the same thrust respect to the previous version). Here the β_{cf} is bounded by the mixing conditions which impose $p_{2f} = p_4$ so that the project parameters are only three (TIT, OPR, BPR)



In the turbofan the thrust is extracted from the hot flux which from the inlet goes into the compressor, that in this case, differently from the turbojet, is divided in the low pressure compressor (also called fan that represents the point where the flow is divided in cold and hot flow) and in the high pressure compressor, here its pressure increase and the speed decrease, then passes through the combustor, later through the turbine, that equally to the compressor is divided in high pressure turbine and low pressure turbine, (they drive respectively the high pressure compressor and the fan) here the flow is expanded and finally it exits from the nozzle where it can be mixed or not with the cold flow that from the inlet goes directly to the nozzle, the flow dynamic is the same as that of the turbojet engine in its internal section, while in the external section the cold flow after its passage from the fan goes directly to the bottom of the engine.

The turbofan with separated flows is schematized in the figure below:

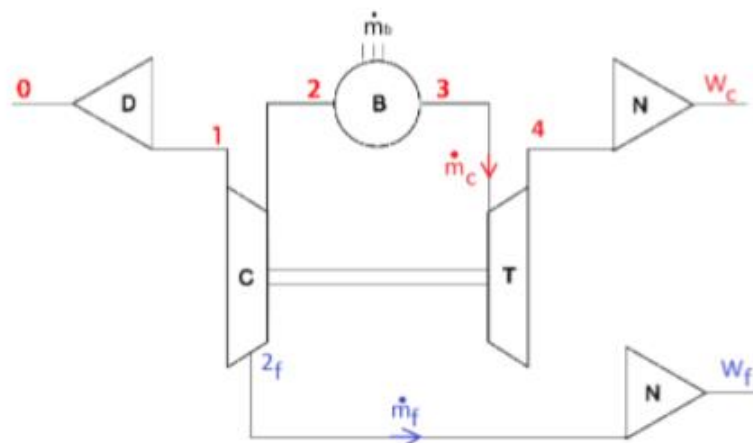


Figure 1.9

Its behaviour can be shown also in this case by a Joule-Brayton Cycle:

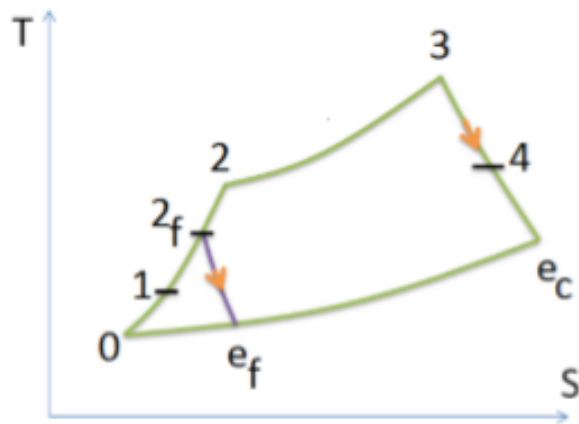


Figure 1.10

On the other hand, in the figure below the scheme of the mixed flows turbofan is shown, here there is the presence of a new component, the mixer:

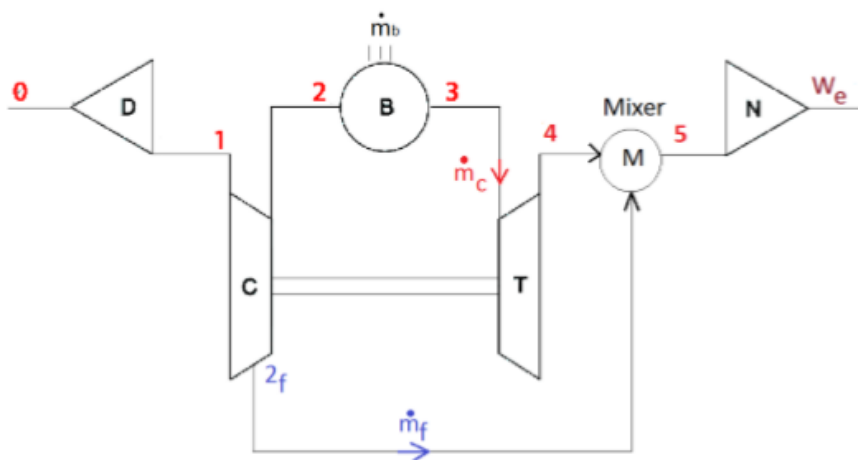


Figure 1.11

And here there is its cycle, in the point 5 the hot and the cold flow are mixed in a unique flux and the continue their evolution to the point e (the nozzle) and then they exit from the engine:

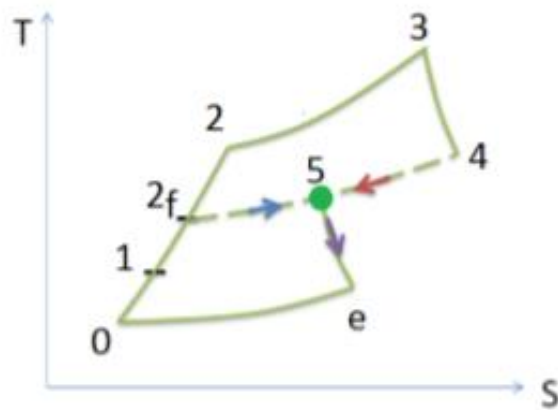


Figure 1.12

In both the turbofan versions, the separated flow turbofan and the mixed flow turbofan, are valid the following relationship for the evaluation of the performances:

$$I_a = \frac{S}{\dot{m}}$$

$$\dot{m} = \dot{m}_c + \dot{m}_f = (1 + \mu)\dot{m}_c$$

$$q_s = \frac{\dot{m}_b}{S} = \frac{\dot{m}_b}{\dot{m}_c} \frac{\dot{m}_c}{S}$$

$$\alpha = \frac{\dot{m}_c}{\dot{m}_b}$$

The influence of the β_{cf} parameter on the performance can be analysed:

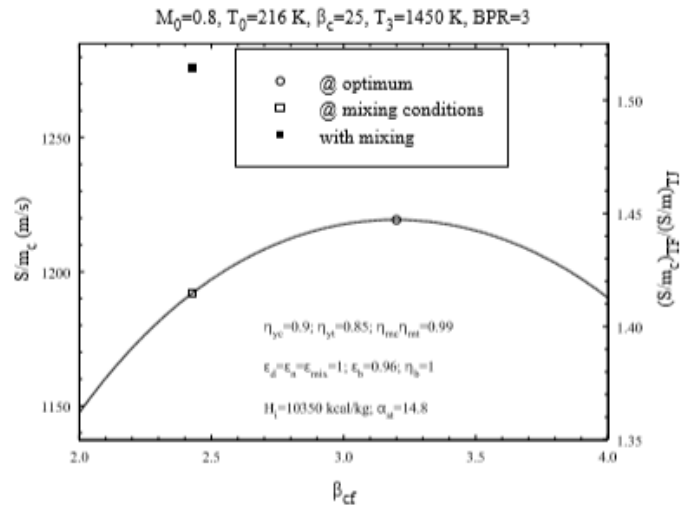


Figure 1.13

Note that the optimum working condition for the maximum generation of specific thrust differ based on the type of turbofan we take in consideration: for separated flow turbofan, the thrust has a parabolic-like evolution in function of the β_{cf} , while the optimum point for mixed flow turbofan is set on a precise value of β_{cf} since there is a constrain on the value of the cold and hot flow pressure, and this value is generally less than that for the other type of turbofan. It is clearly visible that is more convenient the version with mixing.

In the figure below it is presented the effect of the BPR:

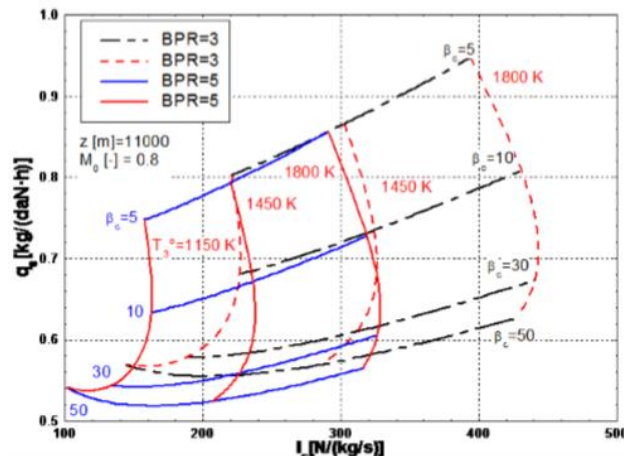
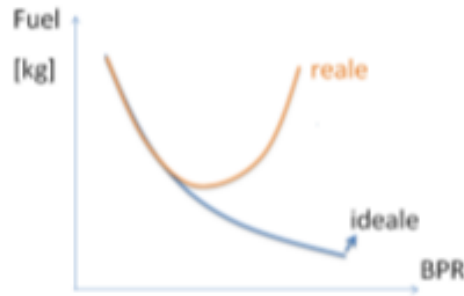


Figure 1.14

Fixed a value of OPR and TIT , an increase in BPR means a reduction of both the specific fuel consumption q_s and the specific thrust, that means an increase in the engine dimensions and weight, but above a certain value of BPR the negative effect of the drag and high weight prevails on the q_s reduction.



1.3.3 Afterburning

A good method to improve the engine's performances is the usage of an afterburning which brings to an increase of the thrust level and a variation to the consumption level, many of the aircrafts analysed in the supersonic first stage database adopt it.

The scheme of the engine with the afterburning will be modified and it will count a new component:

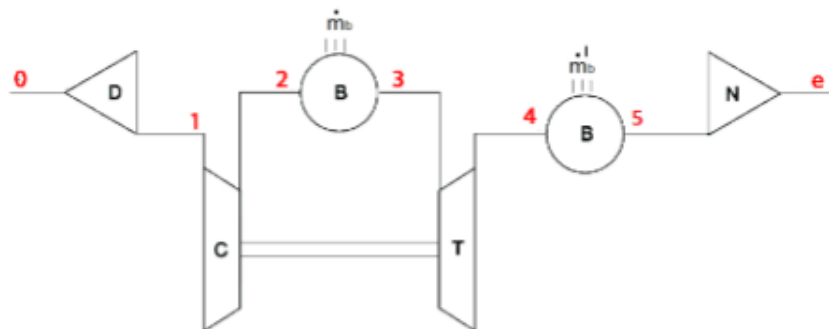


Figure 1.15

Where B stands for burner, the temperature in the point 5 is a new project parameter, in the figure below the new cycle can be seen:

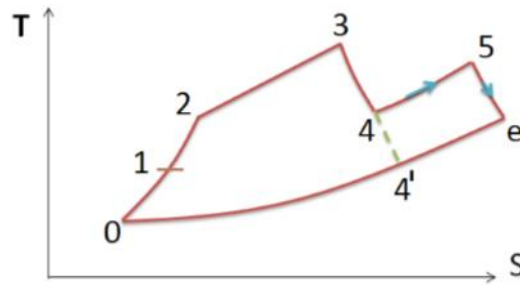


Figure 1.16

It is clearly visible that the useful work, represented by the subtended area of the cycle, is increased. The flow can't be heated up before the entrance in the turbine for the material's temperature limits, but the flow that exits from the turbine, since there is a residue of oxygen, is further heated until a temperature $T_5 > T_3$, in fact it is easier to protect the afterburner from the heat instead of the turbine blades.

The speed of the exhaust gases can be evaluated in both the dry condition (without afterburner) and with afterburner, in particular for the DRY condition is:

$$w_e = \sqrt{2C_p' T_e^\circ \left(1 - \frac{1}{\beta_n \gamma'^{\frac{\gamma'-1}{\gamma'}}} \right)} \propto \sqrt{T_4^\circ}$$

While for the condition with afterburner is:

$$w_e = \sqrt{2C_p' T_e^\circ \left(1 - \frac{1}{\beta_n \gamma'^{\frac{\gamma'-1}{\gamma'}}} \right)} \propto \sqrt{T_5^\circ}$$

Thanks to these formulas the evaluation of the cycle work increase can be justified in fact the expansion work (in total terms) is equal to:

$$L_t^* = L_t + \frac{w_e^2}{2}$$

While the compression work is equal to:

$$L_c^* = L_c + \frac{u_e^2}{2}$$

The expansion work increase due to the effect of the increase of w_e (respect to the case without afterburner) that is proportional to the square root of T_5 , on the other hand the value of u is independent of the presence of the afterburner and thus constant.

The increase of thrust is temporary since an increment in the thrust by means of the afterburner means an increase in the consumption, generally a doubling in the thrust means a doubling in the consumption.

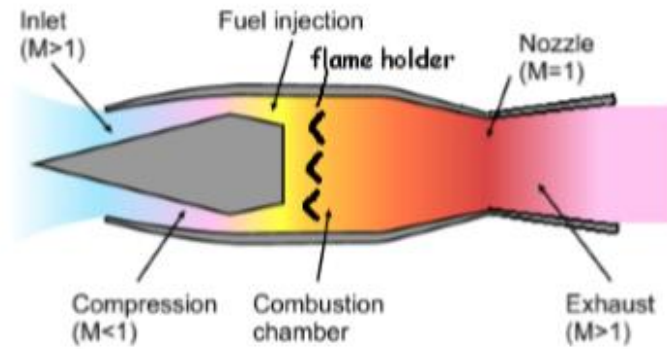
1.3.4 Ramjet and Scramjet

Both ramjet and scramjet are a particular type of reaction engine, their basic functioning is the same of the turbojet and the turbofan, in fact the thrust is created by mean of the air, but the difference from this type of engine and those previously mentioned is that the compression and the expansion are executed thanks to the air intake (compression) and to the convergent-divergent or divergent nozzle (expansion) respectively for ramjet and scramjet where the exhaust gases are accelerated and expanded to generate the thrust.

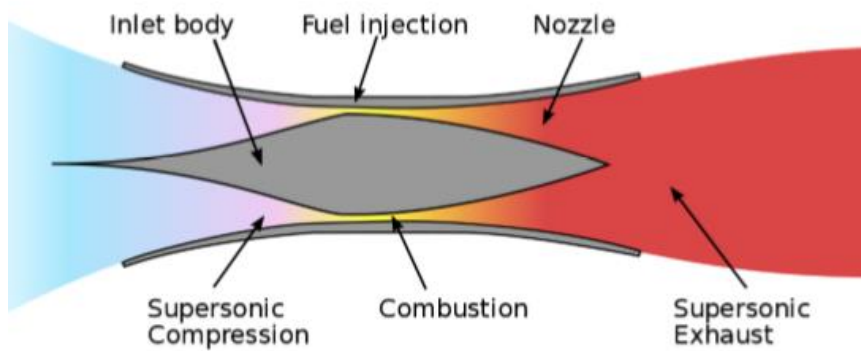
The difference between ramjet and scramjet is that the combustion in the scramjet is supersonic while in the ramjet is subsonic, this is an advantage and let to the vehicle which adopt a scramjet to reach Mach 8 or even more, while the ramjet is capable to reach Mach 3/3.5.

Ramjet and scramjet engines exploit the high operative velocities to compress the air coming in the air intake thanks to oblique bumps and expand it into the nozzle to generate enough thrust to keep it in flight at high speeds.

The scheme of the ramjet is reported below:



The scheme of the scramjet is similar due to the absence of turbine and compressor but with the difference in the nozzle explained in the previous lines:



More simply it can be reduced to the scheme hereunder to which follows the thermodynamic cycle:

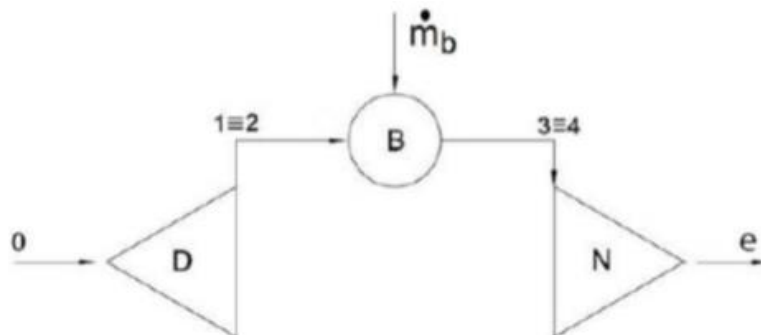


Figure 1.17

It can be noticed that this type of propulsor is made only by an air intake, a combustor and a nozzle, and as previously said, differently from turbojet and turbofan the compressor and the turbine are absent.

The thermodynamic ideal cycle made by the ramjet and scramjet is very similar to the cycle of the others engine, thus a compression, a combustion and an expansion.

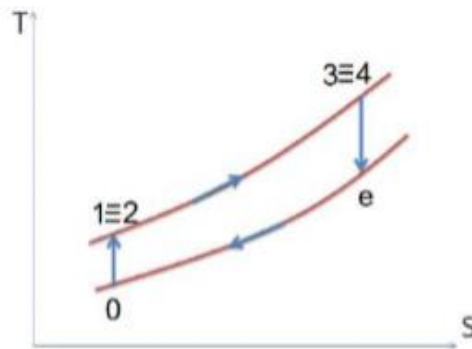


Figure 1.18

From the figure it can be noticed: 0 is the air input into the air intake, from 0 to 1 there is the compression by mean of the air intake, point 2 represents the input in the combustion chamber, from 2 to 3 the combustion is made, then in point 4 there is the input to the nozzle and finally from point 4 to e there is the expansion and the output ad exhaust gases.

For the ramjet and the scramjet, the only project parameter useful for its dimensioning is the Turbine Inlet Temperature (TIT) which is the temperature of the gas leaving the combustor.

These engines are composed by a few components so that the construction and the maintenance are easy specially thanks to the absence of rotative parts such as turbine and compressor, a consequence of this is also the fact that the they are not extremely heavy, moreover generally the ramjet and the scramjet are use as propellant the liquid hydrogen which burning with oxygen generate H_2O in a non-polluting way without producing CO_2 , all these represent the main advantages of these engine but on the other hand some disadvantages may be encountered, the most important is that these propulsor can't take off autonomously but they start to have a good functioning around Mach 2 for ramjet and Mach 4/5 for the Scramjet, so that the aircraft which adopts these kind of engine should be equipped by another type of propulsor (a turbofan or a rocket) that brings them to the operative speeds.

1.3.5 Rocket

This is a type of engine that doesn't use air flow for propulsion but uniquely propellant, energy is given to on-board propellant accelerated and ejected to provide thrust, for this reason its performances doesn't depend from the flight speed and form the external conditions so that they can be used for space applications differently from the air-breathing engine, moreover they can work on a wide range of thrust but their consumption is very high respect to the air-breathing.

The rockets can be classified in thermal, electrostatic or electromagnetic, within the thermal rocket category are comprised the chemical rockets which have high importance for TSTO applications and in turn they can be classified as solid rocket motor (solid propellant), liquid rocket engine (liquid propellant) and hybrid rocket engine (liquid+solid, usually liquid oxidizer).

The main components of a chemical rocket are the tanks, the feed system, the combustion chamber and the nozzle. An example is presented hereunder with the case of a liquid propellant rocket engine where there is a tank for the oxidizer and one for the fuel, while the feed system is made of a pumps and valves:

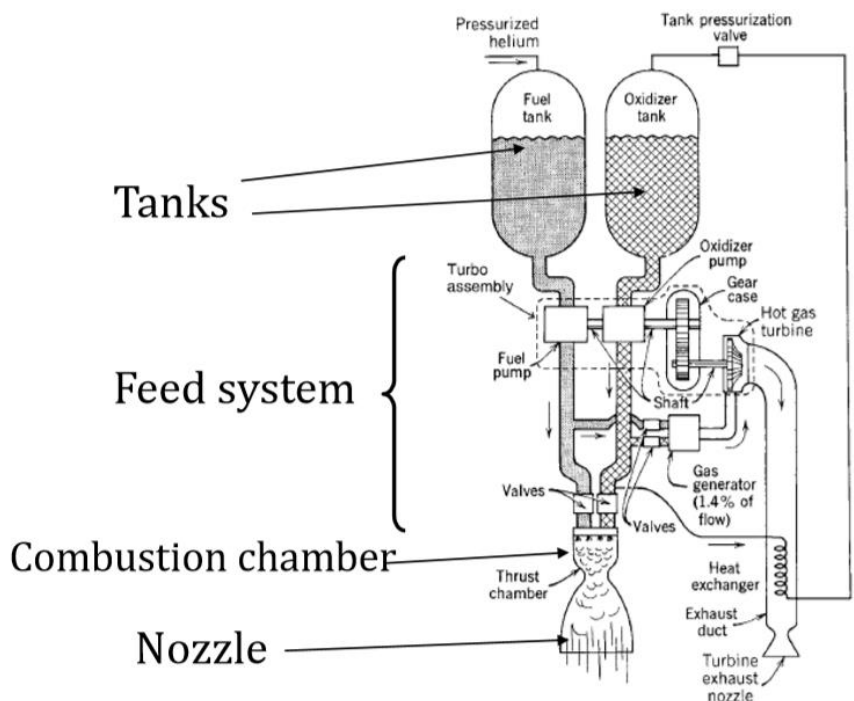


Figure 1.19

A difference emerges in the case of a solid propellant rocket motor where tanks coincide with the combustion chamber and the feed system is absent, so that the architecture of the engine is limited to the combustion chamber and the nozzle:

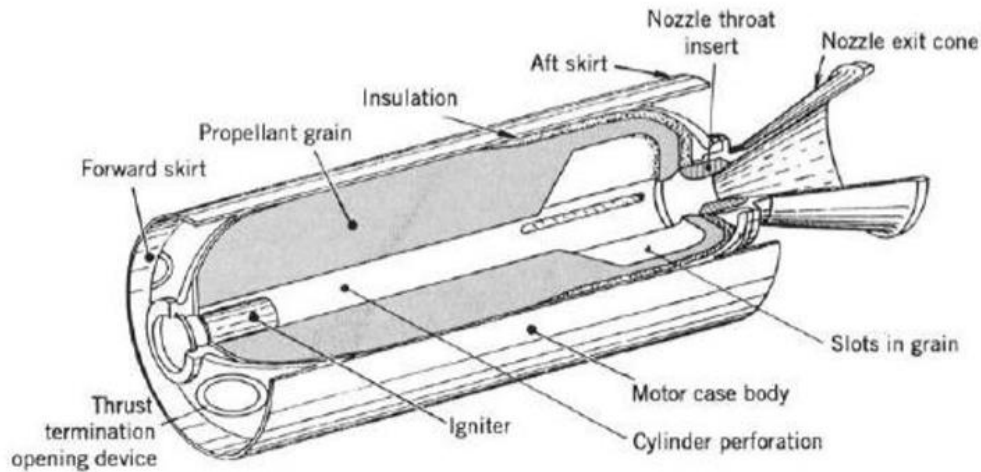


Figure 1.20

A problem of the solid propellant rocket motor, contrary to respect the liquid propellant rocket engine, is the impossibility to stop the combustion once it has started except with impractical methods such as destructive ones, for this type of engine the thrust variation is determined by the shape in which the mixture is cast and can't be actively controlled during the flight.

The hybrid propellant rocket engine is a configuration where generally the oxidizer is liquid and is contained in its own tank, while the fuel is solid and is present in the combustion chamber.

By rockets engine the thrust we obtain, in a 1D model, is equal to:

$$F = \dot{m}w_e + A_e(p_e - p_o)$$

And the specific impulse is:

$$I_s = \frac{I_t}{g_0 M_p} = \frac{F dt}{g_0 dm} = \frac{c}{g_0}$$

Where I_t is the total impulse given by the integral of the force F during the burning time, g_0 is the gravitational acceleration, M_p the propellant mass and c the effective exhaust velocity.

The graph below focuses on a classification of the rocket types, in terms of effective exhaust velocity and acceleration without payload, it is worth noting that from high to low values of effective exhaust thrust the propellant consumption increase while from low to high values of acceleration the thrust to engine mass ratio increase, so that the best performances are obtained moving towards top right values of the graphic.

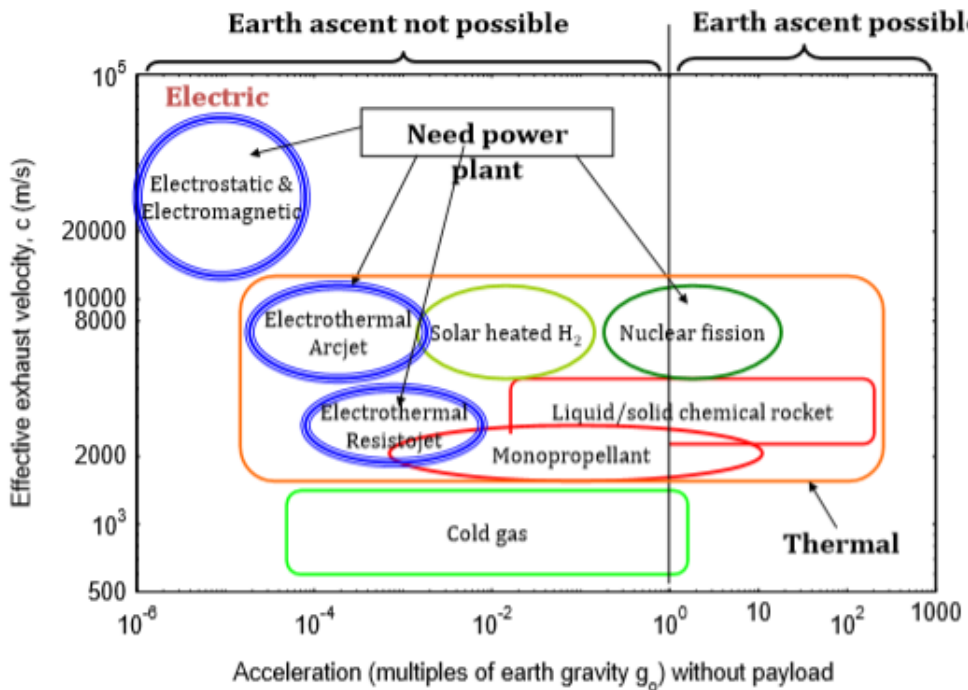


Figure 1.21

Chapter 2

2.1 Statistical Analysis

The preparatory activity to the conceptual design of a TSTO consists in the execution of a statistical analysis: starting from a proper database where are collected all the aircrafts that perform the same mission or that have the same technologies of the spacecraft of interest will be defined those technical data, called guess data, which are useful to start the conceptual design.

Starting from the value of the payload mass in the under-development TSTO thanks to the statistical analysis will be available data on maximum take-off weight, thrust, wing surface, propellant mass fraction (*PMF*), and from the value of desired Mach, the value of specific fuel consumption (*SFC*) will be noted.

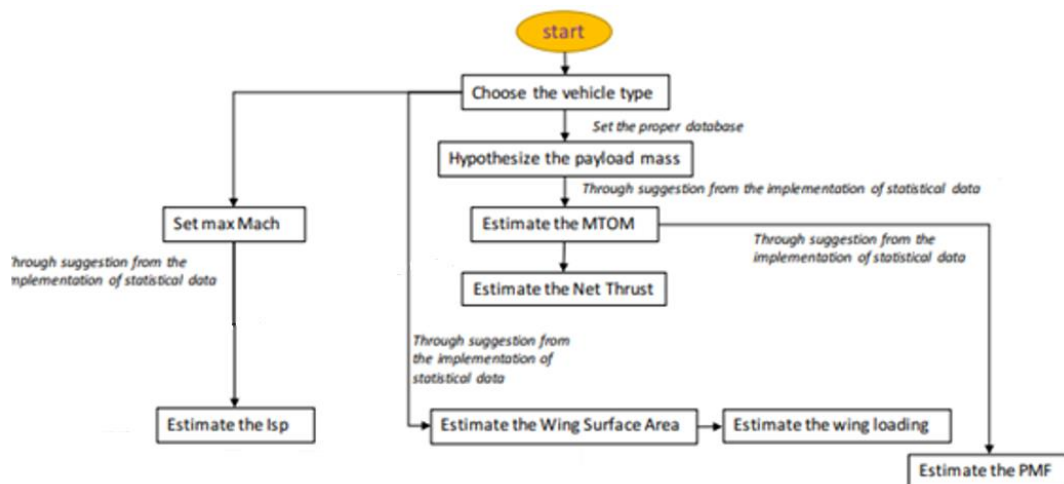


Figure 2.1

The database for the statistical analysis of the TSTO has been defined starting from the type of propulsion of the first stage of the aircraft, in order to do so the main database has been divided into three parts and each characterized a different type of stage: subsonic first stage, high speed first stage, rocket first stage.

For each of these, diagrams have been developed to find the most suitable interpolation law to find guess data.

In the next pages will be presented all the vehicle taken in consideration for each single database and how data will be found.

2.1.1 Subsonic first stage database

In this section have been selected vehicles that could be taken as example as subsonic first stage, in this context also air-launch-to-orbit vehicles have been taken into account as well as some cargo airplanes.

Air launch to orbit is primed to become the main method of placing small satellites into orbit in a quick and cheap manner, most of the vehicle that adopt this kind of launch method carry the payload to an altitude of 12/15 km before changing to rocket propulsion and accelerate it to reach the orbit with the second stage.

Stratolaunch

Stratolaunch is a vehicle born with the aim to transport rocket until an altitude of about 12000m to put into orbit satellites according to any orbital inclination, it is a vehicle with a double fuselage each with its own tail with rudder and elevator in order to leave an empty area to reduce the aerodynamic interference drag during the flight, it is the airplane with the biggest wingspan that have ever been made with an overall wing surface of 1000 m². It has an MTOW of 590 tons and is capable to carry until 230 tons of payload, while the propellant mass is 325 tons.

It has six turbofan engines (three on the left half-wing and three on the right one) with a thrust of 253.3 kN each so that an overall thrust of 1520 kN can be generated reaching Mach 0.78.



Whiteknight II

Whiteknight II is the carrier aircraft, following the concept of air launching space vehicle, used for the SpaceShipTwo's launch which is the world's first passenger carrying spaceship to be built by a private company and operated in commercial service, and transport it to an altitude of 50000 feet.

Whiteknight II aircraft is made of two different fuselages united among them to have a wingspan of 43 metres and a wing surface of 117 m^2 , this type of design provides a large and easily accessible payload area and facilitates clean separation when the spaceship is released.

The thrust is produced by four turbojets Pratt & Whitney Canada PW 308 with a thrust of 30.69 kN each and operates at an attitude of 21000 metres at a speed of Mach 0.8, moreover this aircraft has a MTOW of 21 tons and is capable to carry a payload of 13 tons.



Lockeed L-1011 Tristar

This aircraft was developed by the Lockheed Corporation Company in the late 1960, born as an airliner with a capacity of 400 passengers for destinations if medium to long range such as London or the south America leaving from hub like Dallas and New York, but later it has been taken into account for its application as air-launch-to-orbit vehicle in fact in its version L-1011 "Stargazer" has dropped the rocket Pegasus to an altitude of 12 km and it has been useful to place over 78 satellites in orbit in over 40 launches since 1990, moreover it was used in support of the X-34 and X-43 programs for the NASA aerodynamic research on Orbital Sciences.

This aircraft has a MTOW of 200 tons and in the case of his application mentioned above carried a payload of 23000 Kg and a propellant mass of 50 tons, it has three turbofans installed on board to produce a thrust of 498 kN, the cruise speed is Mach 0.86 and has a ceiling altitude of 11000 metres, also important for our analysis is the wing surface that is equal to 321 m².



Antonov An-225 Mriya

The An-225 is Russian cargo vehicle, it was conceived for the soviet space program which required a new aircraft to transport the components of the Energia rocket, this vehicle is equipped with a large internal hold that allows to increase the payload and make the aircraft to be used for a wider range of tasks, such as transporting the Buran space shuttle on his back.

An-225 has a MTOW of 640 tons and is able to carry a payload of 50000 kg, on each half-wing owns 3 turbofans ZMKB Progress D-18T with a thrust of 229 kN each for an overall thrust of 1380 kN, it is the third airplane the with the largest wingspan and has a wing surface of 905 m², its cruise speed is Mach 0.72.



Myasshchev VM-T

VM-T is a cargo vehicle of Russian origin with the scope to be a transport system for the elements of rockets and the shuttle to the launch pad, and it is the predecessor of the An-225, it was born with the idea to carry a payload of around 40 tons and a diameter of 8 metres, despite the problems of aerodynamic nature it was a successful aircraft with more than 150 flights to transport space components to Baikonur.

Its main properties are a MTOW of 200 tons and a wing surface of 351 m^2 , it is able to reach a speed of 970 km/h, but it decreases its cruise velocities to Mach 0.42 when has a payload on its back to decrease the consumption, it is endowed with four turbofans Dobrynin VD-7M for a total thrust of 424 kN.



Conroy Virtus

The Conroy Virtus was a large transport aircraft intended to carry the Space Shuttle, in fact at its origins Space Shuttle was projected to have airbreathing engine to move from a launch site to another after the re-entry but due to the high weight that this configuration would have involved, it was opted for an aircraft capable to execute a ferry flight for the Shuttle.

Conroy Virtus was made by a pair of Boeing B-52 Stratofortress fuselage to form a new airplane with a wing surface of 2060 m^2 , unfortunately it never enters in service because the Boeing 747-based Shuttle Carrier was preferred to it.

With a MTOW of 386 tons and a thrust of 816 kN produced by four turbofan Pratt & Whitney JT9D-3A the Conroy Virtus was able to carry a payload of 25 tons.



Boeing 747 Space Shuttle carrier

The Space Shuttle carrier from the Boeing family are Boeing 747-100 adapted for the Space Shuttle Transportation, they have been conceived with the idea to carry the Space Shuttle to the Kennedy Space Center whenever for operational reasons they are forced to land on a runway other than NASA Shuttle Landing Facilities.

With an MTOW of 322 tons it has been thought to carry a payload of 49500 kg, it hosts four turbofans Pratt & Whitney JT9D-7J with a thrust of 222 kN each for an overall thrust of 888 kN, which enables the aircraft to reach the speed of Mach 0.78 to a cruise altitude of 5000 metres when the Space Shuttle is carried.

Dimensionally Boeing 747 has a length of 70.5 metres and an height of 19.3 while the wing surface is 510 m².



Guess data estimation

Once that all the aircraft of reference have be set their technical data have been used to define the graphics here below, the following relationship have been studied to find an interpolation law:

- > MTOW = f(Payload)
- > Thrust = f(MTOW)
- > PMF = f(MTOW)
- > Wing Surface = f(MTOW)
- > Isp = f (Mach)

For these relationships it has been used a logarithmic interpolation law for MTOW = f(Payload) and a linear interpolation law for all the others.

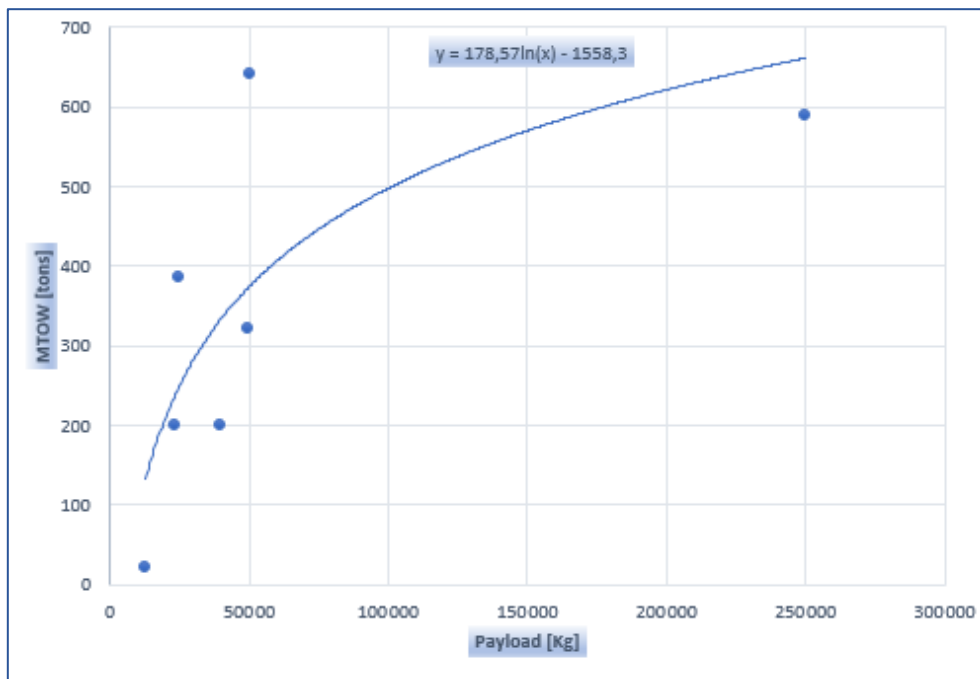


Figure 2.2

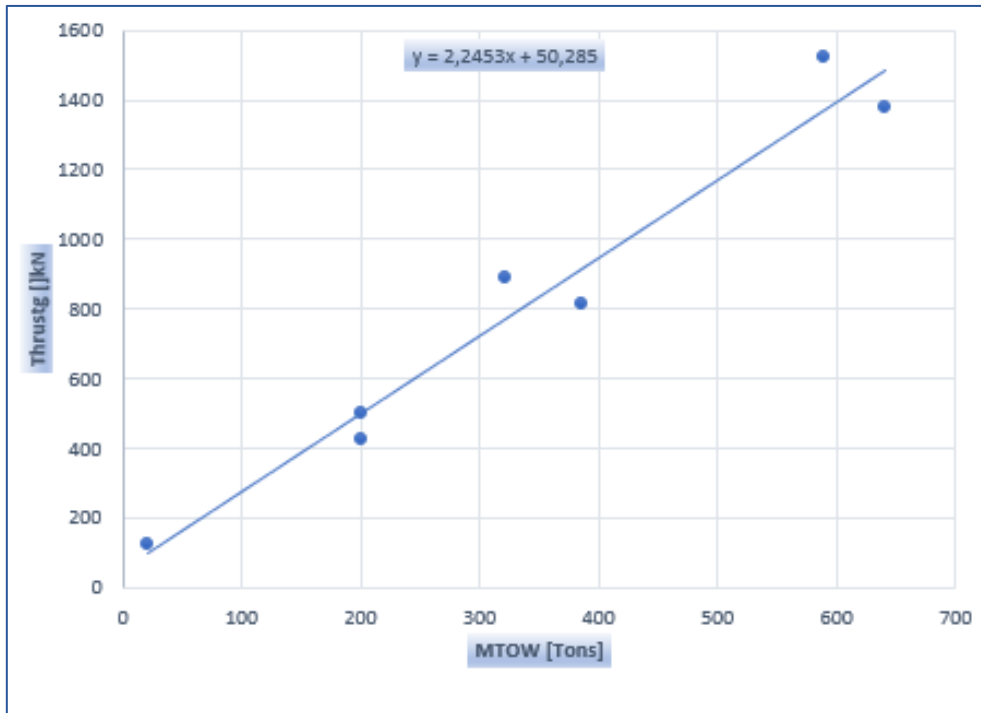


Figure 2.3

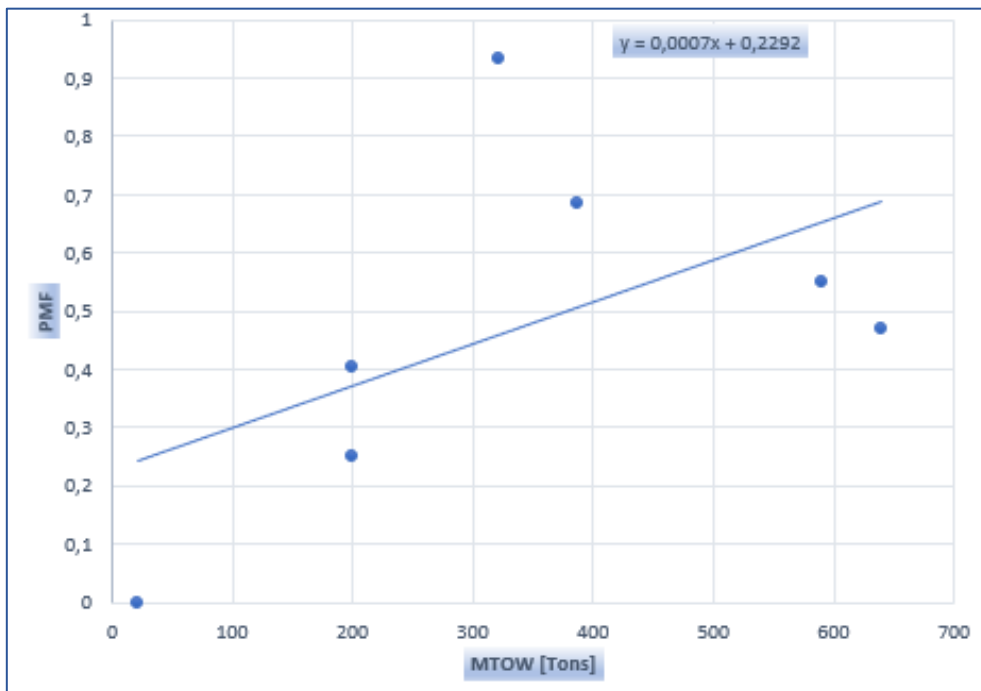


Figure 2.4

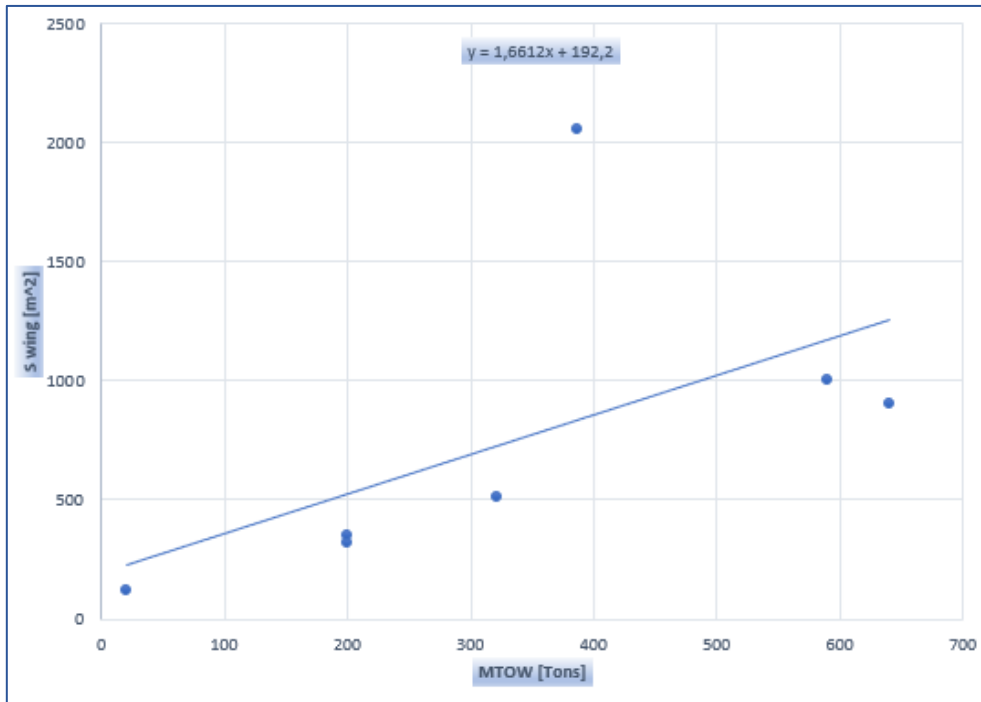


Figure 2.5

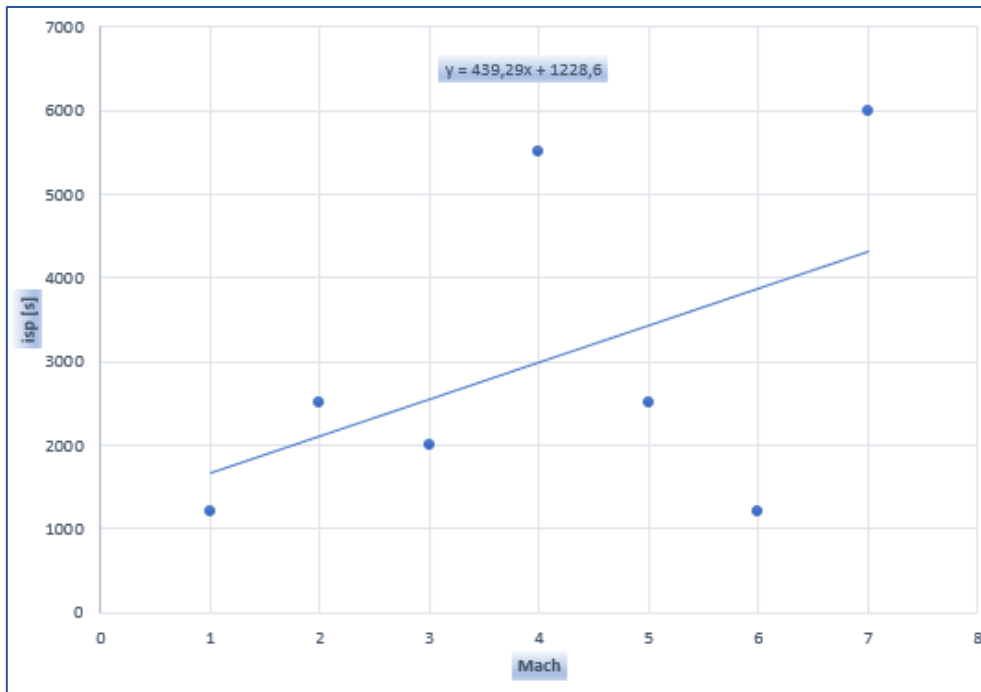


Figure 2.6

2.1.2 Supersonic first stage database

The second type of first stage that has been analysed is the supersonic first stage with an airbreathing type of propulsion, cruise and acceleration vehicle (CAV), aircrafts that can reach a high value of Mach will be taken into consideration for this category.

All the vehicles that belong to this category are conceived to accelerate the second stage and the payload to a value of Mach and to reach an altitude that better suits to the second stage in order to optimize its performances.

In the database have been included also three single stage to orbit (SSTO) which are the Hotol, Tupolev 2000 (space version) and the Skylon, that are propelled by an engine for the initial phase of the mission to let them to reach high speed and for the second phase of the mission they switch to a rocket propulsion.

As it has been done for the subsonic first stage database in the following lines a review of the characteristics of all the aircraft chosen for our scope will be presented and then there will be found the interpolation laws to find the guess data.

Hotol

British Aerospace envisioned the HOTOL as an unmanned, fully reusable single-stage-to-orbit (SSTO) winged spaceplane capable to take off from a conventional runway and re-enter the atmosphere executing a horizontal landing. The original HOTOL airframe design was derived from conventional vertical take-off rockets with the engines mounted at the rear of a blunt fuselage while the payload bay was placed in a projecting forebody.

The engine was intended to switch from jet propulsion to pure rocket propulsion at 26-32 km high by which the aircraft would be travelling at Mach 5 to 7.

It was a vehicle with an MTOW of 250 tons projected with the idea to put a payload of around 8 tons in orbit at 300 km of altitude, the air-breathing engines would be capable of producing a thrust of 735 kN.



Tupolev 2000 (space version)

The Tu-2000 was born in three different versions but only one, the space version, was projected with the idea to furnish a method to carry payload in low earth orbit (until 200 km) in an economic and efficient manner, the propulsion would have consisted in 8 statoreactors ATR and a rocket in the higher altitude.

It was conceived as an aircraft with a MTOW of 260 tons able to carry a payload of 10000 kg, a wing surface of 1250 m², and an overall thrust of 900 kN.



Skylon

The Skylon is an SSTO under-development spaceplane able to depart from and return to a conventional runway to deploy satellites into orbit which uses a particular propulsive technology that is the Synergetic Air-Breathing Rocket Engine (SABRE)

from the British aerospace manufacturer Reaction Engine, it is an hybrid engine capable to work as an airbreathing engine as well as a rocket, this technology enables the aircraft to operate in two different environment (inside the atmosphere and in the space) in fact after a first phase to reach Mach 5 the craft switch to closed-cycle mode and reach the orbit with Mach 9, the thrust that each engine can produce is 1350 kN for a total of 2700 kN.

The Skylon has an MTOW of 325 tons and can carry a payload of 17 tons, it has a wing surface of 240 m².



Lapcat A2

Lapcat A2 is an atmospheric vehicle conceived for an high speed transport mission and belongs to the CAV category and it is part of a program funded by the European Commission and defined by the research of a consortium of 12 partners.

The scope of the A2 is hypersonic antipodal passenger transport with travel times of under five hours, which intrinsically requires a new flight regime which means a technological innovation, it is very similar to the Skylon and has an engine, that is the simplification of the SABRE, called Scimitar and it is adapted for high speed atmospheric cruise until Mach 5.

A2 has an MTOW of 400 tons and a payload mass of 29 tons, thanks to its propulsion system it can generate a thrust of 1488 kN and has a wing surface of 900 m².



XB-70

North American XB-70 Valkyrie was born as a strategic supersonic bomber able to reach Mach 3 to not be intercepted by the soviet air defences, but this program didn't have a long life in fact only two prototypes were built.

It employed a canard configuration and a delta wing with a total surface of 585 m^2 , moreover this aircraft is the only of its size to have movable wingtips to increase aerodynamic stability at supersonic speeds, the engines were six turbojets with afterburner General Electric YJ93-GE-3 with a thrust of 128 kN each positioned in the aft of the fuselage between the two vertical empennage.

The MTOW is equal to 246 tons and the payload mass is equal to 23 tons.



Tupolev 144

Usually considered the “Russian Concorde”, the Tupolev Tu-144 was the Russian response to the supersonic civil transport and on his side it has a double delta wing with a conic curvature and two little retractable canard to increase to lift at low speed. This vehicle could fly at cruise Mach 2 at an average altitude of 16 km going across the ocean in 3 hours and half.

Due to the high operational cost of Tu-144 it was used only in part for people transportation but more frequently it was used as cargo with a payload mass of 20 tons in the face of a MTOW of 205 tons, but after only 8 years from its entry in service its operativity was stopped.



Concorde

The Concorde has been a supersonic transport airliner produced by the Anglo-french consortium formed by the Aerospatiale and the British Aircraft Corporation, it was used only in ocean-crossing routes to prevent sonic boom disturbances over-populated areas.

Its first flight was in 1969 and remained in service for 34 years then the programme was stopped, the factors that brought to this decision were the disastrous accident that took place on the 25th July 2000 but even more the very high maintenance costs and the high operative costs.

It could flight at a maximum Mach of 2 at the cruise altitude of 17 km with seating for 92 to 128 passengers, it relied on four Rolls-Royce/Snecma Olympus 593 turbojets

with afterburner (this was used only in take-off and acceleration phase) that produced an overall thrust of 676 kN, it has a MTOW of 187 tons and could host a payload mass of 15 tons, very accurate was the study of the delta wing which had a surface of 358 m².



Lockheed L-2000

L-2000 was a project proposed by Lockheed Corporation for the development of a supersonic transport aircraft, but the program was cancelled due to political, economic and environmental reasons.

This aircraft had the aim to be a vehicle that could improve Concorde performances, it was designed with a double delta wing and the engines drowned in it. This aircraft has a seating capacity of 250 passengers, a cruise speed of Mach 2 and a MTOW and a payload mass respectively of 267 tons and 30030 kg.



Saenger II

Saenger II was one of the first concept design for a reusable TSTO vehicle, it was developed for a twofold target: as hypersonic passenger airliner and as a two-stage launch vehicle for deploying various payloads into orbit.

As a conventional aircraft it was projected to have been able to reach Mach 3 and transport around 230 passengers.

For space launches to orbit Saenger would have carried a small piloted orbital spaceplane known as Horus that would have been principally used to service and supply space stations with cargo or astronauts; moreover Saenger would have carried also another type of spaceplane called Cargus which would have been used to convey payload into low earth orbit.

In its space launch configuration, which is our case of interest, the first stage of the aircraft would have taken off conventionally and ascended up to a ceiling altitude of 30 km with a maximum speed of Mach 6 thanks to its six turboramjet.



Lapcat MR2

Lapcat MR2 is a cruise passenger vehicle designed for antipodal flight from Brussel to Sydney in less than 4 hours, the leading idea was the optimal integration of a high performance propulsion unit within an aerodynamically efficient wave rider design based upon an adapted osculating cone method enabling to construct the vehicle from the leading edge while reducing integration problems giving enough volume for tanks payload and subsystems. For the propulsion system it has been adopted six air turboramjet and two dual mode ramjet which allow the aircraft to reach very high speeds, up to Mach 8 and able to produce a thrust of 1100 kN.

It could host a payload mass of 30 tons in face of 400 tons of MTOW, moreover the wing surface is estimated to be equal to 1600 m².



Jaxa HST

JAXA has been promoting research and development to establish technologies for a Mach 5 class hypersonic passenger aircraft that can cross the Pacific Ocean in two hours, from this work of research it was projected Jaxa HST that has an MTOW of 284 tons which thanks to a turbojet engine that can work continuously to grant that conditions and with a payload of 10000 kg.

The take off and the landing are executed in a conventional way, the wing is a delta wing with a surface of 242 m².



Guess data estimation

As it has been done with the previous category of aircraft, those that have been taken into consideration for a subsonic first stage, the following relationship have been studied to find an interpolation law:

- > $MTOW = f(\text{Payload})$
- > $\text{Thrust} = f(MTOW)$
- > $PMF = f(MTOW)$
- > $\text{Wing Surface} = f(MTOW)$
- > $Isp = f(\text{Mach})$

For these relationships a linear interpolation law has been used.

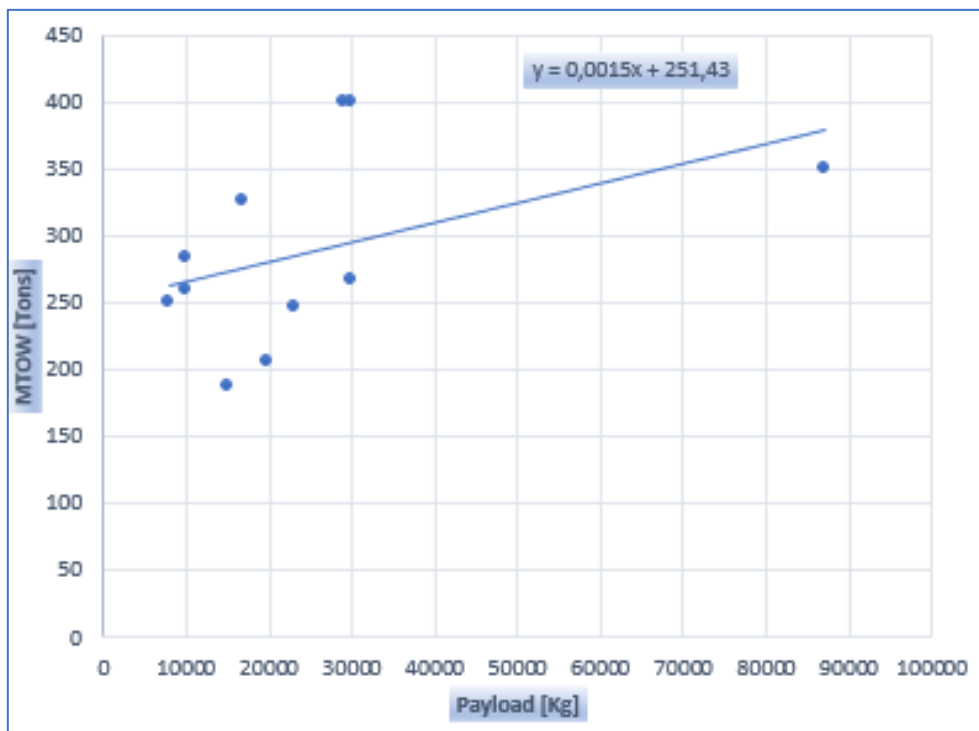


Figure 2.7

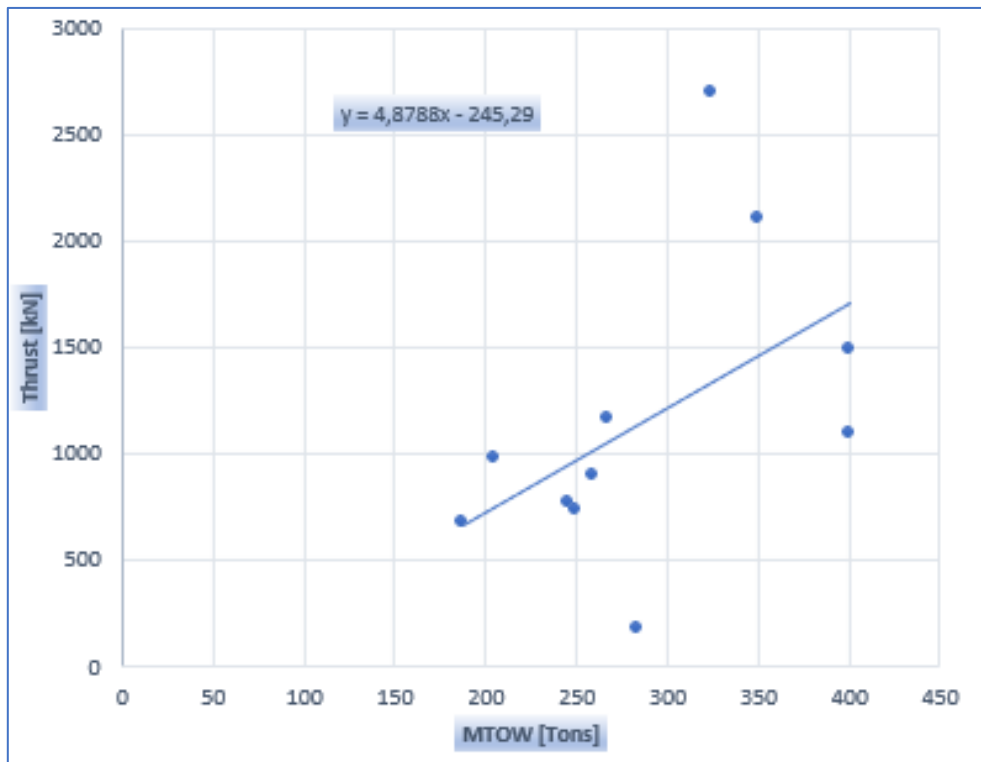


Figure 2.8

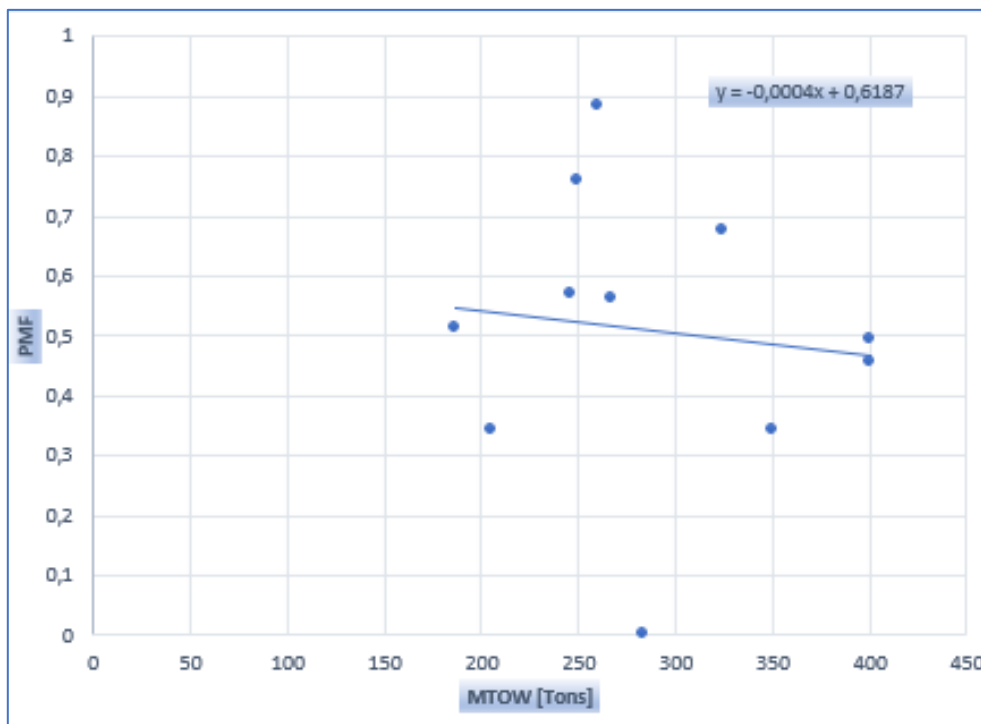


Figure 2.9

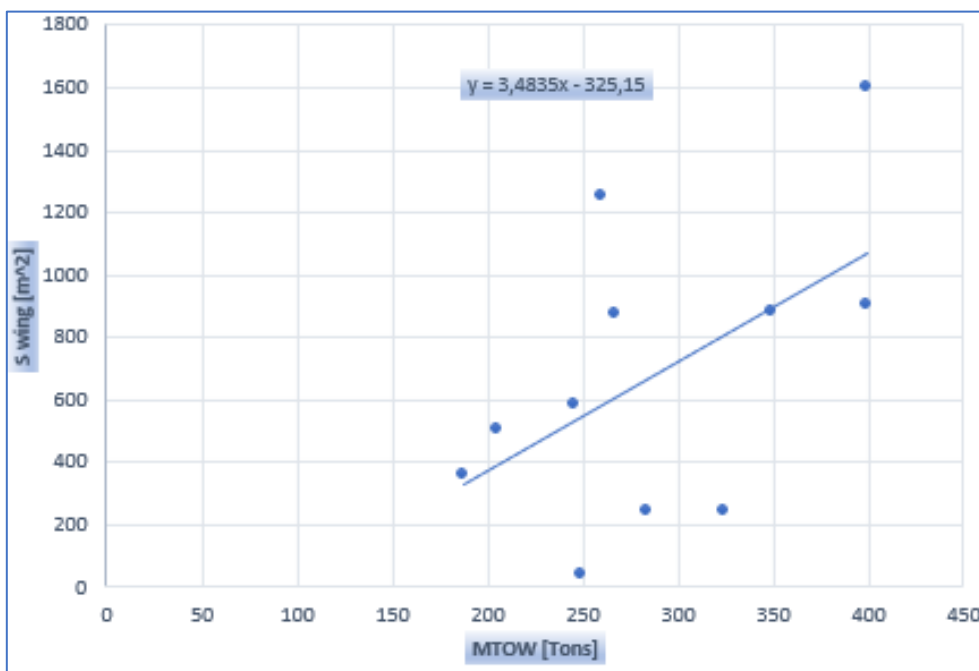


Figure 2.10

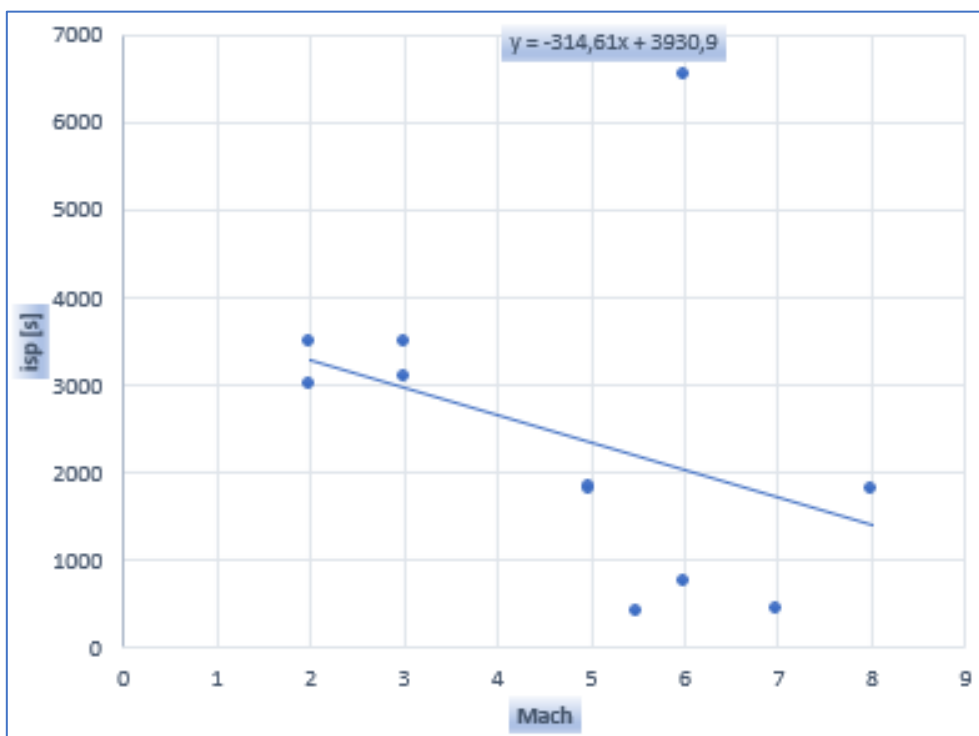


Figure 2.11

2.1.3 Rocket first stage database

This is the third and last category taken into account for the type of first stage that our TSTO can foresee.

In this database also three types of SSTO have been included, those are the Hotol, the Tupolev 2000 space version and the Skylon, all these three aircraft have been presented in the previous section.

To the aircraft just mentioned, others three aircraft have been added to complete the database, the main information are presented in the lines below.

Bristol Spacecab

Spacecab is a fully reusable spaceplane designed by Bristol Aerospace, it consists in a carrier which serves to launch a smaller aircraft identified as its payload with a mass of 41000 kg.

The carrier aircraft, which is the stage of interest, has four turbojet engines to provide the power for take off, acceleration to Mach 2, flyback and landing, plus two rocket engines with a thrust of 1960 kN to accelerate spacecab from Mach 2 to Mach 4, at which point the orbiter will separate.

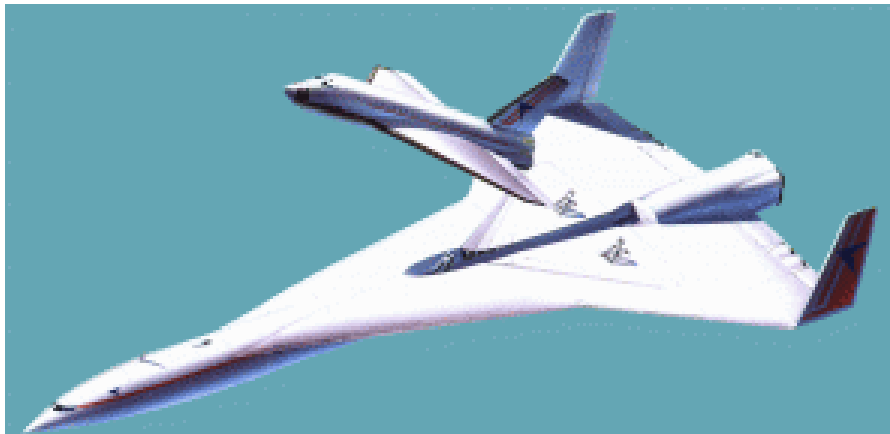
This vehicle can be used for launching satellites, transporting crew and supplies space stations.



Bristol spacebus

This vehicle is the second generation of the orbital spaceplane of the Bristol Aerospace, in particular the Spacebus is the larger version of Spacecab, doubling the MTOW, that is equal to 400 tons, and also the weight of the payload, equal to 90 tons.

The vehicle is capable to take off and land horizontally and as the spacecab has two different types of propulsion for the carrier vehicle: a first phase with jet engine and a second phase switching to rocket to accelerate or reach the altitude and the speed optimized for the functioning of the second stage.



Spaceliner

Spaceliner is a concept for a suborbital hypersonic aircraft for passengers' transport, the first stage of the Spaceliner is intended as a reusable vehicle capable of delivering heavy payloads (370 tons) into orbit. Nowadays this vehicle is under-development and is thought it could be operational in the 2040s.

The vehicle is projected to execute a vertical take-off and a horizontal landing, the system is accelerated by a total of eleven liquid rocket engines (nine for the booster stage and 2 for the passenger stage), for a total thrust of almost 20000 kN for the first stage.

The MTOW of the booster is equal to 1485 tons, with a propellant mass of 1279 tons and a wing surface equal to 1080 m².



Guess data estimation

As it has been done with the previous categories of first stages, the following relationship have been studied to find a interpolation law:

- > $MTOW = f(\text{Payload})$
- > $\text{Thrust} = f(MTOW)$
- > $PMF = f(MTOW)$
- > $\text{Wing Surface} = f(MTOW)$
- > $Isp = f(\text{Mach})$

For these relationships a linear interpolation law has been used.

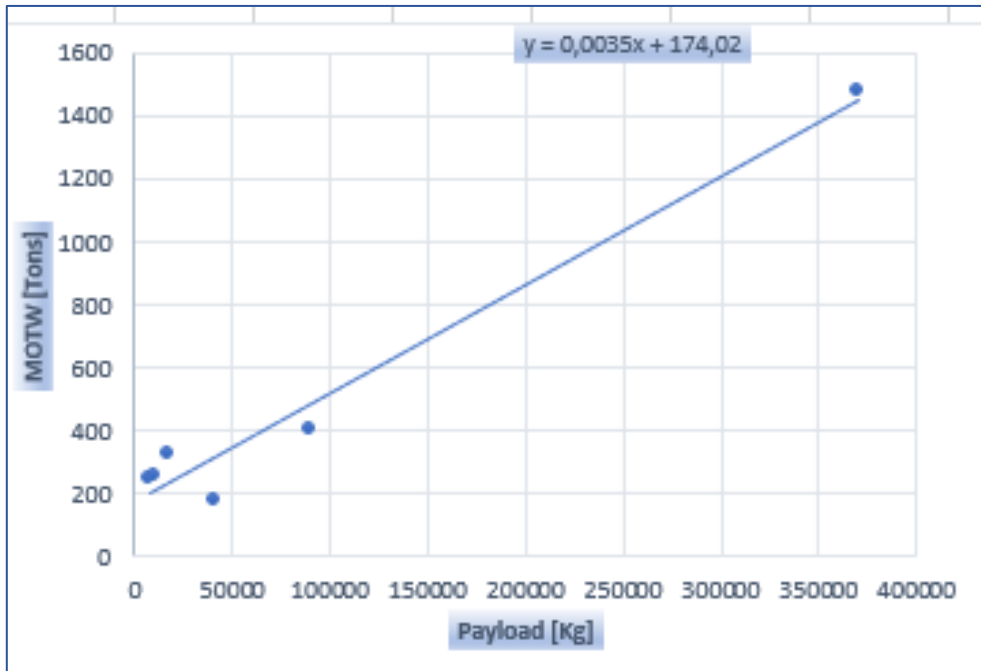


Figure 2.12

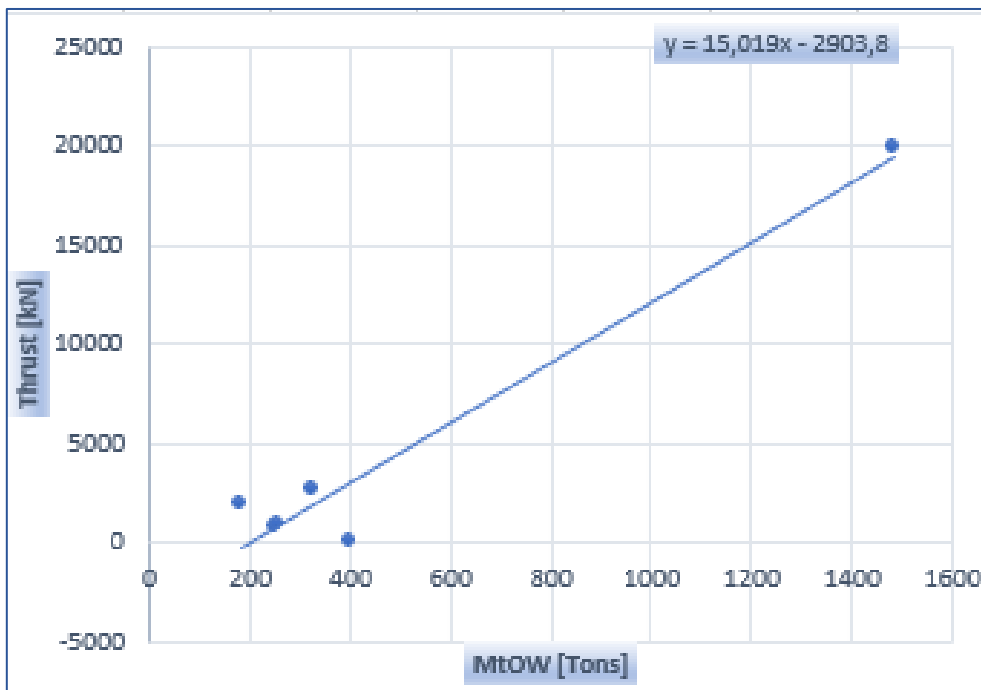


Figure 2.138

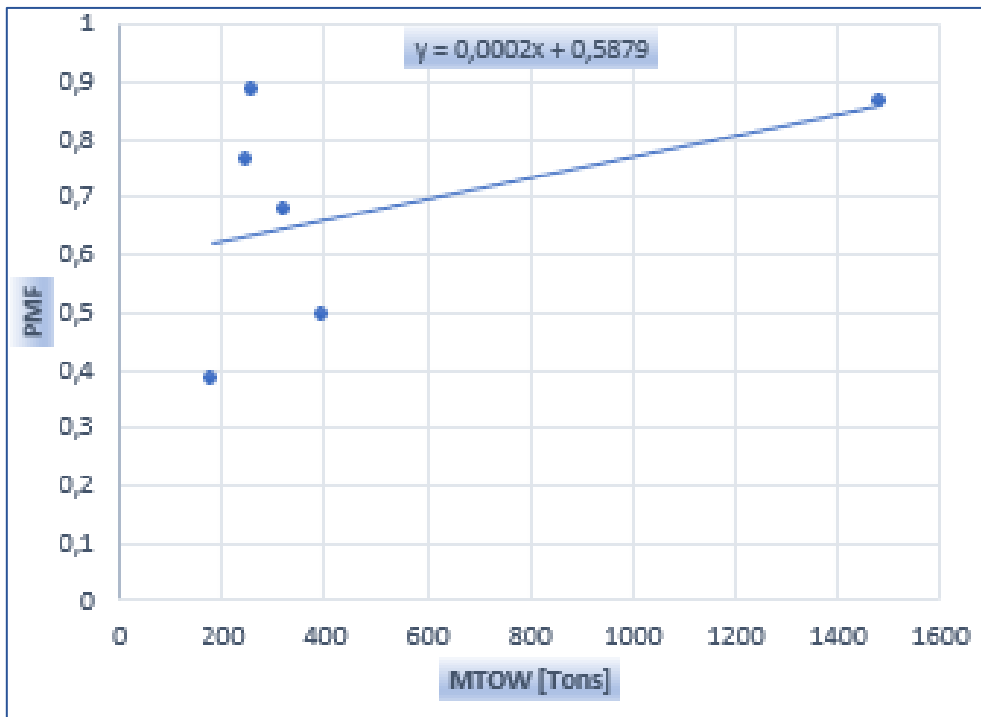


Figure 2.14

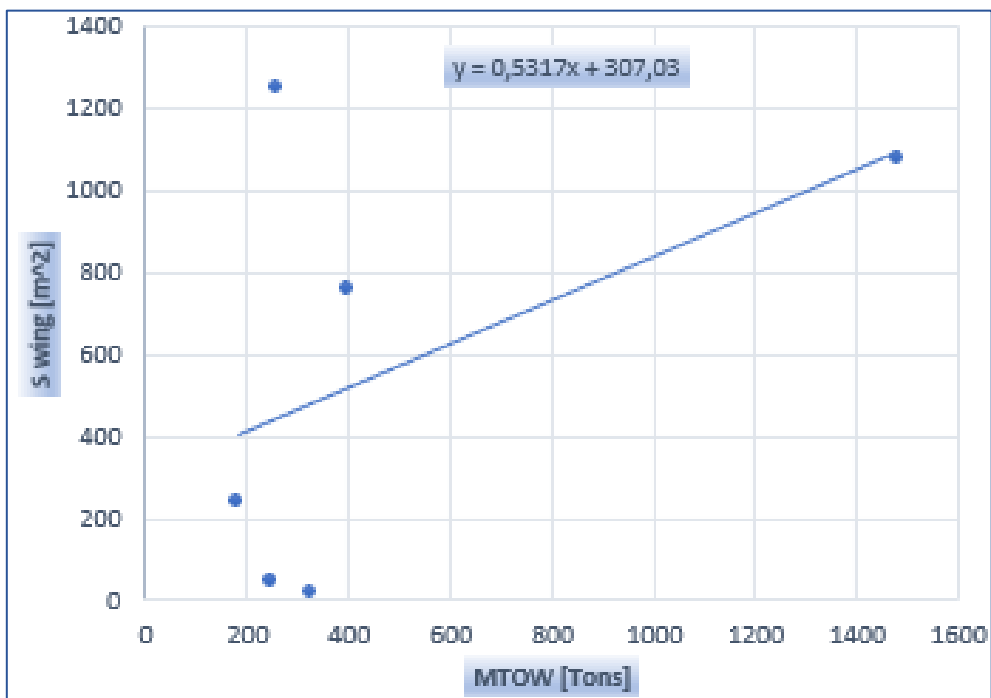


Figure 2.15

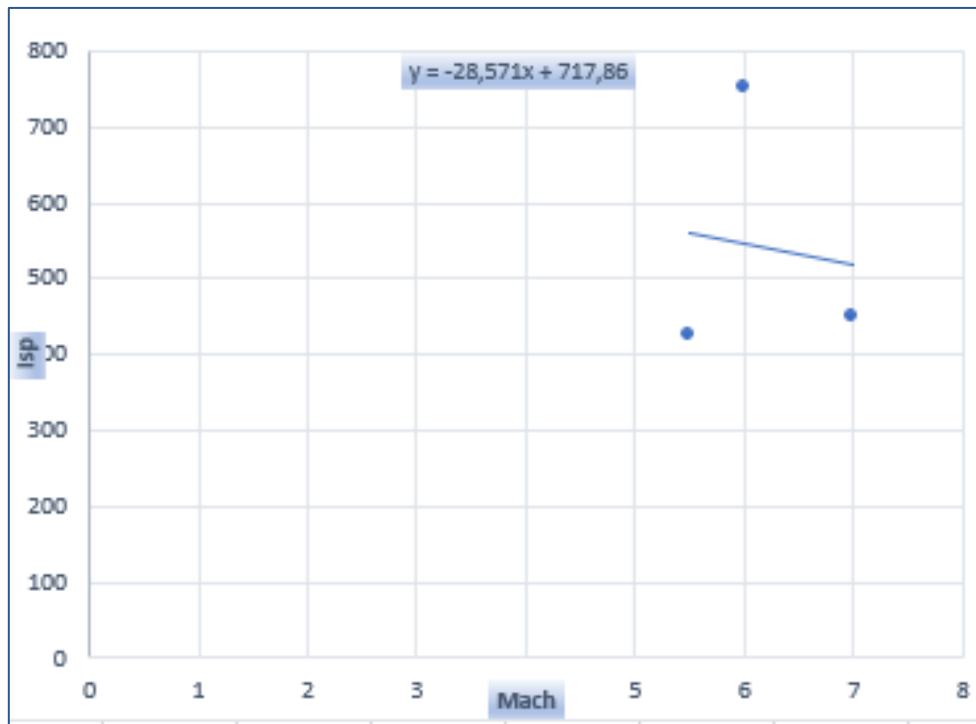


Figure 2.16

2.2 Implementation of the Matlab GUI

Once that the database has been defined, it has been given to a user, by mean of a GUI (graphic user interface), the opportunity to have as output all the guess data that serves to start the conceptual design.

The GUI has been designed in a simple mode: starting from the choice of first stage type to be used which are those examined previously (subsonic first stage, high speed first stage and rocket first stage), the user has to enter the value of payload mass of the under-development aircraft.

From this information and thanks to the interpolation law obtained in the previous work, pushing the 'CALCULATE' button the MTOW value will be calculated and from the latter also the value of wing surface, thrust and propellant mass fraction.

Selecting the checkbox called 'Set the separation Mach' the user can insert this value and then calculate from statistic the value of specific impulse.

Pushing the 'REFRESH' button all the values inserted previously and those defined by the statistical analysis will be put to zero and another calculation can be executed.

The screenshot shows a MATLAB GUI titled "Statistical analysis". It features an "INPUT" section with a dropdown menu for "First Stage type" (set to "Subsonic"), a text input for "Payload [Kg]" (value: 0), a text input for "Mach" (value: 0), and a checkbox for "Set the separation Mach" (unchecked). A black "Calculate" button is to the right. The "OUTPUT" section displays five read-only text boxes: "MTOW [Tons]" (0), "Thrust [kN]" (0), "Wing surface [m^2]" (0), "PMF" (0), and "Isp [s]" (0). A black "Refresh" button is at the bottom.

In the next lines is presented the code used for the GUI implementation:

```

1 | classdef analisisstatistica < matlab.apps.AppBase
2 |
3 |     % Properties that correspond to app components
4 |     properties (Access = public)
5 |         UIFigure                matlab.ui.Figure
6 |         StatisticalanalysisPanel  matlab.ui.container.Panel
7 |         FirstStagetypedropDownLabel  matlab.ui.control.Label
8 |         FirstStagetypedropDown      matlab.ui.control.DropDown
9 |         PayloadKgEditFieldLabel      matlab.ui.control.Label
10 |         PayloadKgEditField          matlab.ui.control.NumericEditField
11 |         INPUTLabel                  matlab.ui.control.Label
12 |         OUTPUTLabel                 matlab.ui.control.Label
13 |         MTOWTonsEditFieldLabel       matlab.ui.control.Label
14 |         MTOWTonsEditField           matlab.ui.control.NumericEditField
15 |         ThrustkNEditFieldLabel       matlab.ui.control.Label
16 |         ThrustkNEditField           matlab.ui.control.NumericEditField
17 |         Wingsurfacem2EditFieldLabel  matlab.ui.control.Label
18 |         Wingsurfacem2EditField      matlab.ui.control.NumericEditField
19 |         IspsEditFieldLabel          matlab.ui.control.Label
20 |         IspsEditField               matlab.ui.control.NumericEditField
21 |         MachEditFieldLabel           matlab.ui.control.Label
22 |         MachEditField                matlab.ui.control.NumericEditField
23 |         CalculateButton              matlab.ui.control.Button
24 |         PMFEditFieldLabel            matlab.ui.control.Label
25 |         PMFEditField                 matlab.ui.control.NumericEditField
26 |         SettheseparationMachCheckBox matlab.ui.control.CheckBox
27 |         RefreshButton                matlab.ui.control.Button
28 |         Label                         matlab.ui.control.Label
29 |     end
30 |
31 |     methods (Access = private)
32 |
33 |         % Button pushed function: CalculateButton
34 |         function CalculateButtonPushed(app, event)
35 |             if (strcmp(app.FirstStagetypedropDown.Value, 'Subsonic'))
36 |
37 |                 if app.MachEditField.Value > 1
38 |                     app.Label.Text = 'Subsonic first stage, the mach must be <1';
39 |                 else
40 |
41 |                     payload = app.PayloadKgEditField.Value;
42 |
43 |                     mtow = 119.22 * log(payload) - 898.61;
44 |                     app.MTOWTonsEditField.Value = mtow;
45 |                     app.MTOWTonsEditField.BackgroundColor = 'w';
46 |
47 |                     thrust = 2.2453 * mtow + 50.285;
48 |                     app.ThrustkNEditField.Value = thrust;
49 |                     app.ThrustkNEditField.BackgroundColor = 'w';
50 |
51 |                     Swing = 1.6612 * mtow + 192.2;

```

```

52 -         app.Wingsurfacem2EditField.Value=Swing;
53 -         app.Wingsurfacem2EditField.BackgroundColor='w';
54
55 -         pmf=0.0007*mtow+0.2292;
56 -         app.PMFEditField.Value=pmf;
57 -         app.PMFEditField.BackgroundColor='w';
58
59 -         mach=app.MachEditField.Value;
60 -         isp=439.29*mach+1228.6; %ricontrollare la formula
61 -         app.IspsEditField.Value=isp;
62
63 -     end
64
65 - else if (strcmp(app.FirstStagetypeDropDown.Value,'High speed (airbreathing
66
67 -     if app.MachEditField.Value<1
68 -         app.Label.Text='Supersonic first stage, the mach must be >1';
69 -     else
70
71 -         payload=app.PayloadKgEditField.Value;
72
73 -         mtow=0.0015*payload+251.43;
74 -         app.MTOWTonsEditField.Value=mtow;
75 -         app.MTOWTonsEditField.BackgroundColor='w';
76
77 -         thrust=4.8788*mtow-245.29;
78 -         app.ThrustkNEditField.Value=thrust;
79 -         app.ThrustkNEditField.BackgroundColor='w';
80
81 -         Swing=3.4835*mtow-325.15;
82 -         app.Wingsurfacem2EditField.Value=Swing;
83 -         app.Wingsurfacem2EditField.BackgroundColor='w';
84
85 -         pmf=-0.0004*mtow+0.6187;
86 -         app.PMFEditField.Value=pmf;
87 -         app.PMFEditField.BackgroundColor='w';
88
89 -         mach=app.MachEditField.Value;
90 -         isp=439.29*mach+1228.6; %ricontrollare la formula
91 -         app.IspsEditField.Value=isp;
92
93 -     end
94
95 - else if (strcmp(app.FirstStagetypeDropDown.Value,'High speed (rocket)'))
96
97 -     if app.MachEditField.Value<1
98 -         app.Label.Text='Supersonic first stage, the mach must be >1';
99 -     else
100
101 -         payload=app.PayloadKgEditField.Value;
102

```

```

103 -         mtow=0.0035*payload+174.02;
104 -         app.MTOWTonsEditField.Value=mtow;
105 -         app.MTOWTonsEditField.BackgroundColor='w';
106 -
107 -         thrust=15.019*mtow-2903.8;
108 -         app.ThrustkNEditField.Value=thrust;
109 -         app.ThrustkNEditField.BackgroundColor='w';
110 -
111 -         Swing=0.5317*mtow+307.03;
112 -         app.Wingsurfacem2EditField.Value=Swing;
113 -         app.Wingsurfacem2EditField.BackgroundColor='w';
114 -
115 -         pmf=0.0002*mtow+0.5879;
116 -         app.PMFEEditField.Value=pmf;
117 -         app.PMFEEditField.BackgroundColor='w';
118 -
119 -         mach=app.MachEditField.Value;
120 -         isp=439.29*mach+1228.6; %ricontrollare la formula
121 -         app.IspsEditField.Value=isp;
122 -
123 -         end
124 -
125 -     end
126 - end
127 -
128 -
129 -
130 - end
131 -
132 - % Button pushed function: RefreshButton
133 - function RefreshButtonPushed(app, event)
134 -     app.FirstStagetypeDropDown.Value='Subsonic';
135 -     app.PayloadKgEditField.Value=0;
136 -     app.MTOWTonsEditField.Value=0;
137 -     app.ThrustkNEditField.Value=0;
138 -     app.Wingsurfacem2EditField.Value=0;
139 -     app.PMFEEditField.Value=0;
140 -     app.MTOWTonsEditField.BackgroundColor=[0.8 0.8 0.8];
141 -     app.ThrustkNEditField.BackgroundColor=[0.8 0.8 0.8];
142 -     app.Wingsurfacem2EditField.BackgroundColor=[0.8 0.8 0.8];
143 -     app.PMFEEditField.BackgroundColor=[0.8 0.8 0.8];
144 -     app.MachEditField.Enable='off';
145 -     app.IspsEditField.Enable='off';
146 -     app.Label.Text='';
147 -     app.SettheseperationMachCheckBox.Value=0;
148 -     app.MachEditField.Value=0;
149 - end
150 -
151 - % Value changed function: SettheseperationMachCheckBox
152 - function SettheseperationMachCheckBoxValueChanged(app, event)
153 -     value = app.SettheseperationMachCheckBox.Value;
154 -     if value==1

```

```

155 -         app.MachEditField.Enable='on';
156 -         app.IspsEditField.Enable='on';
157
158 -     else
159 -         app.MachEditField.Enable='off';
160 -         app.IspsEditField.Enable='off';
161 -         app.MachEditField.Value=0;
162
163
164 -     end
165 - end
166
167
168 % App initialization and construction
169 methods (Access = private)
170
171 % Create UIFigure and components
172 function createComponents(app)
173
174 % Create UIFigure
175 - app.UIFigure = uifigure;
176 - app.UIFigure.Position = [100 100 640 480];
177 - app.UIFigure.Name = 'UI Figure';
178
179 % Create StatisticalanalysisPanel
180 - app.StatisticalanalysisPanel = uipanel(app.UIFigure);
181 - app.StatisticalanalysisPanel.TitlePosition = 'centertop';
182 - app.StatisticalanalysisPanel.Title = 'Statistical analysis';
183 - app.StatisticalanalysisPanel.BackgroundColor = [0.9412 0.9412 0.9412];
184 - app.StatisticalanalysisPanel.FontWeight = 'bold';
185 - app.StatisticalanalysisPanel.Position = [15 35 610 423];
186
187 % Create FirstStagetypDropDownLabel
188 - app.FirstStagetypDropDownLabel = uilabel(app.StatisticalanalysisPanel);
189 - app.FirstStagetypDropDownLabel.HorizontalAlignment = 'right';
190 - app.FirstStagetypDropDownLabel.Position = [180 356 89 15];
191 - app.FirstStagetypDropDownLabel.Text = 'First Stage type';
192
193 % Create FirstStagetypDropDown
194 - app.FirstStagetypDropDown = uidropdown(app.StatisticalanalysisPanel);
195 - app.FirstStagetypDropDown.Items = {'Subsonic', 'High speed (airbreathing e
196 - app.FirstStagetypDropDown.Position = [284 356 147 18];
197 - app.FirstStagetypDropDown.Value = 'Subsonic';
198
199 % Create PayloadKgEditFieldLabel
200 - app.PayloadKgEditFieldLabel = uilabel(app.StatisticalanalysisPanel);
201 - app.PayloadKgEditFieldLabel.HorizontalAlignment = 'right';
202 - app.PayloadKgEditFieldLabel.Position = [87 289 74 15];
203 - app.PayloadKgEditFieldLabel.Text = 'Payload [Kg]';
204

```

```

205 % Create PayloadKgEditField
206 - app.PayloadKgEditField = uieditfield(app.StatisticalanalysisPanel, 'numeric'
207 - app.PayloadKgEditField.ValueDisplayFormat = '%.0f';
208 - app.PayloadKgEditField.Position = [176 285 100 22];
209
210 % Create INPUTLabel
211 - app.INPUTLabel = uilabel(app.StatisticalanalysisPanel);
212 - app.INPUTLabel.FontWeight = 'bold';
213 - app.INPUTLabel.Position = [18 275 41 15];
214 - app.INPUTLabel.Text = 'INPUT';
215
216 % Create OUTPUTLabel
217 - app.OUTPUTLabel = uilabel(app.StatisticalanalysisPanel);
218 - app.OUTPUTLabel.FontWeight = 'bold';
219 - app.OUTPUTLabel.Position = [300 220 54 15];
220 - app.OUTPUTLabel.Text = 'OUTPUT';
221
222 % Create MTOWTonsEditFieldLabel
223 - app.MTOWTonsEditFieldLabel = uilabel(app.StatisticalanalysisPanel);
224 - app.MTOWTonsEditFieldLabel.HorizontalAlignment = 'right';
225 - app.MTOWTonsEditFieldLabel.Position = [185 187 77 15];
226 - app.MTOWTonsEditFieldLabel.Text = 'MTOW [Tons]';
227
228 % Create MTOWTonsEditField
229 - app.MTOWTonsEditField = uieditfield(app.StatisticalanalysisPanel, 'numeric'
230 - app.MTOWTonsEditField.Editable = 'off';
231 - app.MTOWTonsEditField.BackgroundColor = [0.8 0.8 0.8];
232 - app.MTOWTonsEditField.Position = [277 183 100 22];
233
234 % Create ThrustkNEditFieldLabel
235 - app.ThrustkNEditFieldLabel = uilabel(app.StatisticalanalysisPanel);
236 - app.ThrustkNEditFieldLabel.HorizontalAlignment = 'right';
237 - app.ThrustkNEditFieldLabel.Position = [199 154 63 15];
238 - app.ThrustkNEditFieldLabel.Text = 'Thrust [kN]';
239
240 % Create ThrustkNEditField
241 - app.ThrustkNEditField = uieditfield(app.StatisticalanalysisPanel, 'numeric'
242 - app.ThrustkNEditField.Editable = 'off';
243 - app.ThrustkNEditField.BackgroundColor = [0.8 0.8 0.8];
244 - app.ThrustkNEditField.Position = [277 150 100 22];
245
246 % Create Wingsurfacem2EditFieldLabel
247 - app.Wingsurfacem2EditFieldLabel = uilabel(app.StatisticalanalysisPanel);
248 - app.Wingsurfacem2EditFieldLabel.HorizontalAlignment = 'right';
249 - app.Wingsurfacem2EditFieldLabel.Position = [154 119 108 15];
250 - app.Wingsurfacem2EditFieldLabel.Text = 'Wing surface [m^2]';
251
252 % Create Wingsurfacem2EditField
253 - app.Wingsurfacem2EditField = uieditfield(app.StatisticalanalysisPanel, 'num
254 - app.Wingsurfacem2EditField.Editable = 'off';

```

```

255 -     app.Wingsurfacem2EditField.BackgroundColor = [0.8 0.8 0.8];
256 -     app.Wingsurfacem2EditField.Position = [277 115 100 22];
257
258     % Create IspsEditFieldLabel
259 -     app.IspsEditFieldLabel = uilabel(app.StatisticalanalysisPanel);
260 -     app.IspsEditFieldLabel.BackgroundColor = [0.9412 0.9412 0.9412];
261 -     app.IspsEditFieldLabel.HorizontalAlignment = 'right';
262 -     app.IspsEditFieldLabel.Enable = 'off';
263 -     app.IspsEditFieldLabel.Position = [226 49 36 15];
264 -     app.IspsEditFieldLabel.Text = 'Isp [s]';
265
266     % Create IspsEditField
267 -     app.IspsEditField = uieditfield(app.StatisticalanalysisPanel, 'numeric');
268 -     app.IspsEditField.Editable = 'off';
269 -     app.IspsEditField.BackgroundColor = [0.8 0.8 0.8];
270 -     app.IspsEditField.Enable = 'off';
271 -     app.IspsEditField.Position = [277 45 100 22];
272
273     % Create MachEditFieldLabel
274 -     app.MachEditFieldLabel = uilabel(app.StatisticalanalysisPanel);
275 -     app.MachEditFieldLabel.HorizontalAlignment = 'right';
276 -     app.MachEditFieldLabel.Enable = 'off';
277 -     app.MachEditFieldLabel.Position = [125 258 35 15];
278 -     app.MachEditFieldLabel.Text = 'Mach';
279
280     % Create MachEditField
281 -     app.MachEditField = uieditfield(app.StatisticalanalysisPanel, 'numeric');
282 -     app.MachEditField.Enable = 'off';
283 -     app.MachEditField.Position = [175 254 100 22];
284
285     % Create CalculateButton
286 -     app.CalculateButton = uibutton(app.StatisticalanalysisPanel, 'push');
287 -     app.CalculateButton.ButtonPushedFcn = createCallbackFcn(app, @CalculateButt
288 -     app.CalculateButton.BackgroundColor = [0.149 0.149 0.149];
289 -     app.CalculateButton.FontWeight = 'bold';
290 -     app.CalculateButton.FontColor = [1 1 1];
291 -     app.CalculateButton.Position = [472 258 110 46];
292 -     app.CalculateButton.Text = 'Calculate';
293
294     % Create PMFEditFieldLabel
295 -     app.PMFEditFieldLabel = uilabel(app.StatisticalanalysisPanel);
296 -     app.PMFEditFieldLabel.HorizontalAlignment = 'right';
297 -     app.PMFEditFieldLabel.Position = [233 83 30 15];
298 -     app.PMFEditFieldLabel.Text = 'PMF';
299
300     % Create PMFEditField
301 -     app.PMFEditField = uieditfield(app.StatisticalanalysisPanel, 'numeric');
302 -     app.PMFEditField.Editable = 'off';
303 -     app.PMFEditField.BackgroundColor = [0.8 0.8 0.8];
304 -     app.PMFEditField.Position = [278 79 100 22];
305

```

```

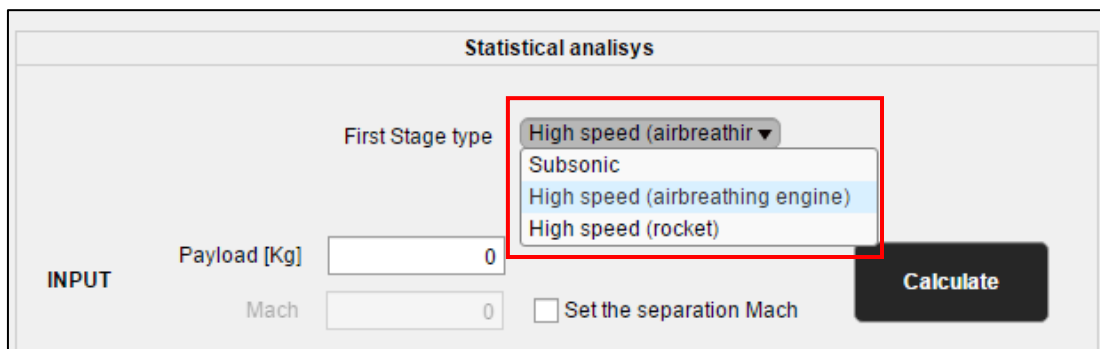
306         % Create SettheseparationMachCheckBox
307 -       app.SettheseparationMachCheckBox = ucheckbox(app.StatisticalanalysisPanel);
308 -       app.SettheseparationMachCheckBox.ValueChangedFcn = createCallbackFcn(app, @S
309 -       app.SettheseparationMachCheckBox.Text = 'Set the separation Mach';
310 -       app.SettheseparationMachCheckBox.Position = [292 258 154 15];
311
312         % Create RefreshButton
313 -       app.RefreshButton = uibutton(app.StatisticalanalysisPanel, 'push');
314 -       app.RefreshButton.ButtonPushedFcn = createCallbackFcn(app, @RefreshButtonPu
315 -       app.RefreshButton.BackgroundColor = [0.149 0.149 0.149];
316 -       app.RefreshButton.FontWeight = 'bold';
317 -       app.RefreshButton.FontColor = [1 1 1];
318 -       app.RefreshButton.Position = [277 8 100 22];
319 -       app.RefreshButton.Text = 'Refresh';
320
321         % Create Label
322 -       app.Label = uilabel(app.StatisticalanalysisPanel);
323 -       app.Label.FontSize = 10;
324 -       app.Label.FontColor = [1 0 0];
325 -       app.Label.Position = [176 240 280 15];
326 -       app.Label.Text = '';
327 -       end
328     end
329
330     methods (Access = public)
331
332         % Construct app
333         function app = analisisstatistica
334
335             % Create and configure components
336 -           createComponents(app)
337
338             % Register the app with App Designer
339 -           registerApp(app, app.UIFigure)
340
341 -           if nargin == 0
342 -               clear app
343 -           end
344 -       end
345
346         % Code that executes before app deletion
347         function delete(app)
348
349             % Delete UIFigure when app is deleted
350 -           delete(app.UIFigure)
351 -       end
352     end
353 end

```

2.3 Example of GUI's use

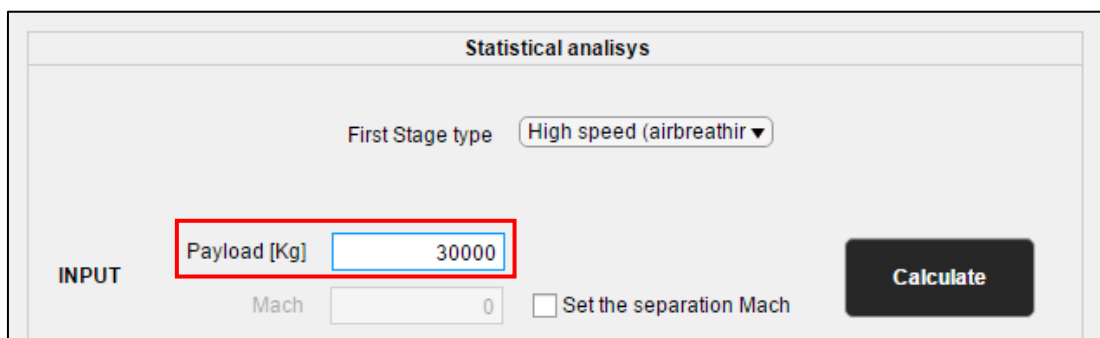
In this section a simple example of the use of the Graphic User Interface will be shown, in particular the guess data for high speed first stage with air-breathing engine will be defined.

First of all the user should choose the type of first stage to use in the project, as it has been said it will be an high speed for our case of interest, once that “High speed (airbreathing engine)” has been selected the alghoritm will take into consideration exclusively the high speed database excluding those that use the rocket.



The screenshot shows a window titled "Statistical analysis" with an "INPUT" section. The "First Stage type" dropdown menu is open, showing four options: "High speed (airbreathir", "Subsonic", "High speed (airbreathing engine)", and "High speed (rocket)". The "High speed (airbreathing engine)" option is highlighted. Below the dropdown, there are input fields for "Payload [Kg]" (value 0) and "Mach" (value 0), and a checkbox labeled "Set the separation Mach". A "Calculate" button is located to the right.

The next step is to set the payload that the under-project aircraft should host, that value should be insert in the proper box in kilograms, for this example a payload of 30000 kg will be used:



The screenshot shows the same "Statistical analysis" window. The "First Stage type" dropdown is now closed and shows "High speed (airbreathir". The "Payload [Kg]" input field is highlighted with a red box and contains the value "30000". The "Mach" input field still shows "0". The "Set the separation Mach" checkbox is unchecked. The "Calculate" button is visible on the right.

In the GUI it is possible to insert the value of separation mach that is supposed to be the maximum mach that the first stage will reach, in order to do that it is necessary to insert a tick in the checkbox, in this way the box will be editable and the user can insert the value, in our case it will be Mach 4:

Example of GUI's use

Statistical analysis

First Stage type High speed (airbreathir ▼)

INPUT

Payload [Kg] 30000

Mach 4 Set the separation Mach

Calculate

As it has been explained in the database development section, from the value of the payload thanks to the statistical analysis the value of the MTOW will be available and from the latter also the value of the thrust, the PMF and the wing surface, while from the value of Mach, the value of Isp will be known.

By means of the button “Calculate” the results are shown in the GUI:

Statistical analysis

First Stage type High speed (airbreathir ▼)

INPUT

Payload [Kg] 30000

Mach 4 Set the separation Mach

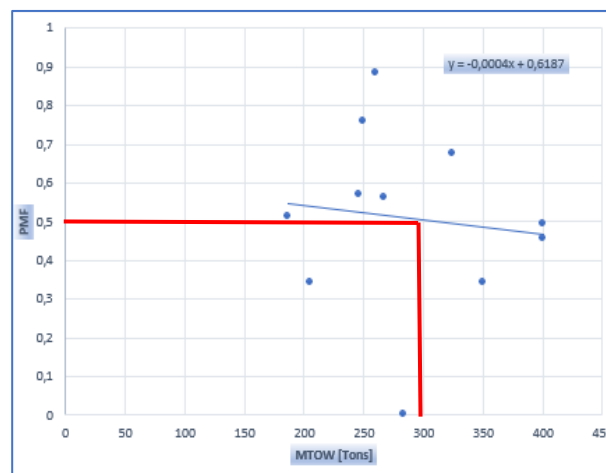
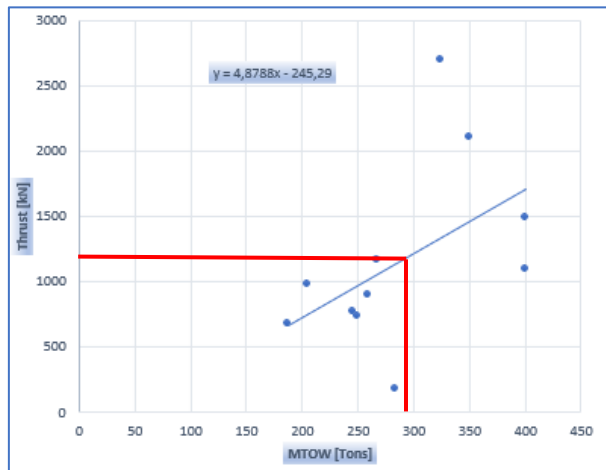
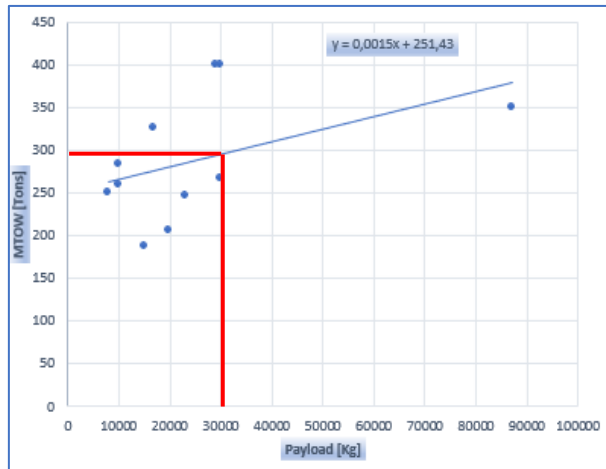
Calculate

OUTPUT

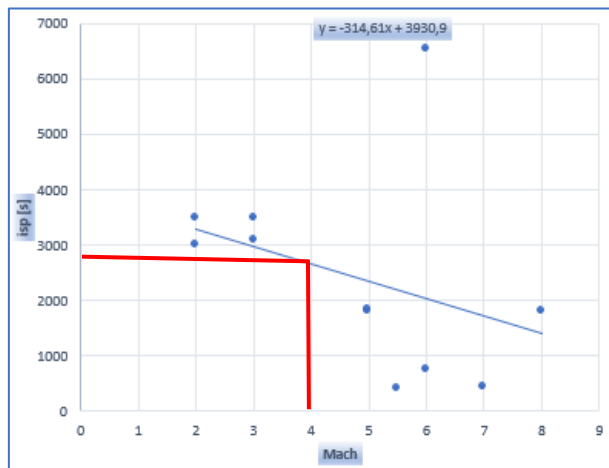
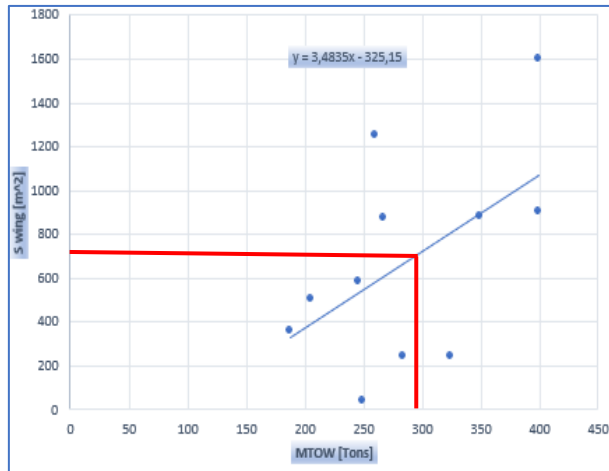
MTOW [Tons]	296.4
Thrust [kN]	1201
Wing surface [m ²]	707.5
PMF	0.5001
Isp [s]	2986

Refresh

Example of GUI's use



Example of GUI's use



Chapter 3

3.1 Iteration logic

In this section the overall calculation to define the matching chart for the first and the second stage is presented thanks to a block diagram.

The calculation starts from the definition of the payload weight and the coefficients connected to both the stages, the first iteration concern the second stage and the calculation of its weight, the latter will be an input for the evaluation of the first stage weight.

Known the weight of the overall TSTO, thanks to the user input regards the mission phases, all the requirements are calculated, firstly for the first stage and secondly for the second stage, until the definition of the design point.

The iteration will continue until five constrains are fulfil: the planform surface both of the first and the second stage must will be higher than the wing surface plus a contribution defined as a percentage of the wing surface, the total volume of the second stage must be higher than the propellant volume needed plus a contribution defined as a percentage of the propellant volume, and lastly, both the value of first stage and second stage Thrust, supposed at the beginning of the calculation to a first iteration value, must meet the design point.

3.2 Matching Chart Analysis

The Matching chart is as the final goal of the conceptual design phase and it assess the feasibility of the mission's completion and the achievement of the vehicle's operational and technical targets so it can be defined as a verification instrument.

The Matching chart was firstly developed by NASA and it is presented as a 2D graph with the value of the Thrust-to-weight ratio on the y-axes and the value of the wing loading on the x-axes so that through this instrument the feasible design space can be highlighted and in it the design point can be chosen taking into account the optimal configuration in terms of Maximum Thrust, Maximum Take-off Mass and Wing Surface for the meeting of all the high level requirements.

To complete the matching chart the user needs to have initial aerodynamic knowledges such as the landing lift coefficient, the take-off lift coefficient or the efficiency which are necessary to define the requirements as it can be seen from the figure below:

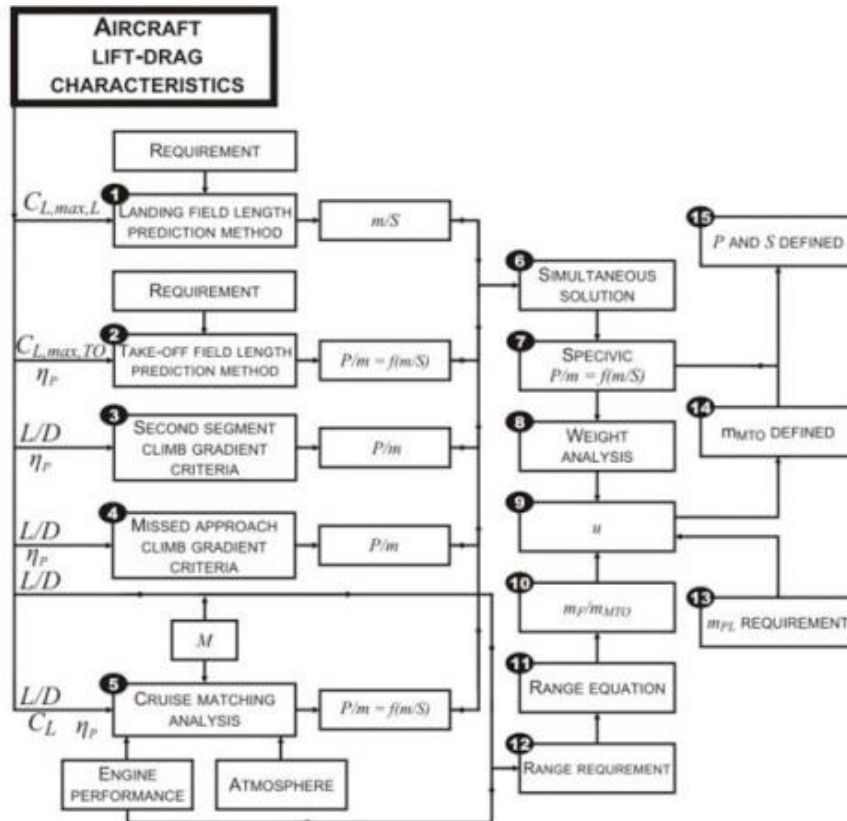


Figure 3.1

Starting from the aircraft lift-drag characteristics all the high-level requirements are calculated thanks to flight mechanics equations. The output of the requirements boxes are horizontal/vertical lines or curves which tie the T/W value to the W/S value.

Once defined the curve for each requirement the design space can be identified as the part of the graph characterized by T/W higher than the most stringent requirement and with W/S lower than the most stringent requirement, in particular the design point is located where the minimum Thrust-to-Weight ratio is reached, coupled with consistent Wing Loading value.

3.3 TSTO Mission Profile

The determination of a mission profile is the starting point for the definition of the requirements that the aircraft should accomplish, in the case of a TSTO of our interest the general mission profile is similar to that shown in the figure hereunder.

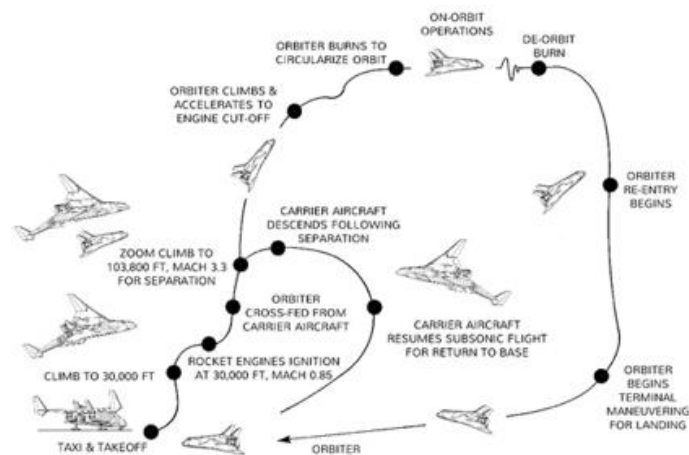


Figure 3.2

The vehicle's mission starts with the take-off from the launch site with a subsequent ascent to reach an altitude, called Separation Altitude, where after a brief cruise the first stage separates from the second stage.

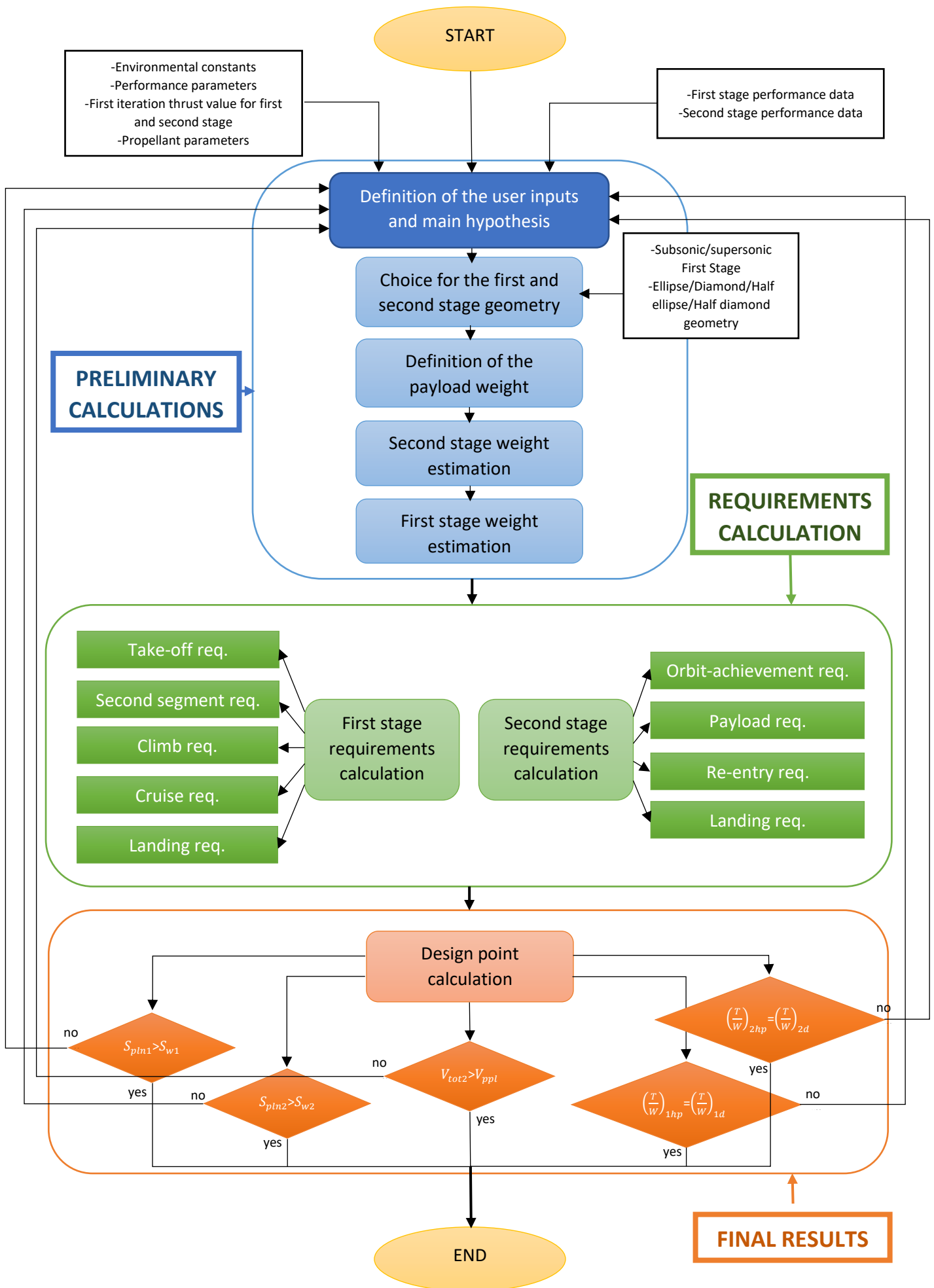
After the separation the first stage starts its descent and then its landing, on the contrary the second stage continues the ascent to reach the target orbit and after completed the on-orbit operation start the de-orbit, afterwards it proceeds with the re-entry into the atmosphere and then completes the descent and the landing.

The requirements that will be analysed are different on the base of the first and the second stage, concerning the first stage the main requirements for the mission presented above are:

- Take-off requirement
- Second segment requirement
- Climb requirement
- Cruise requirement
- Landing requirement

On the other hand, the main requirements for the second stage of the TSTO are:

- Orbit-reaching requirement
- Payload requirement
- Re-entry requirement
- Landing requirement



3.4 Weight analysis

In this chapter the iteration to define both the first stage and the second stage weight to start all the calculations needed in the definition of the matching chart will be analysed.

In the weight estimation two different types of calculation will be analysed, the first for the case of TSTO with subsonic first stage and the second for the case of TSTO with supersonic first stage, so that the case of subsonic and supersonic separation will be taken into account.

3.4.1 Subsonic first stage weight estimation

Starting from a weight value of first iteration and supposed the payload weight that will be put into orbit in addition to the length of the first and the second stage, the analysis will bring to the evaluation of a convergence point thanks to the following equations.

The subsequent analysis will be used in consequence to the second stage weight estimation, in fact, the latter value will be equal to the payload weight of the first stage.

The total weight is evaluated as the sum of the following three terms:

$$W_{TO} = W_{payload} + W_{fuel} + OEW$$

Each of these terms can be broken down into the several contributions, for example the payload weight is composed by the sum of the dropped payload and the passengers weight which in turn is calculated by the product of the single passenger weight and the number of passenger:

$$W_{payload} = W_{passengers} + W_{dropped\ payload}$$

$$W_{passengers} = n_{passengers} W_{single\ passenger}$$

The fuel weight for the first stage is calculated taking into account the take off phase, included the taxi phase, and the fuel for the climb and the cruise phases, as well as for descent and landing, moreover it will count also an additional contribution for safety reasons.

The last contribution is the operative empty weight that is composed by six terms:

$$OEW = W_{wing} + W_{tail} + W_{fuselage} + W_{installed\ engine} + W_{gear} + W_{systems}$$

Each of them can be calculated thanks to the following equations:

$$W_{wing} = \left[MTOW \frac{\lambda}{1000} (1 - 0.35K_{composite}) K_{delta\ con} \right]$$

$$W_{tail} = W_{wing} K_{tail}$$

$$W_{fuselage} = \left(0.002 \frac{MTOW}{1000} + 0.8 \right) \left[MTOW \frac{L_{fus}}{1000} n_{fus} (1 - 0.35K_{composite}) K_{delta\ con} \right]$$

$$W_{installed\ engine} = n_{engines} W_{single\ engine} K_{installation}$$

$$W_{gear} = MTOW \frac{K_{gear}}{1000}$$

$$W_{systems} = W_{fc} + W_{hyd} + W_{electrical} + W_{fuel\ sys} + W_{ecs} + W_{av} + W_{engsys} + W_{furn}$$

$$W_{systems} = MOTW (K_{fc} + K_{hyd} + K_{el} + K_{fuel\ sys} + K_{ecs} + K_{av} + K_{engsys} + K_{furn})$$

For a better comprehension of the weight break-down of the subsonic first stage, refer to the diagram below.

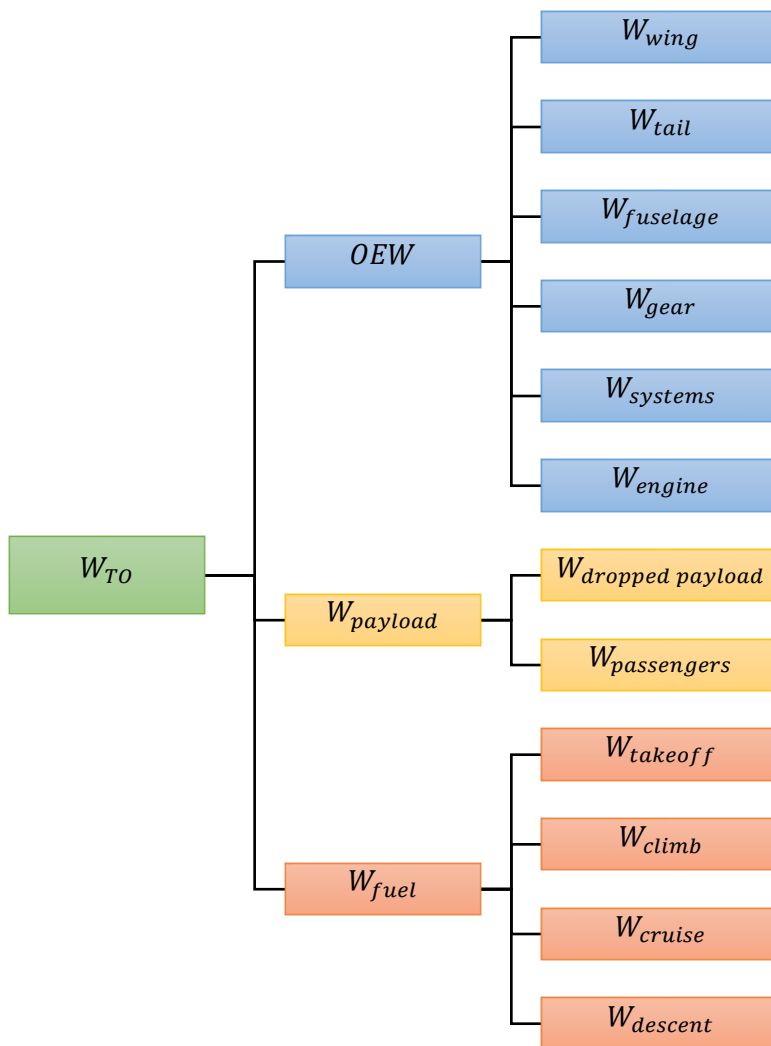


Figure 3,3

As it can be seen in these equations there are many coefficients that must be chosen by the user on the base of the used technology. Here below the guidelines to evaluate them are presented:

- K composite = 0.2 composite skin only
0.85 composite skin and some structure component
1 all composite (skin and structure)
- K delta configuration = 0.9 for delta configuration
1 if not
- K tail = from 0.1 to 0.3 (value proportional to tail dimension)

- K installation = 1.25
- K gear = from 2.2 (fixed gear) to 4.5 (high complexity gear)
- K flight control system = from 0.015 to 0.04 depending by complexity
- K hydraulic system = from 0.005 to 0.03 depending by complexity
- K electric system = from 0.02 to 0.04 depending by complexity
- K fuel system = from 0.015 to 0.02 depending by complexity (number of engines, afterburner, ...)
- K air conditioning = from 0.005 to 0.07 depending by complexity (number of passengers)
- K avionic system = from 0.03 to 0.06 depending by complexity
- K engine system = from 0.005 to 0.015 depending by complexity
- K furnishing system = from 0.005 to 0.04 depending by complexity (number of passengers)
- K secondary fuel = from 0.05 to 0.2 depending by complexity

3.4.2 Supersonic first and second stage weight estimation

For the supersonic and hypersonic first stage, as well as for the second stage, the VDK sizing approach will be used as iterative method of calculation. The main equation that will drive the evaluation of the stage weight is the following:

$$W_{oe} = (1 + \mu_a)(W_{str} + W_{eng} + W_{sys} + W_{crew\ prov})$$

Where the main terms of weight can be expressed as:

$$W_{str} = I_{str}K_W S_{pln} + W_{cprv}$$

$$W_{sys} = C_{sys} + f_{sys}W_{oe}$$

$$C_{sys} = C_{un} + f_{mnd}N_{crew}$$

$$W_{eng} = \frac{TW_0W_R}{E_{TW}}(W_{pay} + W_{crw} + W_{oe})$$

$$W_{cprv} = f_{cprv}N_{crew}$$

$$W_{crew} = f_{crew}N_{crew}$$

Even for this method there are many parameters that must be defined, in particular, their value range are expressed here below:

$$17 \leq I_{str} \leq 21 \text{ kg/m}^2$$

$$1.9 \leq C_{un} \leq 2.1 \text{ ton}$$

$$1.15 \leq f_{mnd} \leq 0.95 \frac{\text{ton}}{\text{person}}$$

$$0.16 \leq f_{sys} \leq 0.05 \frac{\text{ton}}{\text{person}}$$

$$0.06 \leq k_{sup} \leq 0.05 \frac{\text{ton}}{\text{person}}$$

$$0.21 \leq f_{cprv} \leq 0.22 \frac{\text{ton}}{\text{person}}$$

$$0.14 \leq f_{crew} \leq 0.15 \frac{\text{ton}}{\text{person}}$$

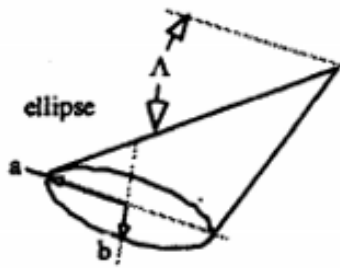
The choice of these values is related to prospective of the project: for current application the higher value will be chosen while for future applications a lower value is considered.

Once made explicit the weight parameters, the W_{oe} can be rewritten:

$$W_{oe} = \frac{I_{str}K_W S_{pln} + C_{sys} + W_{cprv} + \frac{TW_0W_R}{E_{TW}}(W_{pay} + W_{crw} + W_{oe})}{\left[\left(\frac{1}{1 + \mu_a}\right) - f_{sys} - \frac{TW_0W_R}{E_{TW}}\right]}$$

Here the value of $\left(\frac{1}{1+\mu_a}\right) - f_{sys}$ can be supposed to be between 0.63 and 0.71 in relation to the technology advancement, while the value of $\frac{TW_0WR}{E_{TW}}$ will be of order of magnitude of tenths for the first stage and of hundredths for the second stage as consequence of the value of E_{TW} that is estimated to be between 5 and 15 kg/kg for the first stage and about between 70 and 80 kg/kg for the second stage, always in relation to the technological improvement.

In this form it is visible that the main parameters of this equation are both propulsion and geometric terms, in particular $K_W = \frac{S_{wet}}{S_{pln}}$ where both the values of surface depends on the configuration type, here below are reported the main solutions which are ellipse diamond, half-ellipse, half-diamond:

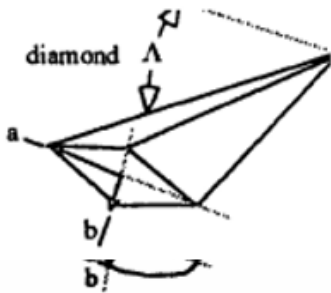


$$S_{pln} = a^2 \tan \Delta$$

$$S_{wet} = \pi a^2 \frac{(1+e)}{\cos \Delta} \left(1 + \frac{R^2}{4} + \frac{R^4}{64} + \frac{R^6}{256}\right) + \pi a^2 e$$

$$V_{tot} = \frac{\pi a^3 e}{3} \tan \Delta$$

$$e = \frac{b}{a} \quad R = \frac{1-e}{1+e}$$

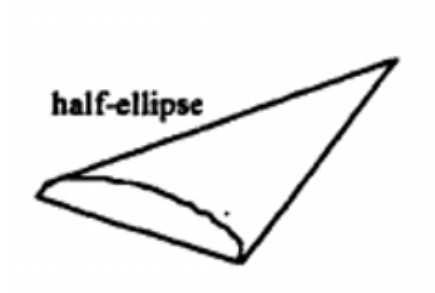


$$S_{pln} = a^2 \tan \Delta$$

$$S_{wet} = 2a^2 \sqrt{1+e^2} \tan \Delta + 2a^2 e$$

$$V_{tot} = \frac{2a^3 e}{3} \tan \Delta$$

$$e = \frac{b}{a}$$

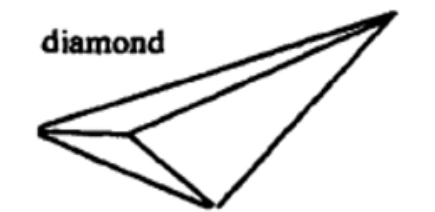


$$S_{pln} = a^2 \tan \Lambda$$

$$S_{wet} = \frac{\pi a^2}{2} \left[\frac{(1+e)}{\cos \Lambda} \left(1 + \frac{R^2}{4} + \frac{R^4}{64} + \frac{R^6}{256} \right) + e \right] + S_{pln}$$

$$V_{tot} = \frac{\pi a^3 e}{6} \tan \Lambda$$

$$e = \frac{b}{a} \quad R = \frac{1-e}{1+e}$$



$$S_{pln} = a^2 \tan \Lambda$$

$$S_{wet} = a^2 (\sqrt{1 + e^2} \tan \Lambda + e) + S_{pln}$$

$$V_{tot} = \frac{a^3 e}{6} \tan \Lambda$$

$$e = \frac{b}{a}$$

Figure 3.4

Once calculated the value of W_{oe} , the value of the take-off weight can be found, in fact the latter is defined by the sum of the overall empty weight the payload weight and the propellant weight:

$$W_{TO} = W_{oe} + W_{payload} + W_{ppl}$$

Chapter 4

4.1 First Stage Requirements

Starting from the knowledge of the flight mechanics the methods of calculation of the first stage requirements are analysed in the next pages.

4.2 Take-off requirement

On statistic base there is a law that binds the take-off distance FAR 25 to the take-off parameter TOP that contains the Thrust-to-Weight ratio to the Wing Loading, it can be expressed as

$$S_{T0} = 37,5 * TOP_{25}$$

$$TOP_{25} = \frac{\left(\frac{W}{S}\right)_{takeoff}}{\sigma C_{Lmax TO} \left(\frac{T}{W}\right)_{takeoff}}$$

The take-off distance can be evaluated following the figure below:

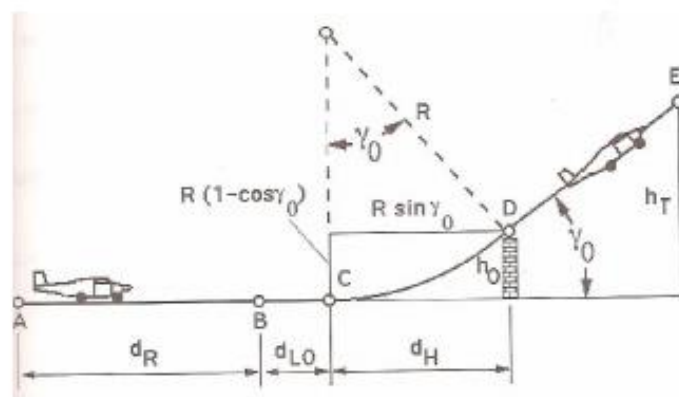


Figure 4.1

As it is shown the take-off distance is divided into three sections in reference to three different phases of the entire maneuver. Starting from the point A the vehicle reaches the speed it needs in the point B defined by manual called V_r and above this value it is possible to execute the subsequent maneuver which brings the vehicle to have a lift equal to the weight, until B there is a growing acceleration but the lift is less than the weight. The distance necessary to reach this value of lift is called taxi distance. The second section is the one between B and C where the lift-off distance is calculated and here the pitch of the vehicle is executed in a brief time interval at the same speed V_r , with this maneuver the vehicle's incidence is changed in such a way to have a lift higher than the weight, at this point the vehicle will be capable to get up from the ground and it will travel the CD line where D is the point that coincide to the 35ft obstacle overcoming.

From this analysis it can be inferred that the total take-off distance is equal to:

$$D_{takeoff} = D_{taxi} + D_{lift-off} + D_{pitch}$$

For our purpose the take-off distance could be defined by statistic from analysis of similar vehicles starting from the take-off distance and then thanks to the graph below the TOP_{25} can be correlated.

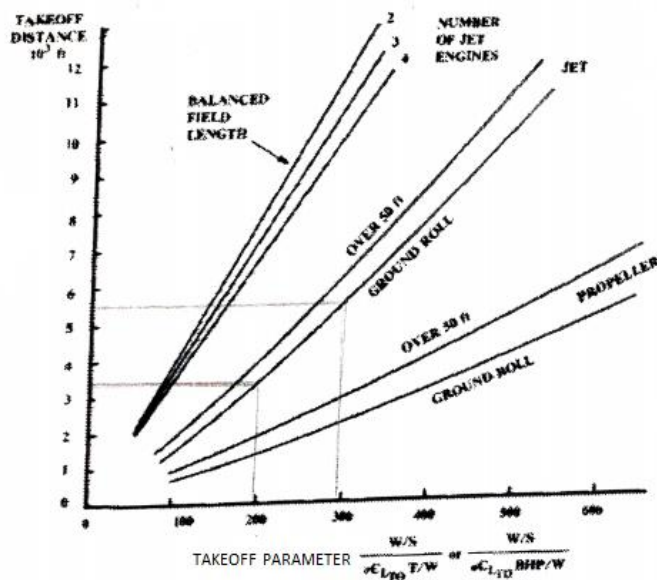


Figure 4.2

Once defined the propulsion type of the aircraft taken into consideration (jet vehicle or propelled vehicle), on the base of the typology of take-off requirement (BLF, ground roll or over 50ft), from the entry value of take-off distance it is possible to find the value of the Take Off Parameter, by a linear equation which brings to the previous relation where the angular coefficient is equal to 37.5.

Beyond the TOP_{25} value the other two quantities unknown are σ and $C_{Lmax TO}$, the first can be calculated from the knowledge if the altitude of the take-off airport through the density variation equation:

$$\sigma = \frac{\rho}{\rho_0} = \left(\frac{T_0 - hZ}{T_0} \right)^{4,2561}$$

Where h is the variation of the temperature per kilometer and is equal to $-6.5 \text{ }^\circ\text{C/km}$ in the troposphere.

On the other hand, $C_{Lmax TO}$ will be supposed that in the take-off phase the vehicle can employ flaps and slats to increase the lift.

Airplane Type	C_{Lmax}	$C_{Lmax TO}$	$C_{Lmax L}$
1. Homebuilts	1.2 - 1.8	1.2 - 1.8	1.2 - 2.0*
2. Single Engine Propeller Driven	1.3 - 1.9	1.3 - 1.9	1.6 - 2.3
3. Twin Engine Propeller Driven	1.2 - 1.8	1.4 - 2.0	1.6 - 2.5
4. Agricultural	1.3 - 1.9	1.3 - 1.9	1.3 - 1.9
5. Business Jets	1.4 - 1.8	1.6 - 2.2	1.6 - 2.6
6. Regional TBP	1.5 - 1.9	1.7 - 2.1	1.9 - 3.3
7. Transport Jets	1.2 - 1.8	1.6 - 2.2	1.8 - 2.8
8. Military Trainers	1.2 - 1.8	1.4 - 2.0	1.6 - 2.2
9. Fighters	1.2 - 1.8	1.4 - 2.0	1.6 - 2.6
10. Mil. Patrol, Bomb and Transports	1.2 - 1.8	1.6 - 2.2	1.8 - 3.0
11. Flying Boats, Amphibious and Float Airplanes	1.2 - 1.8	1.6 - 2.2	1.8 - 3.4
12. Supersonic Cruise Airplanes	1.2 - 1.8	1.6 - 2.0	1.8 - 2.2

* The Rutan Varienze reaches 2.5, based on stall speed data from Ref.9.

Notes: 1. The data in this table reflect existing (1984) flap design practice.
 2. Considerably higher values for maximum lift coefficient are possible with more sophisticated flap designs and/or with some form of circulation control.
 3. Methods for computing C_{Lmax} values are contained in Ref.6.

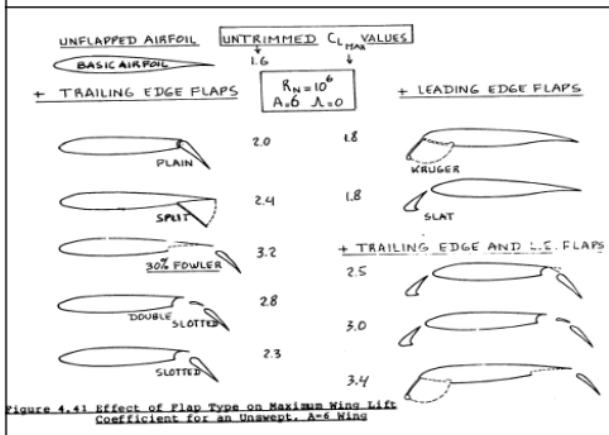


Figure 4.3

Once that each term of the equation is known the relationship between T/W and W/S can be calculated, the result is plotted on the graph below:

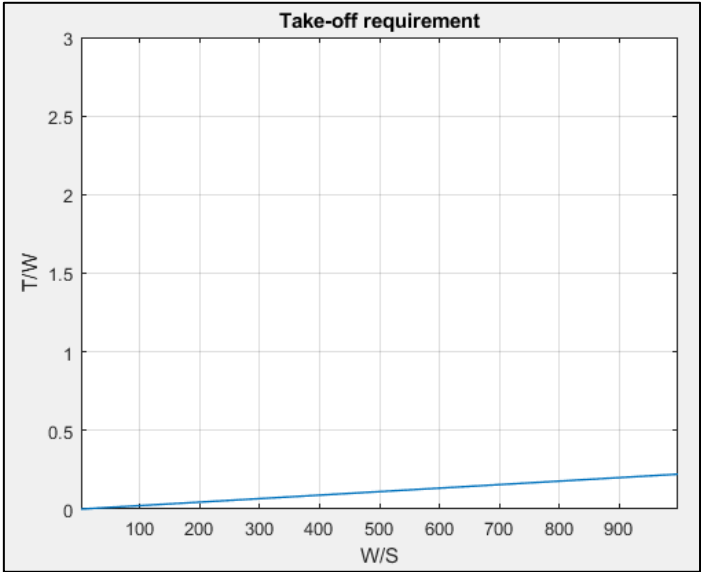


Figure 4.4

The requirement can be analysed for different values of $C_{Lmax TO}$ or for different values of the take-off site.

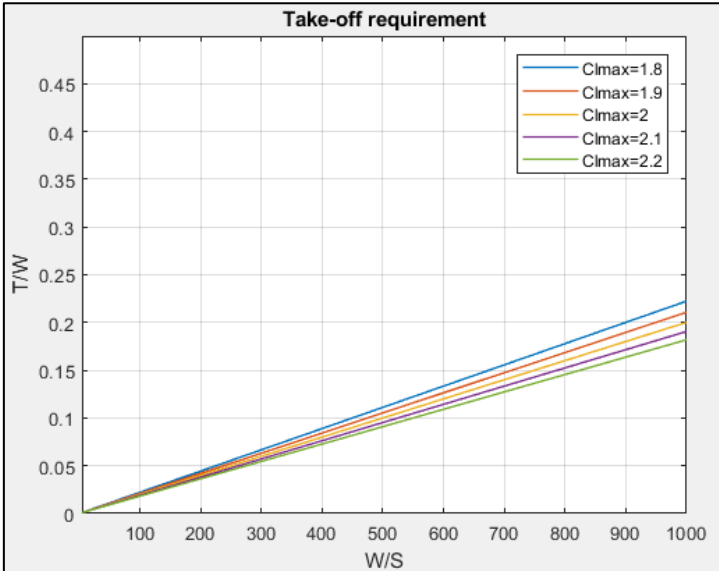


Figure 4.5

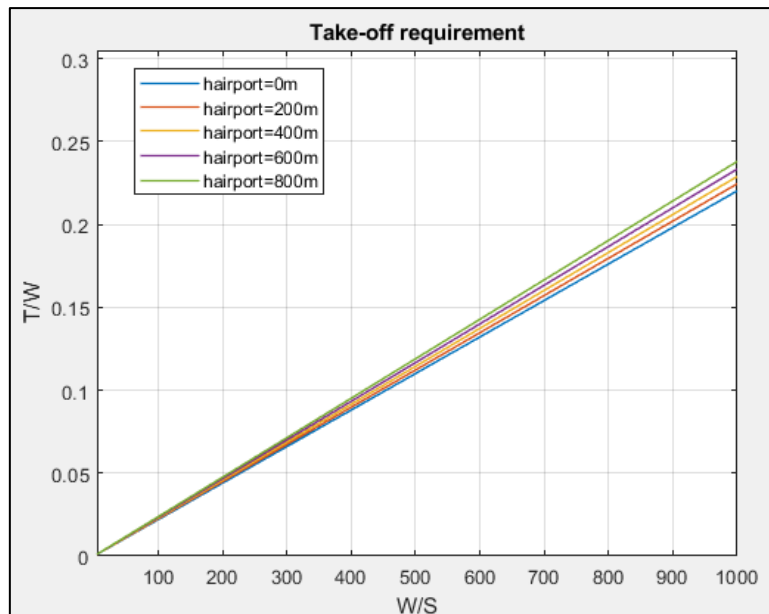


Figure 4.6

In both the cases presented as the $C_{Lmax TO}$ and the $\sigma = \frac{\rho}{\rho_0}$ (the altitude decrease) increase the angular coefficient decrease so that there will be a less pending straight line.

4.3 Second segment requirement

After the take-off the vehicle should be able to continue its mission accomplishing the requirements of the segmented climb, and this should be done taking into account an engine failure.

The first segment is short, it ends when the gear is retracted, then there is the second segment that is often the most difficult to meet, it begins when the gear is up and locked, it has the steepest climb gradient (about 2,5%) and ends at 400 feet, so it could take up to a minute or more to fly this segment. The third climb begins at 400 feet and the climb gradient is approximately the half it was before (1,2%) and it is required to accelerate to a speed called final segment climb speed, this segment is represented as a flat line for the acceleration, when this speed is reached the third segment of the climb ends and the fourth segment starts. The fourth and final segment defines the completion of the climb process, here the thrust is reduced and set to Maximum Continuous, the climb gradient is again around 2,5% and the speed is equal to the final segment climb speed until 1500 feet.

First Stage Requirements

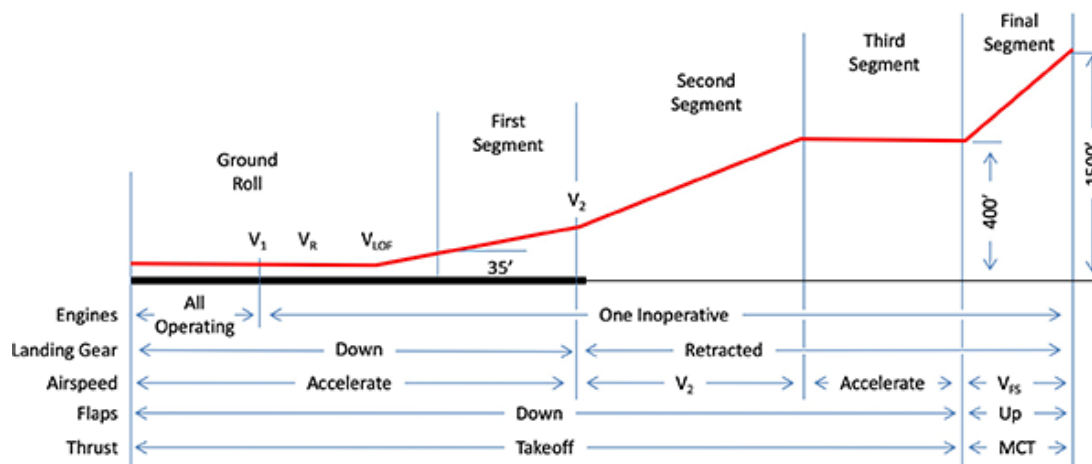


Figure 4.7

As it has been said the second segment requirement is the most difficult to meet and it will be represented in the matching chart.

The relation in second segment between T/W and W/S can be defined by the following equation:

$$\frac{T}{W} = \frac{n_e}{n_e - 1} \left[\left(\frac{C_{D_{TO}}}{C_{L_{TO}}} \right) + \sin \gamma \right]$$

In this equation n_e is the number of operative engines, γ is the climb angle in radiant and the term $\left(\frac{C_{D_{TO}}}{C_{L_{TO}}} \right)$ represent the reverse of the efficiency at the take-off. The result is a flat line as reported in the graph below:

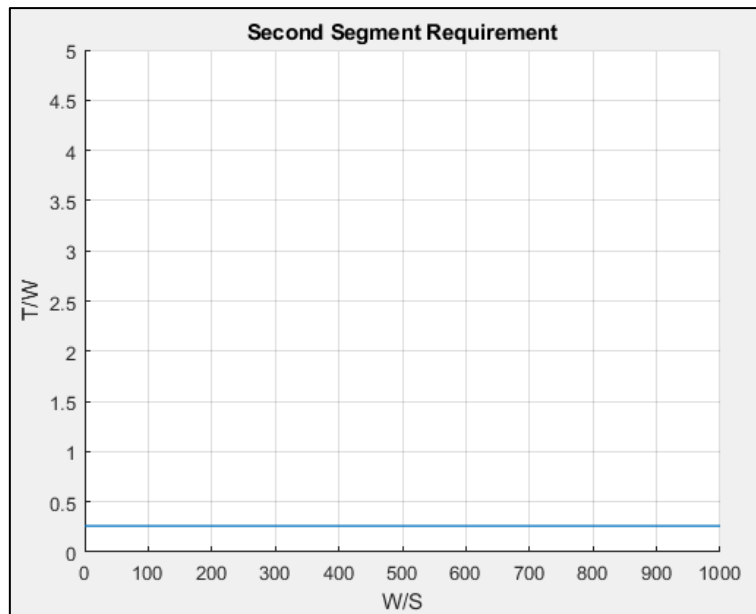


Figure 4.8

The fact that there is a flat line means that this requirement doesn't depend on the wing loading W/S . The value of $C_{D_{T0}}$ and $C_{L_{T0}}$ are the main quantities that influence the equations in fact for greater values of $C_{D_{T0}}$ the line moves upward while if the value of $C_{L_{T0}}$ becomes greater the line moves downward.

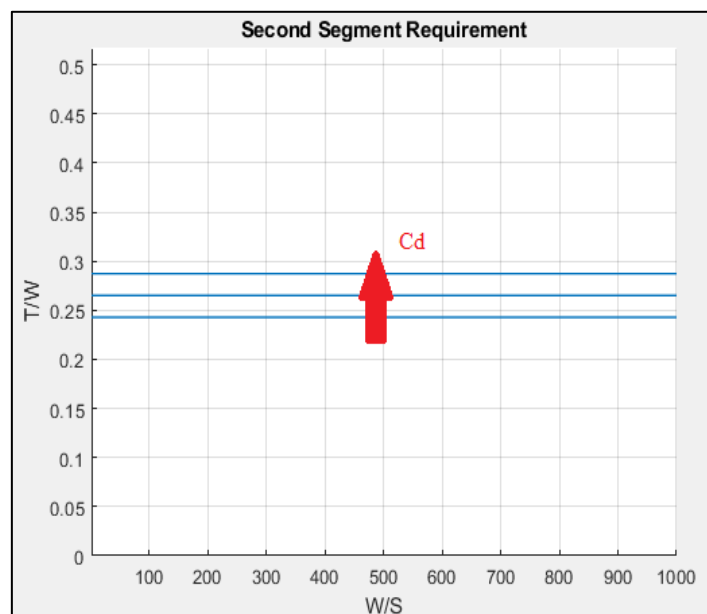


Figure 4.9

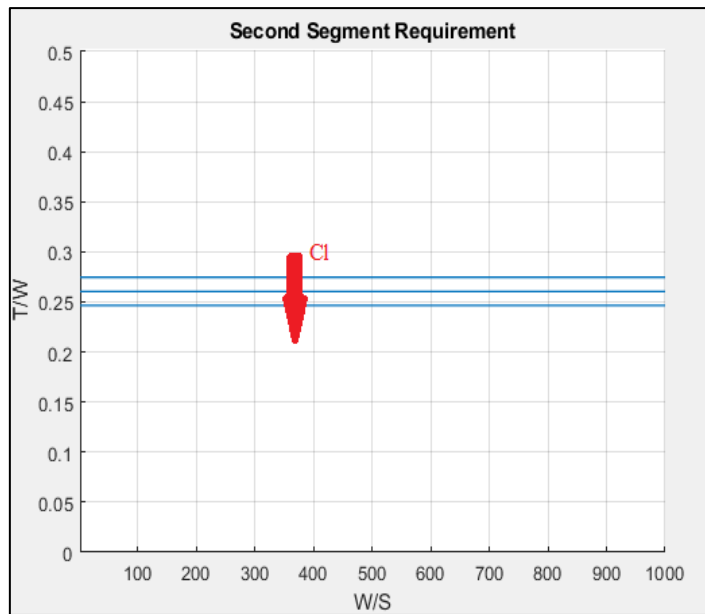


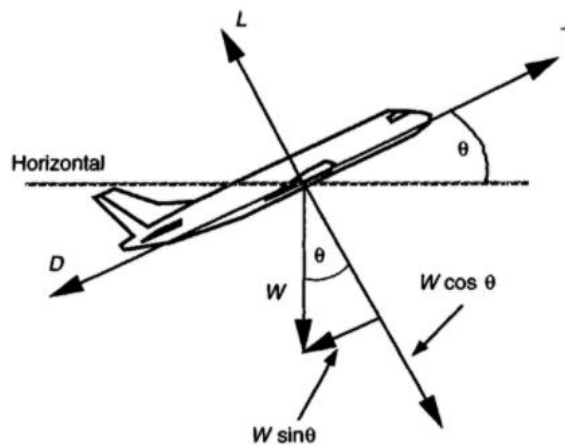
Figure 4.10

4.4 Climb and Cruise Requirements

In this section both the Climb and Cruise requirements will be presented in fact the method for their calculation is almost the same and lays the foundation on the evaluation of the flight mechanics in equilibrium conditions.

Immediately afterwards the second segment phase, the vehicle has to complete the climb to reach the cruise altitude, which is the phase of the aircraft while it is flying in longitudinal balance

In the climb phase the condition of the aircraft in terms of forces is the following:



For a uniform motion, the lift is balanced by the y-axis weight's component (perpendicular to the direction of the motion) while the thrust balances the sum of the drag and the x-axis weight's component (parallel to the direction of the motion).

$$L = W \cos \theta$$

$$T = D + W \sin \theta$$

On the other hand, in the cruise phase the aircraft can be schematized as below:

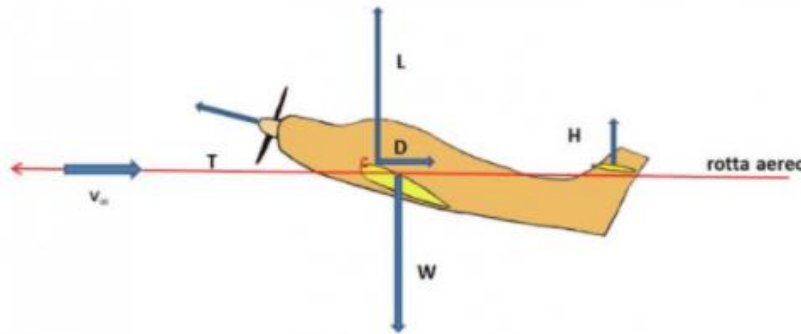


Figure 4.12

As it can be seen the lift and the weight are balanced and the same do the thrust and the drag so it can be written:

$$L = W$$

$$D = T$$

It is observed that, in the cruise phase, under normal conditions the vehicle often flies with its longitudinal axis slightly inclined with respect to the trajectory, with a flight condition called nose-up, here the angle formed between the axis of the plane and the horizontal plane is called pitch attitude.

It is possible to note that, by increasing the incidence angle, the centre of pressure c (the point of application on the forces lift and drag) moves forward on the wing.

However, the weight W is always applied in the center of gravity of the aircraft, it happens that L and W are no longer aligned and this generates a small moment that would tend to roll the plane backwards, this effect is avoided by acting on the tail increasing its lift H , which generates a balancing moment of opposite sign.

In both the conditions, climb and cruise phases, the lift L and the drag D are expressed with the following equations:

$$L = \frac{1}{2} \rho V^2 S C_L$$

$$D = \frac{1}{2} \rho V^2 S C_D$$

the term $q = \frac{1}{2} \rho V^2$ is called dynamic pressure which is the air pressure created by the relative movement between the vehicle and the air.

To express the drag coefficient C_D the quadratic relation is used:

$$C_D = C_{D0} + \frac{C_L^2}{e\pi\lambda}$$

In this equation C_{D0} represent the zero-lift drag coefficient and e is the Oswald factor. The dependence between the two variables can be graphed as following:

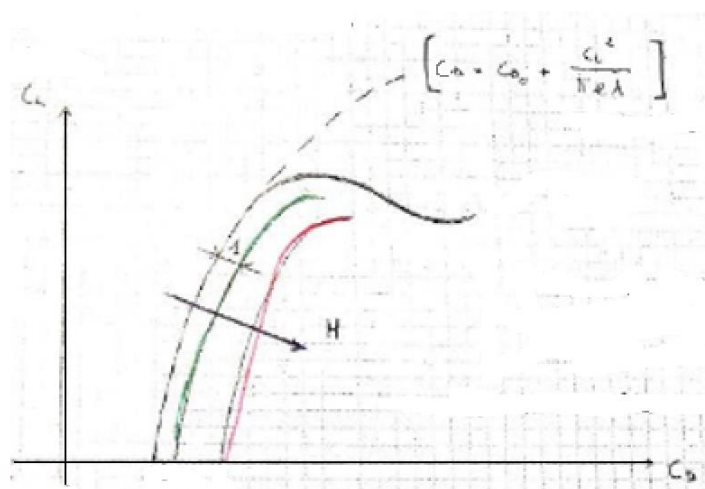


Figure 4.13

The dotted line represents the quadratic expression while the continuous line is made by experimental studies.

Due to the quadratic relation, the equation of the drag D can be rewritten in the following manner:

$$D = qS \left(C_{D0} + \frac{C_L^2}{e\pi\lambda} \right) = qS C_{D0} + qS \frac{C_L^2}{e\pi\lambda}$$

$$D = qS \left(C_{D0} + \frac{C_L^2}{e\pi\lambda} \right) = \frac{1}{2} \rho V^2 S \left(C_{D0} + \frac{\left(\frac{W}{S}\right)^2}{\left(\frac{1}{2} \rho V^2\right)^2 e\pi\lambda} \right)$$

The drag D is composed by a linear term called form resistance and a hyperbolic term called induced resistance. The contribution of both the terms is highlighted in the figure below where the form resistance is the red curve and the induced resistance is the curve in blue:

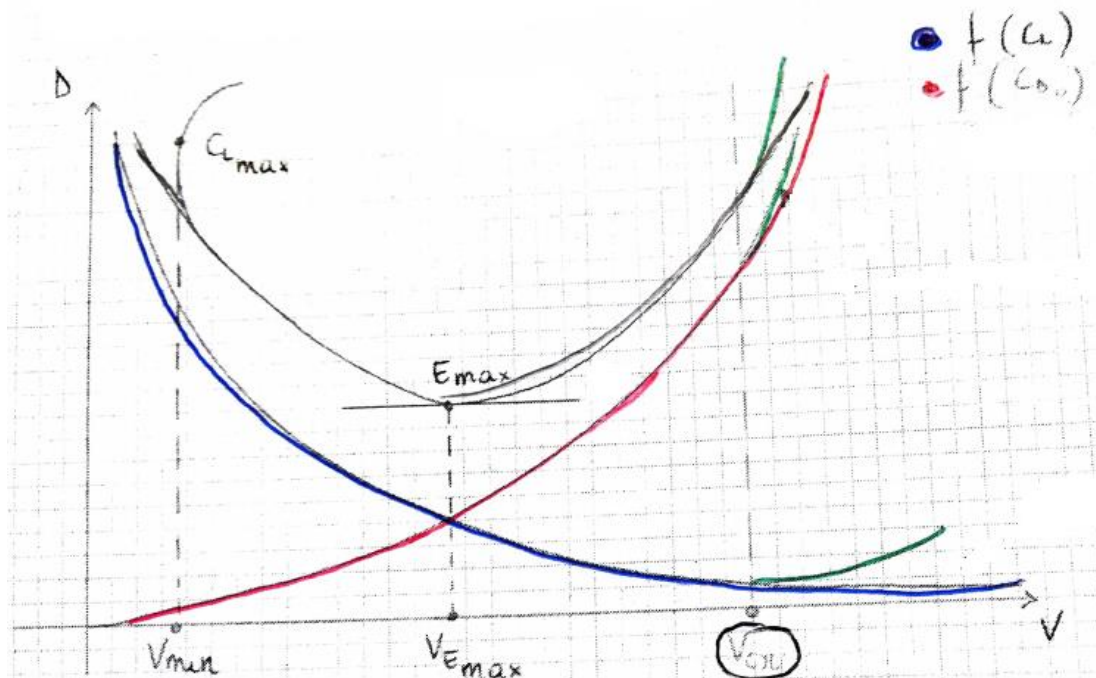


Figure 4.14

Starting from the drag equation, knowing that it is equal to the thrust T , it is possible to find the expression of the Thrust-to-Weight Ratio during the climb and the cruise phase:

$$\left(\frac{T}{W}\right)_{climb} = \frac{qC_{D0}}{W_{climb}/S} + \frac{W_{climb}/S}{q\pi e\lambda} + \sin\gamma$$

$$\left(\frac{T}{W}\right)_{cruise} = \frac{qC_{D0}}{W_{cruise}/S} + \frac{W_{cruise}/S}{q\pi e\lambda}$$

On the base of these equations it is possible to find the term that most interest for the matching chart analysis that is the Thrust-to-Weight ratio at the take-off:

$$\left(\frac{T}{W}\right)_{takeoff} = \left(\frac{qC_{D0}}{W_{takeoff}/S} \frac{W_{takeoff}}{W_{climb}} + \frac{W_{takeoff}/S}{q\pi e\lambda} \frac{W_{climb}}{W_{takeoff}} + \sin\gamma \right) \frac{W_{climb}}{T_{climb}} \frac{T_{climb}}{T_{takeoff}}$$

$$\left(\frac{T}{W}\right)_{takeoff} = \left(\frac{qC_{D0}}{W_{takeoff}/S} \frac{W_{takeoff}}{W_{cruise}} + \frac{W_{takeoff}/S}{q\pi e\lambda} \frac{W_{cruise}}{W_{takeoff}} \right) \frac{W_{cruise}}{T_{cruise}} \frac{T_{cruise}}{T_{takeoff}}$$

The value of the thrust during cruise can be tied to the value of the thrust during take-off through the following relation:

$$T = T_{takeoff} * \varphi(n) * \chi(V, z) * \psi(z)$$

Here the relation between the two quantities is due to three functions that depend on the throttle, the speed and the altitude, in particular they can be made explicit in the following manner:

$$\varphi(n) = \left(\frac{n}{n_0}\right)^{3,5}$$

$$\psi(z) = \left(\frac{p}{p_0}\right)\left(\frac{T_0}{T}\right)^{1,75}$$

$$\chi(V, z) = \left(1 - \frac{V}{w_g}\right)$$

in the first function n_0 is the max number of engine revolutions, while in the second equation there are the temperature and the pressure that are influenced by the altitude and in the third equation w_g is the speed of the outflow gases.

As noted above the climb and the cruise curve are sum of a linear term and a hyperbolic term so the previous equation respects the relation below:

$$y = \left(\frac{A}{x} + Bx\right) C$$

$$\left(\frac{T}{W}\right)_{takeoff} = \left(\frac{A}{\frac{W_{takeoff}}{S}} + B \frac{W_{takeoff}}{S}\right) C$$

So the term A, B and C, which are constant, can be written as (the same for the climb where W_{climb} and T_{climb} will be used respectively instead of W_{cruise} and T_{cruise}):

$$A = \frac{C_{D0}q}{\frac{W_{cruise}}{W_{takeoff}}}$$

$$B = \frac{\frac{W_{cruise}}{W_{takeoff}}}{q\pi e\lambda}$$

$$C = \frac{\frac{W_{cruise}}{W_{takeoff}}}{\frac{T_{cruise}}{T_{takeoff}}}$$

Once defined these three constants it is possible to find the Thrust-to-Weight ratio for different value of Wing Loading. An example is shown hereunder.

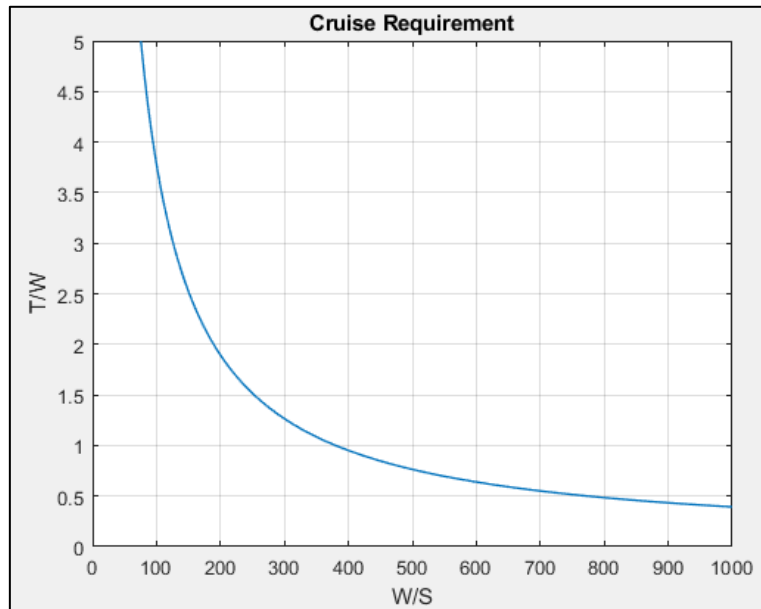


Figure 4.15

The line trend varies if the speed, the altitude and the zero-lift drag coefficient change, it is highlighted in the figures below:

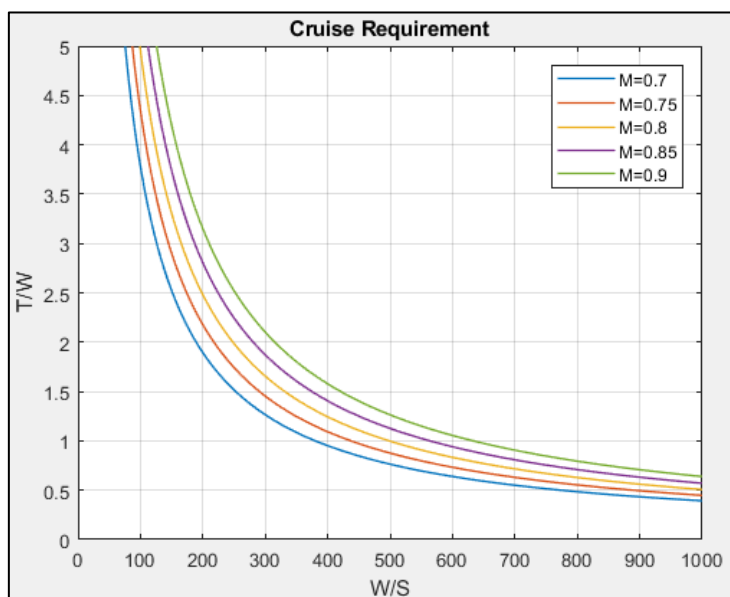


Figure 4.16

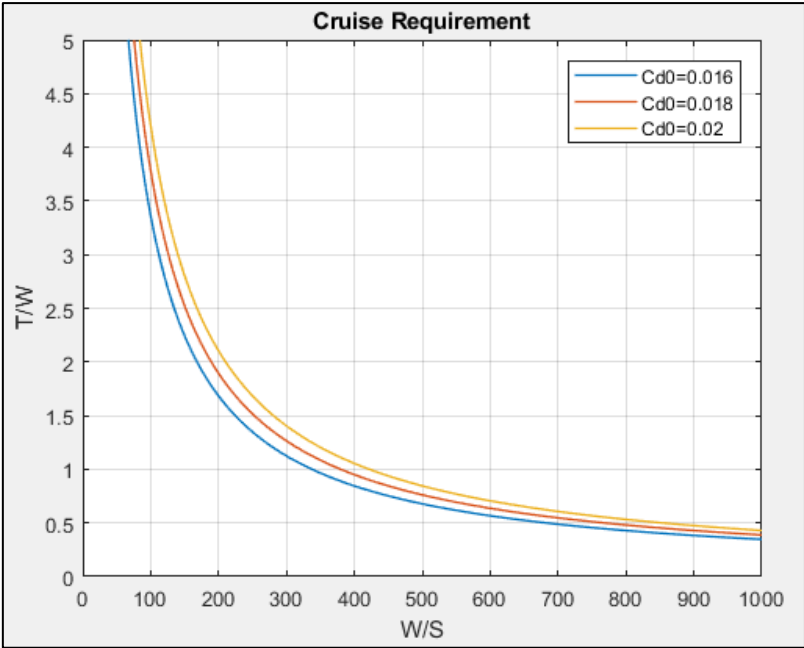


Figure 4.17

The trend for the climb will be the same and even the influence parameters are the same, here is an example:

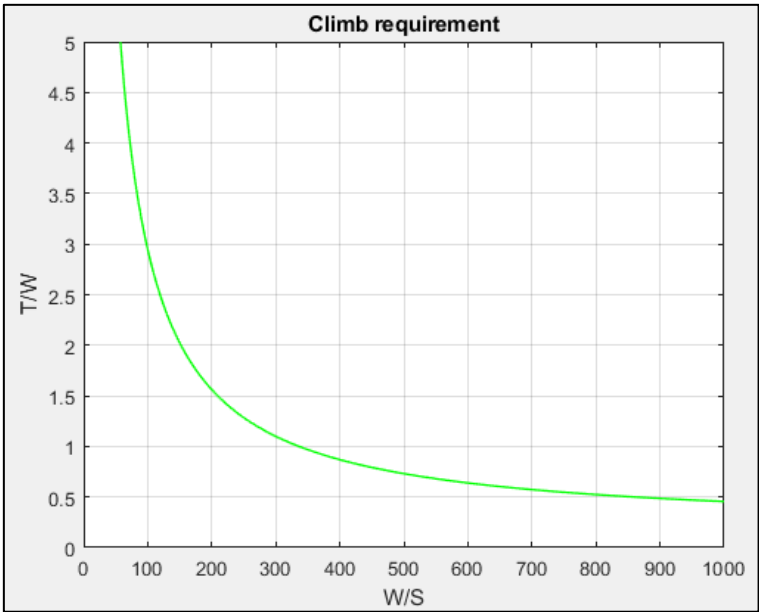


Figure 4.18

4.5 Landing Requirement

The landing is the final maneuver of a flying vehicle and consists on its return to the ground and the subsequent deceleration to stop itself.

In the same way as take-off there is a law on statistic base that bind the landing distance on FAR25 to the approach speed calculate with the stall speed in landing configuration:

$$S_{landing} = 0,3 * (V_{approch})^2 = 0,3 * (1,3 * V_{stall\ landing})^2 = 0,507 * (V_{stall\ landing})^2$$

The landing distance can be divided into four different sections: the first, which is the part AB is the descent, then from B to C the attitude angle is reduced until it becomes equal to zero, from C to D all the braking equipment is used and from D to E there is the effective braking. Here under all the landing contribute are highlighted:

$$D_{landing} = D_{approach} + D_{maneuver} + D_{braking} + D_{taxi}$$

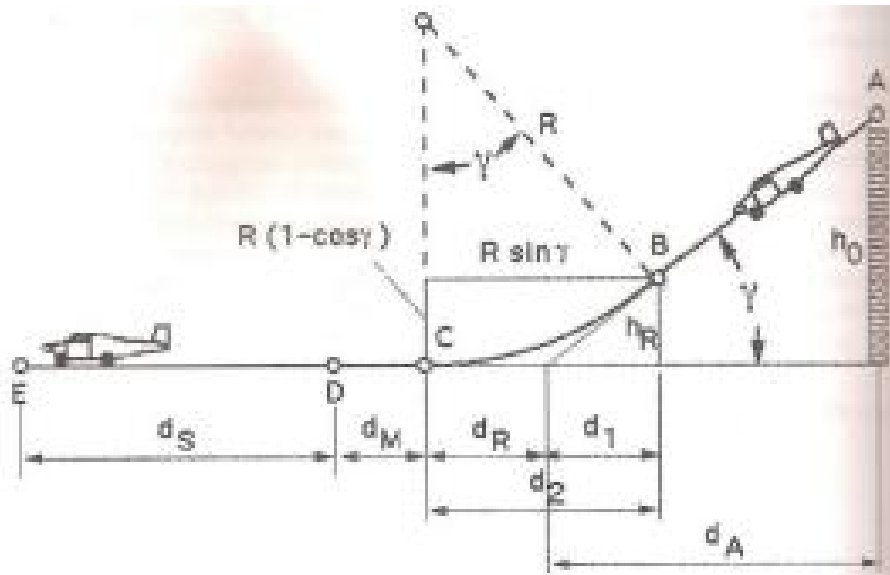


Figure 4.19

In our case the landing distance can be supposed and from the previous equation the stall speed can be found:

$$V_{sl} = \sqrt{\frac{S_L}{0,507}}$$

And from the equation of the lift the Wing Loading can be calculated as following supposing the value of lift coefficient keeping in mind the contribution of all the secondary movable surfaces used to increase the value con C_L .

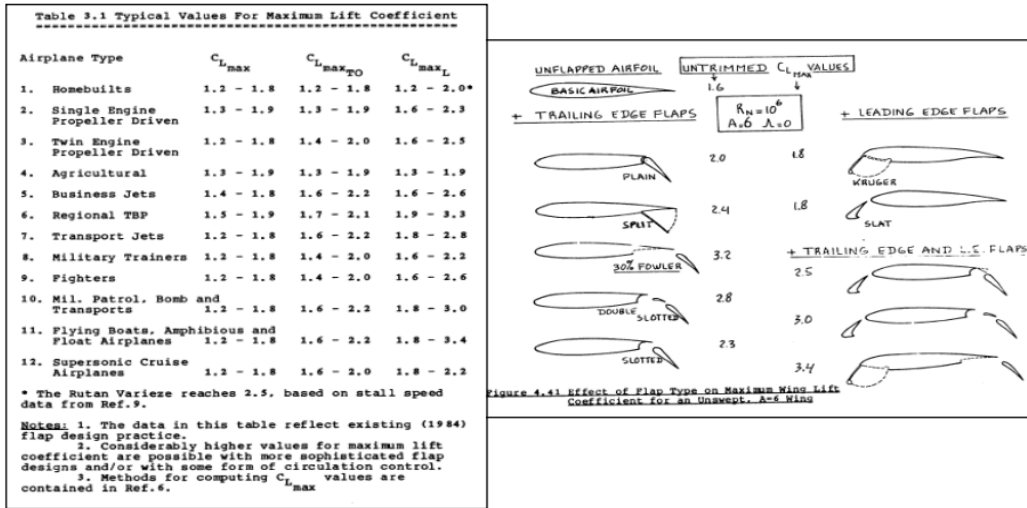


Figure 4.20

$$\frac{W_L}{S} = \frac{1}{2} \rho V_{sl} C_{L_{max}} L$$

But in the matching chart analysis the quantity that most interest is the Wing Loading at the take-off so the equation that will be plotted is:

$$\left(\frac{W}{S}\right)_{takeoff} = \frac{1}{2} \rho V_{sl} C_{L_{max}} L * \frac{W_{TO}}{W_L}$$

It emerges that there is no dependence from the Thrust-to-Weight ratio so in the matching chart will appear a vertical line. An example is reported below:

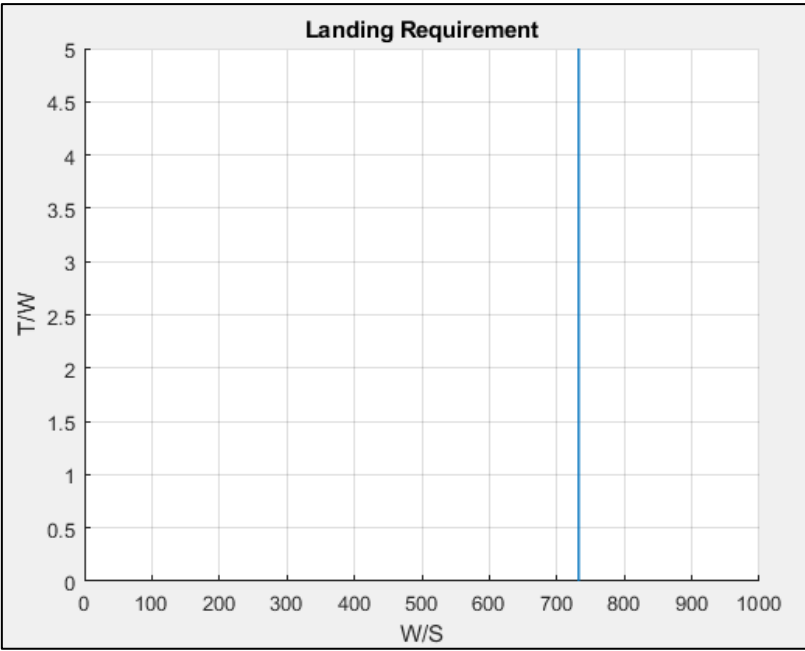


Figure 4.21

It is possible notice the dependence from the main parameters such as $C_{Lmax L}$ that is highlighted in the first figure hereunder and from the take-off and landing weight ratio that is reported in the second figure.

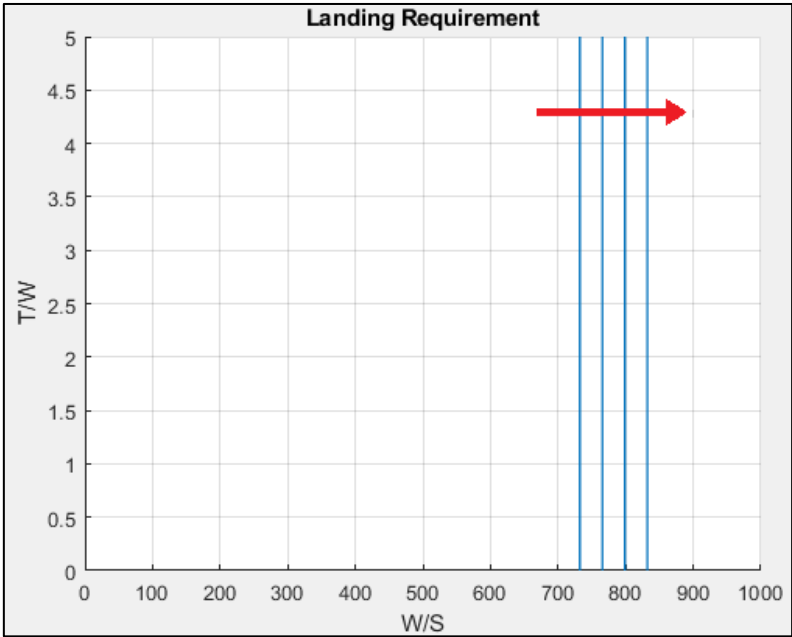


Figure 4.22

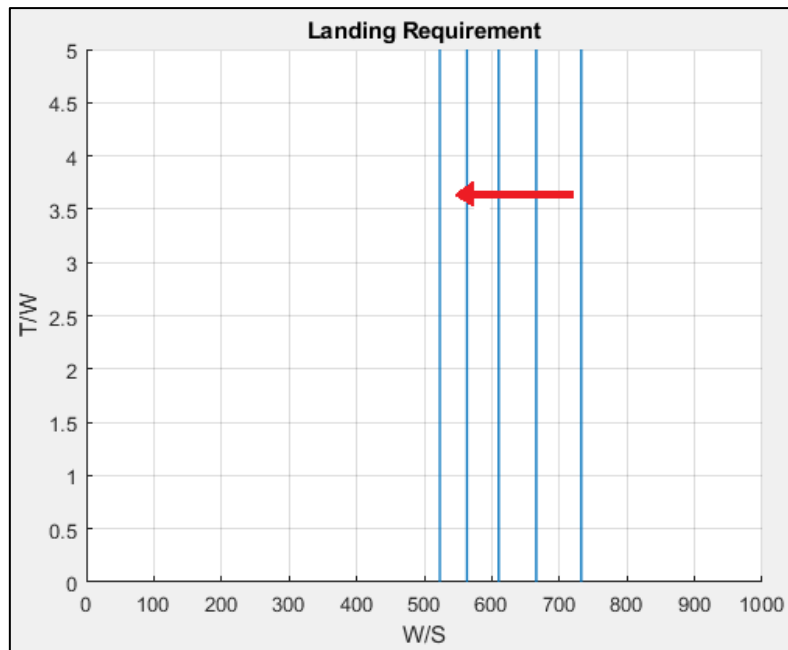


Figure 4.23

The influence of the two quantities is opposite, increasing C_{LmaxL} the value of the Wing Loading increase, while increase the value of the take-off-to-landing weight ratio the value W/S becomes smaller.

Chapter 5

5.1 Second Stage Requirements

In this section all the main requirements for the matching chart analysis of the second stage will be presented, in particular the requirements that will be introduced are the orbit-achievement requirement, the re-entry requirement and the payload requirement.

The second stage must respect also the landing requirement but the analysis of the latter is the same as that seen for the first stage so it will be omitted and introduced directly in the subsequent definition of the design point in the next section.

5.2 Orbit-achievement Requirement

The second stage, immediately after its separation from the first stage, has to reach the target orbit altitude from this it derives the orbit-reaching requirement which express in terms of Thrust-to-weight ratio and Wing Loading which is the possible combination that make it feasible.

For the definition of this requirement the starting point are the two following equations:

$$W_{oe} = \frac{V_{ppl}}{S_{pln}} \frac{\rho_{ppl}}{W_R - 1} S_{pln} = \frac{V_{ppl}}{V_{tot}} \frac{V_{tot}}{S_{pln}^{1.5}} I_p S_{pln}^{1.5}$$

$$I_p = \frac{\rho_{ppl}}{W_R - 1} = \left[\frac{\rho_{fuel}(1 + r_{o/f})}{1 + r_{o/f} \frac{\rho_{fuel}}{\rho_{oxid}}} \right] * \left\{ \exp \left[\frac{\Delta V \frac{T}{D}}{g I_{sp} \left(\frac{T}{D} - 1 - \sin \gamma \right)} \right] - 1 \right\}^{-1}$$

As it emerges from these equations the W_{oe} , the operation empty weight is made by the product of three terms, the first $\frac{V_{ppl}}{S_{pln}}$ is determined by the geometry, the second $\frac{\rho_{ppl}}{W_R - 1}$ by the aero-thermo-propulsion system and the third S_{pln} by the size.

The second equation is related to the propulsion index I_p which itself is product of two terms, the first directly related to the density of the propellants chosen and to the oxidizer to fuel ratio, while the second is function of the propellant and the engine selection, engine size, excess thrust over drag and the climb angle for a given speed.

Rearranging the previous two equations it is possible to find the relation that directly show the link between the Thrust-to-Weight ratio and the Wing Loading and that will be plotted and used in the matching chart analysis:

$$\left(\frac{T}{W}\right)_{TO} = \frac{qC_D(1 + \sin\gamma)}{1 - \frac{\Delta V}{YgI_{sp}}} \left(\frac{W}{S}\right)_{TO}^{-1}$$

Where:

$$Y = \ln \left[1 + \left(\frac{W_{gto}}{W_R} \frac{V_{tot}}{V_{ppl}} \frac{1}{\tau X S_{pln}^{1.5}} \right)^{-1} \right]$$

$$X = \left[\frac{\rho_{fuel}(1 + r_{o/f})}{1 + r_{o/f} \frac{\rho_{fuel}}{\rho_{oxid}}} \right]$$

The X value can be found simply by the knowledge of the type of propellants that the vehicle will use and the mixture ratio $r_{o/f}$.

Related to the propellant is the propellant volume of the second stage that is given by the ratio between the propellant mass and the value of the propellant bulk density, it is computable by the following equations:

$$V_{ppl} = \frac{M_{ppl}}{\rho_{ppl}}$$

$$\rho_{ppl} = \frac{(1 + r_{o/f})}{\frac{1}{r_{o/f}} + \frac{r_{o/f}}{\rho_{oxid}}}$$

The propellant mass is calculated taking into account how much distance the second stage has to travel in fact into the calculation of the M_{ppl} there is the value of burning time of the rocket.

$$M_{ppl} = \frac{T_{rocket} t_{burn}}{g I_{sp}}$$

At this point it is important to find a method to calculate the t_{burn} value: supposing the ceiling of the first stage as the altitude where the separation occur it has been calculated the difference from the altitude of the target orbit.

For the calculation it has been used the standard variation of the air characteristic with a reduction of $-6.5^{\circ}/\text{km}$ in the troposphere, a constant value of -60° in the tropopause and an increase of $1.3^{\circ}/\text{km}$ in the stratosphere.

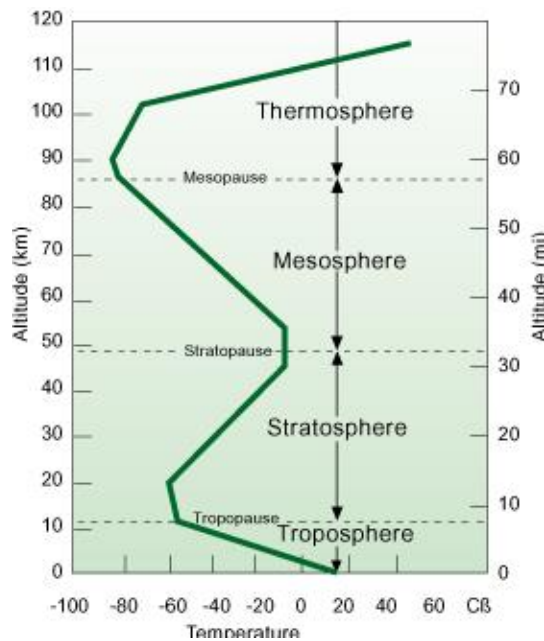


Figure 5.1

For the calculation of the first stage ceiling altitude it has been supposed to fly in a configuration of max efficiency because considering the curve of the available thrust on function of the speed, the ceiling point, that means having climb speed equal to zero, coincide with the lowest point of the curve.

In the figure below there is the evolution of the necessary thrust in function of the speed at the change of the altitude, the curve moves slightly to the right as the altitude increase.

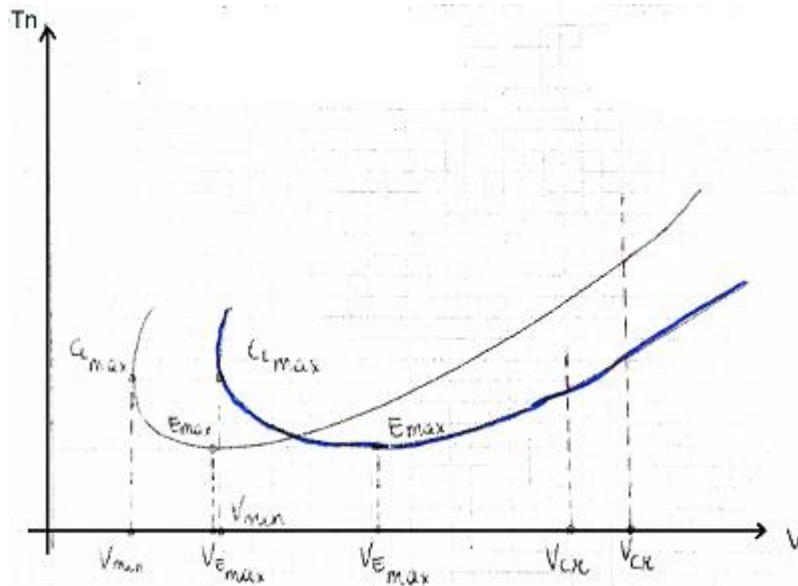


Figure 5.2

On the other hand, for the available thrust it has been used the relation already introduced that presents the thrust as function of the throttle, the altitude and the speed:

$$T_a = T_{s0} * \varphi(n) * \chi(V, z) * \psi(z)$$

Where T_{s0} is the maximum static thrust that the engine can supply at a fixed point at an altitude of 0m and with the maximum number of revolutions.

Assuming the throttle constant its evolution for different values of altitude is reported hereunder:

In the next figure it is possible to notice the mutual behaviour of the available thrust that decrease with the necessary thrust with an increase of the altitude.

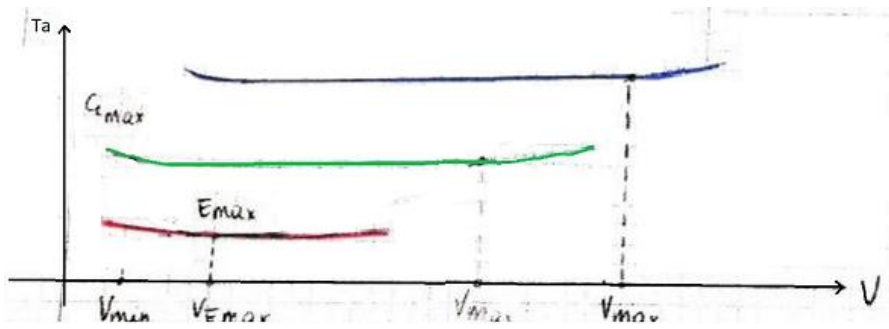


Figure 5.3

On the basis of these considerations it is possible to analyse the mutual behaviour of both the available thrust and the necessary thrust and see how the ceiling, the point where for the highest value of altitude T_a and T_n are the same coincides with the max efficiency, as reported in the next figure:

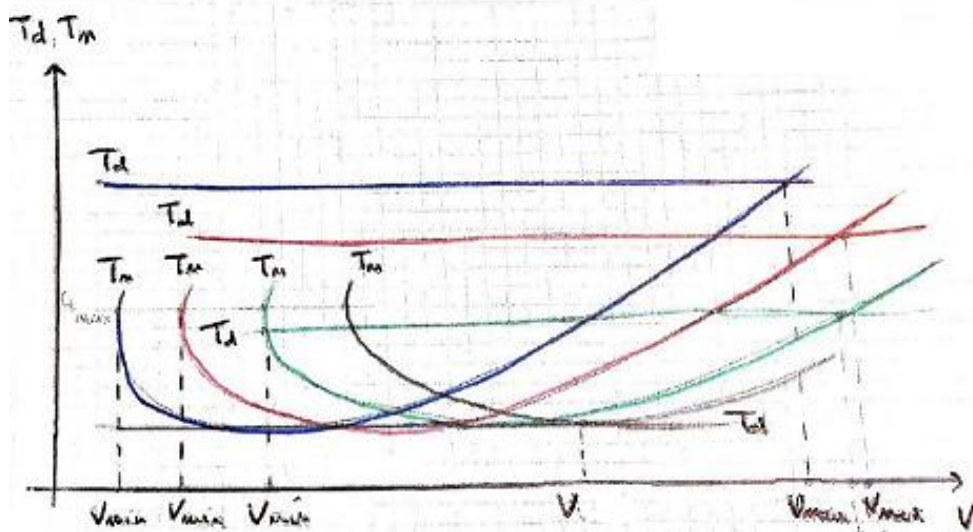


Figure 5.4

The value of ceiling is calculated starting from the speed of ascent value obtained from the equilibrium equations in ascent flight:

$$T - D = W \sin \gamma$$

Multiplying both the terms for the speed V , the ascent speed is calculated, and it can be isolated:

$$(T - D)V = WVsiny$$

$$w = \frac{(T - D)V}{W}$$

Equalizing this equation to zero the ceiling condition is obtained, and the vehicle is supposed to flight in horizontal:

$$\frac{TV}{W} = \frac{DV}{W} = \frac{DV}{L} = \frac{V}{E_{max}}$$

$$T = \frac{W}{E_{max}}$$

But using the previous definition of T and supposing the throttle equal to 1 ($\varphi(n) = 1$):

$$T = T_{s0} * \chi(V, z) * \psi(z) = \frac{W}{E_{max}}$$

$$\chi(V, z) * \psi(z) = \frac{W}{E_{max}T_{s0}}$$

this relation let to calculate the value of the ceiling altitude in a graphic way, in fact all the quantities at the second term are known and for different values of z the quantities at the first term are varied, so that when both the terms are equals the ceiling altitude is found:

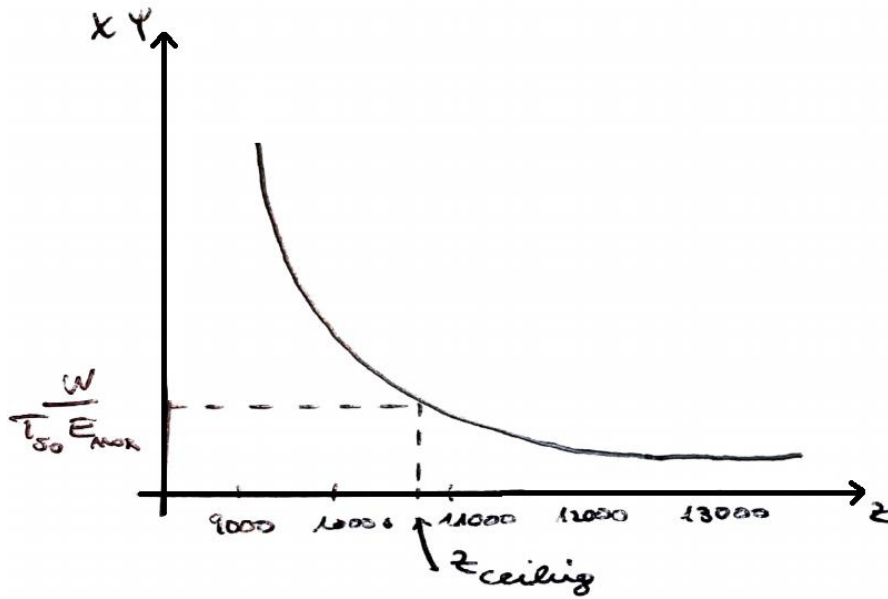


Figure 5.5

Therefore, the trend of $\chi(V, z) * \psi(z)$ is built, then you enter in the graph with the value $\frac{W}{E_{max} T_{50}}$ from the y-axis and finally, in correspondence of the latter, on the x-axis the value of the ceiling altitude can be found.

Once that the ceiling is calculated, it is also known the value of the distance that the second stage should travel to reach the target orbit, for the computation of the burning time the uniformly accelerated motion laws are used supposing a value of average acceleration during the entire distance, in particular it is important to find the value of the ΔV required to reach the orbital speed of the target orbit, it is obtained as a different from the latter and the vehicle speed at the moment of the separation at the ceiling altitude and then:

$$t_{burn} = \frac{\Delta V}{a_{max}}$$

All the quantities in the mass propellant formula are known and the latter can be calculated and then also the V_{ppl} .

At this point it is possible to compute the value of Thrust-to-Weight in function of the Wing Loading using the equation previously introduced:

$$\left(\frac{T}{W}\right)_{TO} = \frac{qC_D(1 + \sin\gamma)}{1 - \frac{\Delta V}{YgI_{sp}}} \left(\frac{W}{S}\right)_{TO}^{-1}$$

An example of the trend of the curve that came out from this equation is reported hereunder:

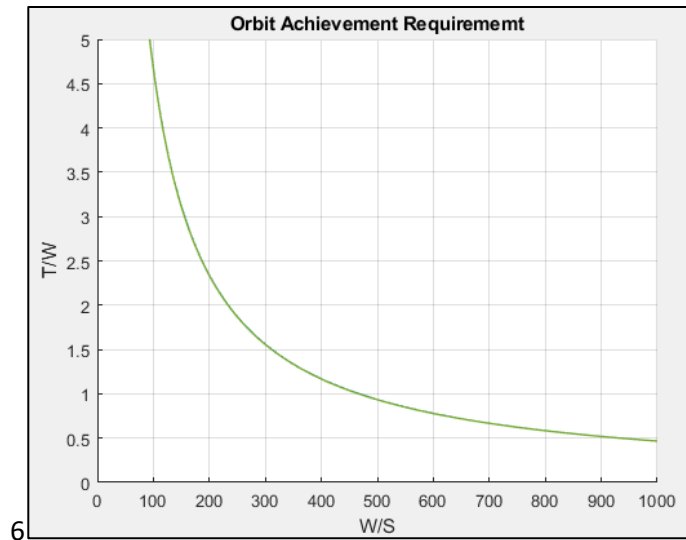


Figure 5.6

It is important to note that the main factor that determine a variation on the curves is the term in the denominator, in fact if it decreases the curve translates upward.

The main variables that characterize the methods are the weight W of the entire vehicle, intended as first stage and second stage not separated, the weight of the second stage W_{ss} and the thrust of their engine, T_{s0} for the first stage and T_{rocket} for the second stage, and the altitude of the target orbit.

From the choice of these values it is possible to analyse how the values of ceiling altitude, and the feasible transportable payload in the second stage.

Hereunder it is highlighted the variation of the payload weight with a change in the values of second stage weight and thrust on the x-axis and y-axis respectively, in addition to the variation of the orbit altitude that the second stage has to reach.

Analysing the point with the same W_{ss} and T_{rocket} with an increase of the z_{orbit} the solution moves upward, while for at parity of the orbital target and at fixed W_{ss} with an increase of T_{rocket} the payload weight admissible decrease linearly because the

propellant mass to be transport increase with the thrust, this is highlighted in the third figure. On the contrary, as the second figure shows, with a fixed Trocket and with an increase in Wss the payload weight allowed increase in a linear manner.

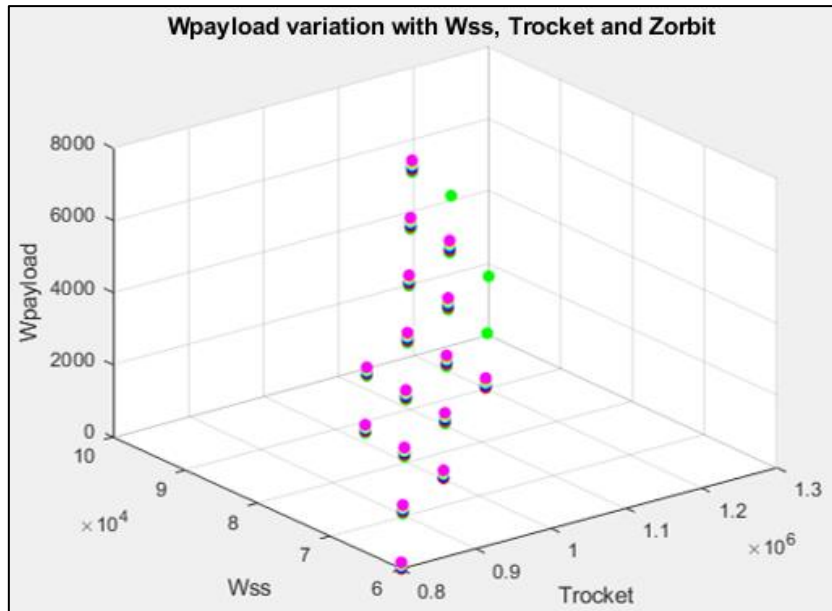
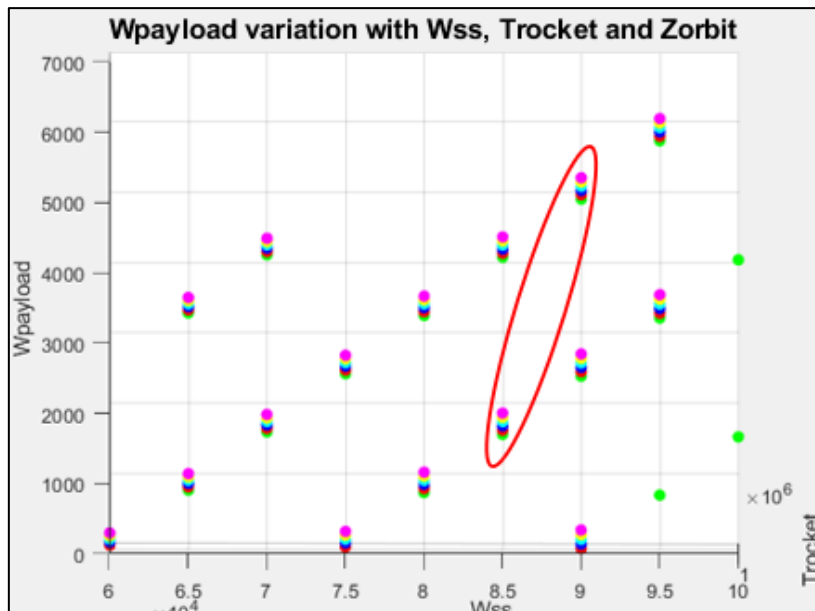
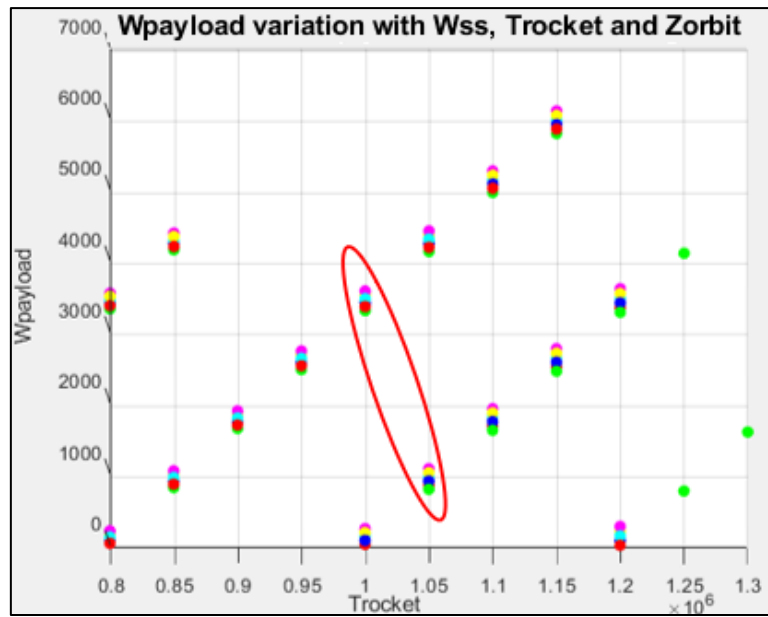


Figure 5.7





The same analysis can be performed considering the effect of Mach on the payload weight, in particular the study below has been developed with Mach equal to 6, 7 and 8.

From the graphs below it can be noticed how the payload weight admissible comprises an higher range of values of Trocket and Wss, while the evolution with the target orbit altitude doesn't change and involves a translation upward of the curves.

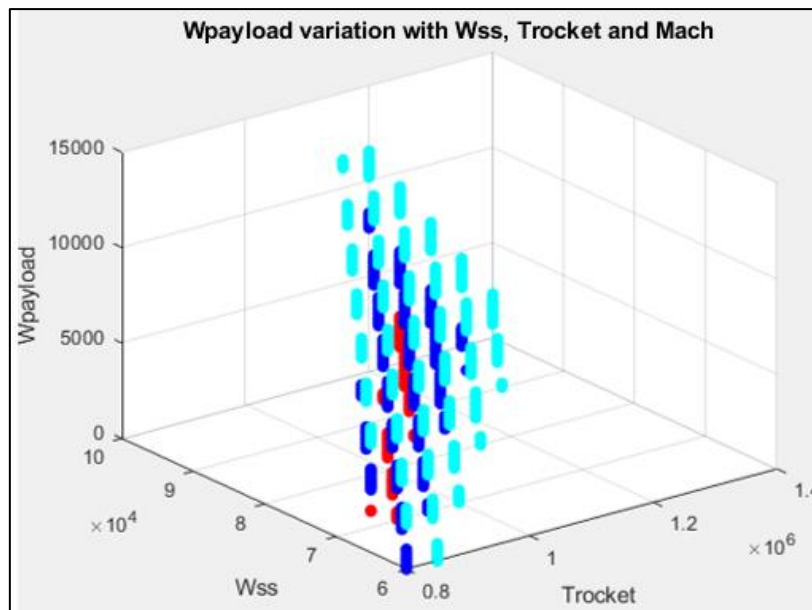
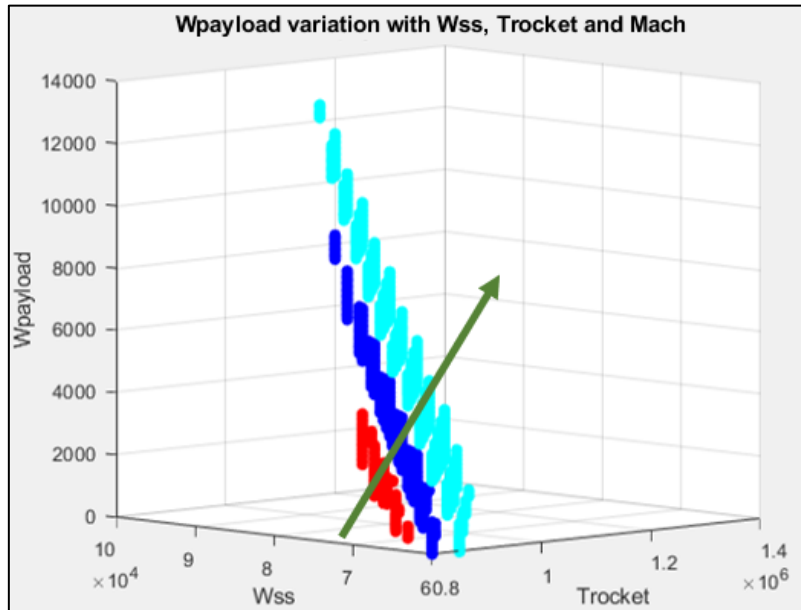


Figure 5.8



As anticipated, it is interesting analyse the evolution of the ceiling with a change in the vehicle value and its thrust T_{s0} .

The figures below show that at fixed values of the maximum static thrust as the vehicle weight increases, the ceiling is reached for smaller altitudes, on the contrary for fixed values of W as the T_{s0} increases also the ceiling altitudes becomes higher.

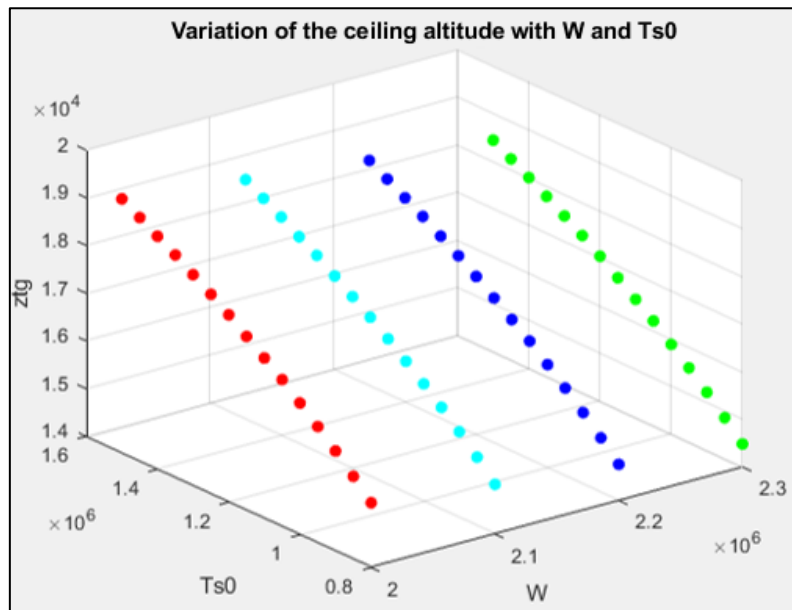
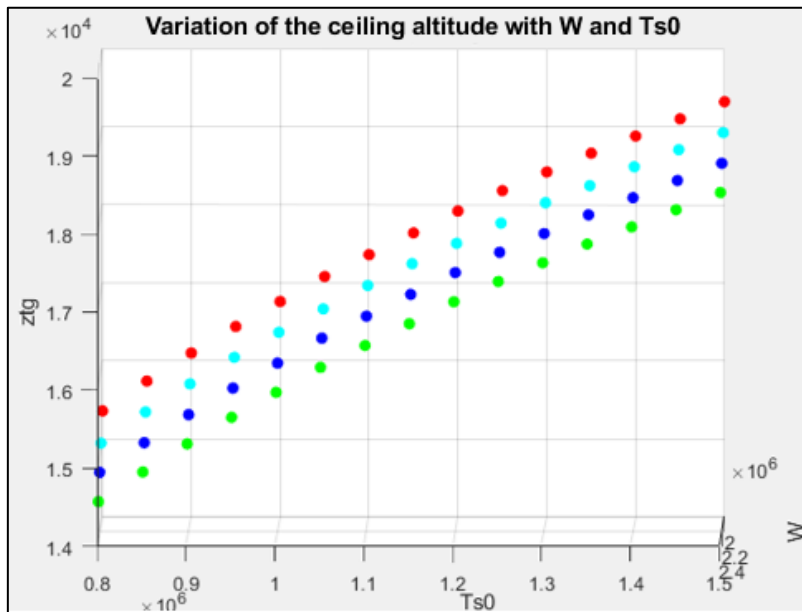
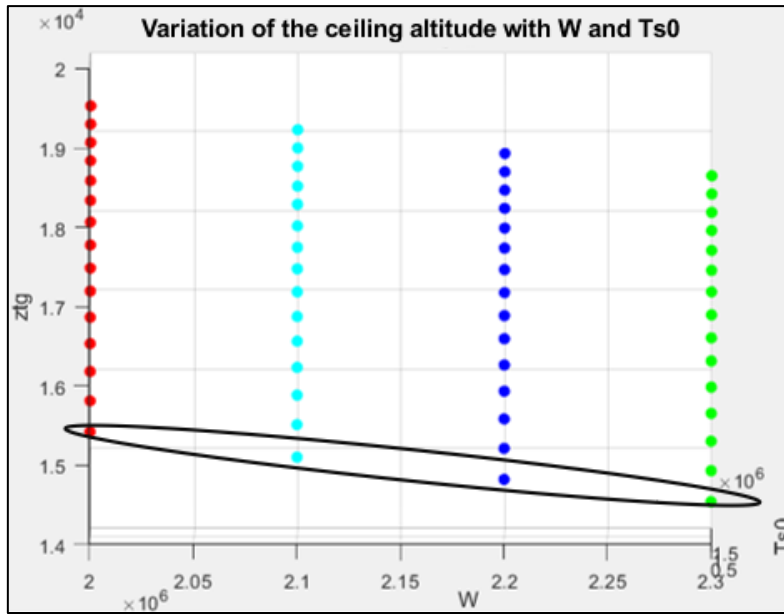


Figure 5.9



In addition to the vehicle weight and the maximum static thrust it is possible to study the dependence from the value of Mach in the same mode as did for the previous analysis. The influence of the Mach is highlighted in the figure below where it is easily visible how the curves translate upward as the Mach increase.

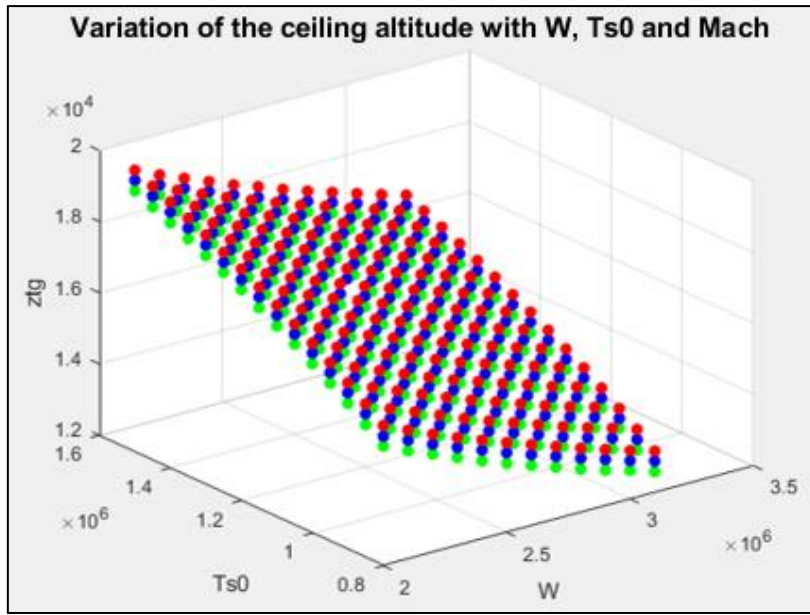
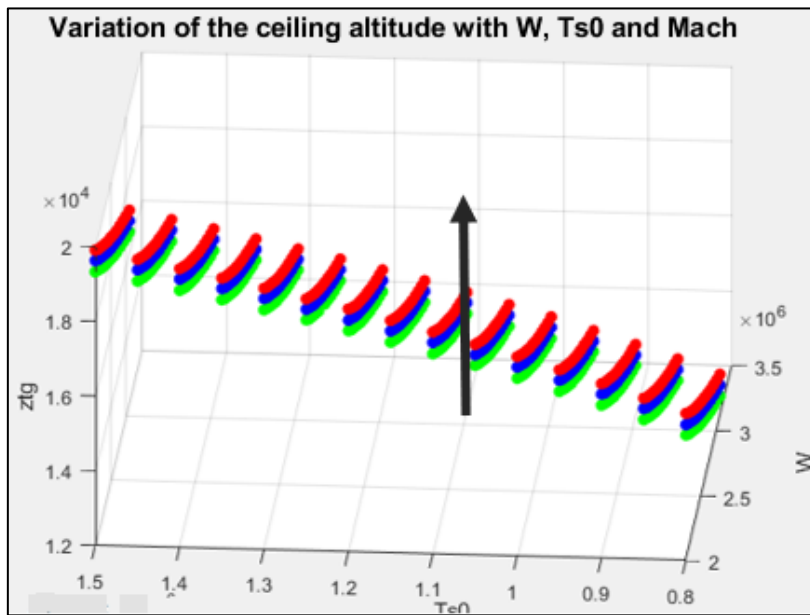


Figure 5.10



5.3 Re-entry requirement

After putting the payload into orbit the second stage has to re-enter into the atmosphere, during this phase the primary thermodynamic principle involved in re-entry is that almost all of the very high energy of the orbiting spacecraft, present at the start of re-entry, is converted into raising the internal thermal energy of the gas layer passing through the bow shock wave surrounding the vehicle.

In thermodynamic terms, the total change in kinetic energy is approximately equal to the work produced by the aerodynamic drag force acting during the descent path. This equivalence is used to find the necessary wing loading to proceed with the maneuver safely.

For a vehicle of mass W and velocity V_e the kinetic energy is:

$$KE = \frac{1}{2}mV_e^2$$

As previously mentioned it is assumed that the total initial vehicle KE is reduced to approximately zero by aerodynamic drag (the gravitational potential energy represents only a small fraction of the total energy so it is assumed negligible), so the following equation can be written:

$$\int_0^{l_D} D dx = KE = \frac{1}{2}WV_e^2$$

An average drag force over the fully re-entry distance can be defined:

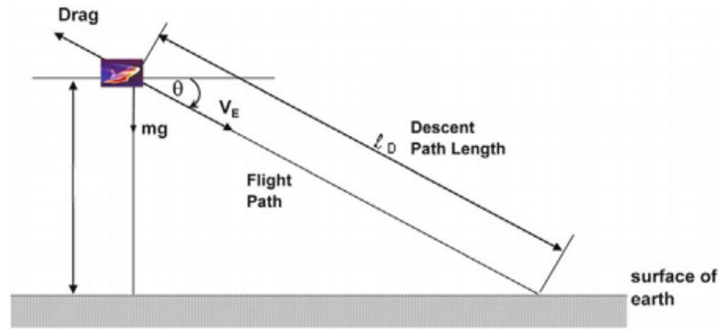
$$\bar{D} = \frac{1}{l_D} \int_0^{l_D} D dx$$
$$\bar{D}l_D = qC_DAl_D = \frac{1}{2}\rho V^2C_DAl_D = \frac{1}{2}WV_e^2$$

Where it has been assumed that ρ is the average density over the full re-entry path, and even V is the average velocity supposed to be half the velocity at the start of the deorbit.

Form the previous equation the value of the wing loading can be calculated as:

$$\frac{W}{S} = \rho C_D l_D \frac{V^2}{V_e^2}$$

Once defined the drag coefficient, that in this phase is evaluated from similar vehicle that fulfil the same mission, the only parameter unknown remains the path length l_D , the latter can be calculated as following starting form the value of the descent angle θ :



$$l_D = \frac{h_{deorbit}}{\sin\theta}$$

From the knowledge of this parameter and, noted all the others, the previous law can be evaluated, so that the requirement will be outlined in the matching chart by means of a vertical line, the latter will be influenced by the value of descent angle and of deorbit height, this variation is highlighted in the figures below in the same order as mentioned.

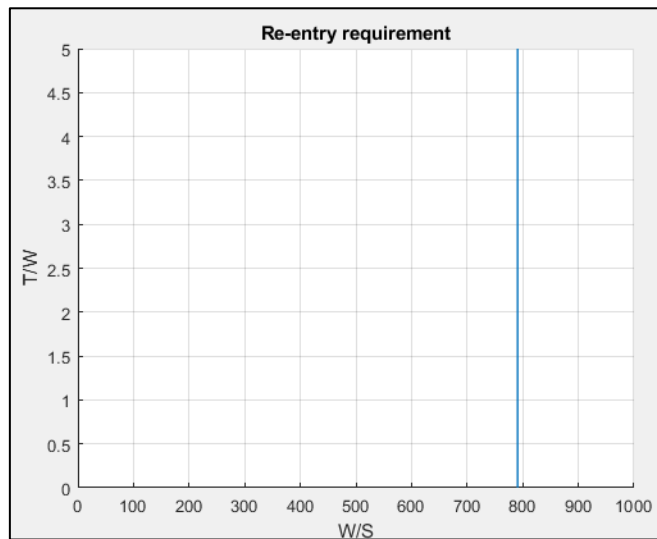


Figure 5.11

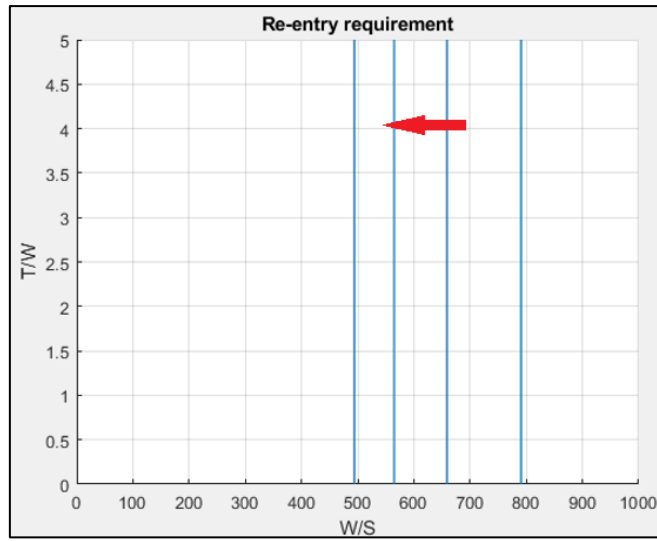


Figure 5.12

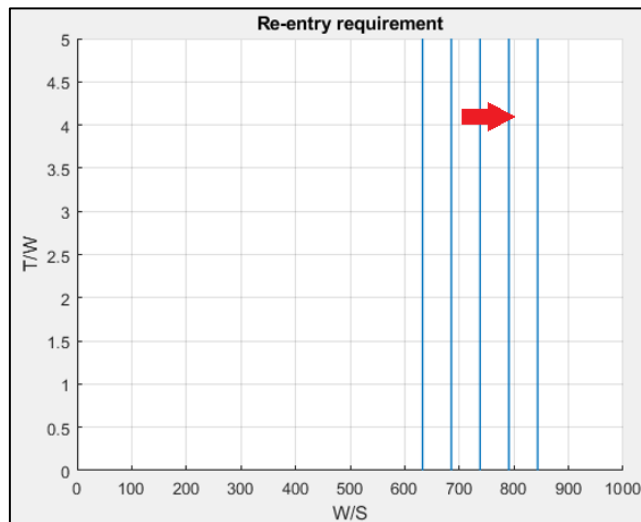


Figure 5.13

5.4 Payload requirement

In this section an analysis on the payload weight will be analysed starting from an equation that directly relates geometry-based parameter with the material/structure and propulsion parameters:

$$\frac{W_{str}}{S_{wet}} = \left(\frac{\rho_{ppl}}{Wr - 1} \right) \left(\frac{V_{ppl}}{V_{tot}} \right) \frac{r_{str}}{1 + r_{use}} \frac{S_{pln}^{1.5} \tau}{K_w}$$

Where τ is called non-dimensional volume index and can be considered a slenderness parameter, it is also bounded to the order of magnitude of the fuel density: as the latter increase the same does the value of τ so that the drag coefficient increases and the efficiency decreases. Another new parameter that appears in the equation is K_w that represents the ratio between the wet surface and the planform surface.

The previous equation can be rewritten in the following manner in such a way to highlight the relationship between the payload weight and the values of Thrust-to-Weight ratio and the wing loading:

$$\frac{W}{S} = W^2 \left(\frac{\rho_{ppl}}{Wr - 1} \right) \left(\frac{t_{burn}}{\rho_{ppl} I_{sp} g} \right) \frac{1}{1 + \frac{W_{payload}}{OEW}} \frac{1}{OEW} \frac{T}{W}$$

The value of W and OEW is available by an iteration on the weights that will be presented in the following section, while the payload density, the burning time are evaluated as done in the orbit-achievement requirement section knowing the type of propellant used during the mission, finally the $W_{payload}$ is a value chosen by the user and is the only value that influences the result on the matching chart, the evolution of the latter is shown in the following figure.

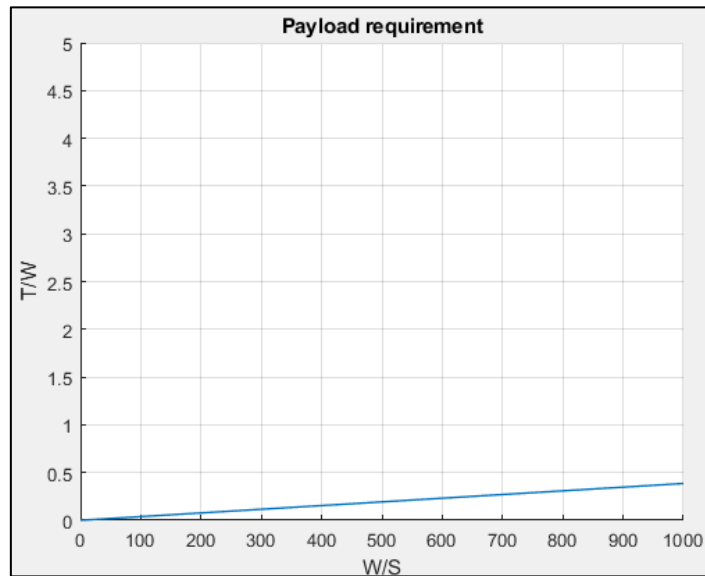


Figure 5.14

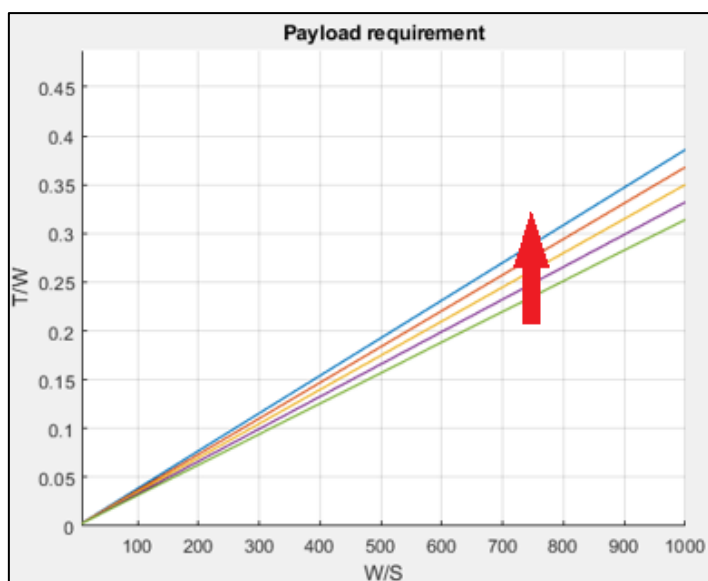


Figure 5.15

5.5 Matlab GUI implementation

As consequence of the previous analysis of all the requirements that the spacecraft must fulfil and of the weight estimation, in this section a new graphic user interface will be presented to the reader in order to show how the matching chart for the two stage to orbit vehicle can be obtained.

The GUI consists in three different tab group, one for the performance data, one for the geometry and weight data, and one to view the results.

In the first tab the introduction of the main performance data is required, in order to calculate the requirements curve, both for the first stage and the second stage, moreover the value of the payload weight is defined.

The screenshot displays a Matlab GUI with three tabs: "Performance Data", "Geometry and weight data", and "Results". The "Performance Data" tab is active, showing two sections: "First Stage" and "Second Stage".

First Stage

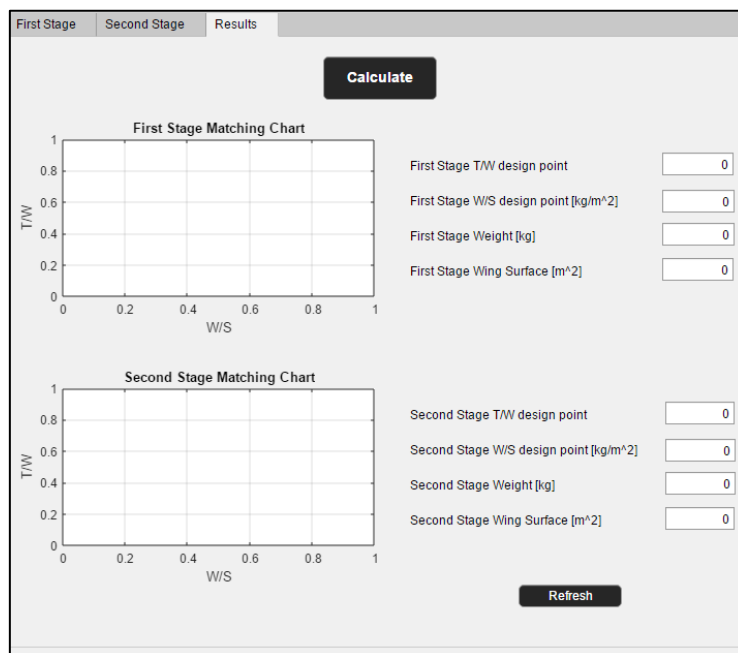
Maximum mach	<input type="text" value="0"/>	Landing maximum lift coefficient	<input type="text" value="0"/>
Take-off distance [m]	<input type="text" value="0"/>	Climb mach	<input type="text" value="0"/>
Take-off airport altitude [m]	<input type="text" value="0"/>	Climb angle [°]	<input type="text" value="0"/>
Take-off maximum lift coefficient	<input type="text" value="0"/>	Cruise mach	<input type="text" value="0"/>
Landing distance [m]	<input type="text" value="0"/>	Oswald factor	<input type="text" value="0"/>
Landing airport altitude [m]	<input type="text" value="0"/>	Aspect ratio	<input type="text" value="0"/>

Second Stage

Payload weight [kg]	<input type="text" value="0"/>		
Landing distance [m]	<input type="text" value="0"/>	Ascent angle [°]	<input type="text" value="0"/>
Landing airport altitude [m]	<input type="text" value="0"/>	Target orbit altitude [m]	<input type="text" value="0"/>
Landing maximum lift coefficient	<input type="text" value="0"/>	Deorbit start altitude [m]	<input type="text" value="0"/>

In the second tab the user has to define the first stage type, on the base of this choice the routine for either the subsonic or the supersonic weight estimation will be used, in case of subsonic first stage the user has to choose the weight coefficient following the guide lines listed before, while in case of supersonic first stage, for both the stages the geometry choice is required, four types of geometries are available and they are all defined by the values of the two axis and the sweep angle.

Once that all the field have been completed the user can swipe to the third tab where pushing the ‘Calculate’ button all the results will be available, in particular the view of both the first stage and the second stage matching chart is presented in two graphs taking into consideration all the requirements seen in the previous chapters, in addition the values of the design point in terms of T/W and W/S, the stage’s take-off weight and the optimal wing surface are calculated and shown in their appropriate boxes.



An example of the GUI's functioning will be presented here below using the following data:

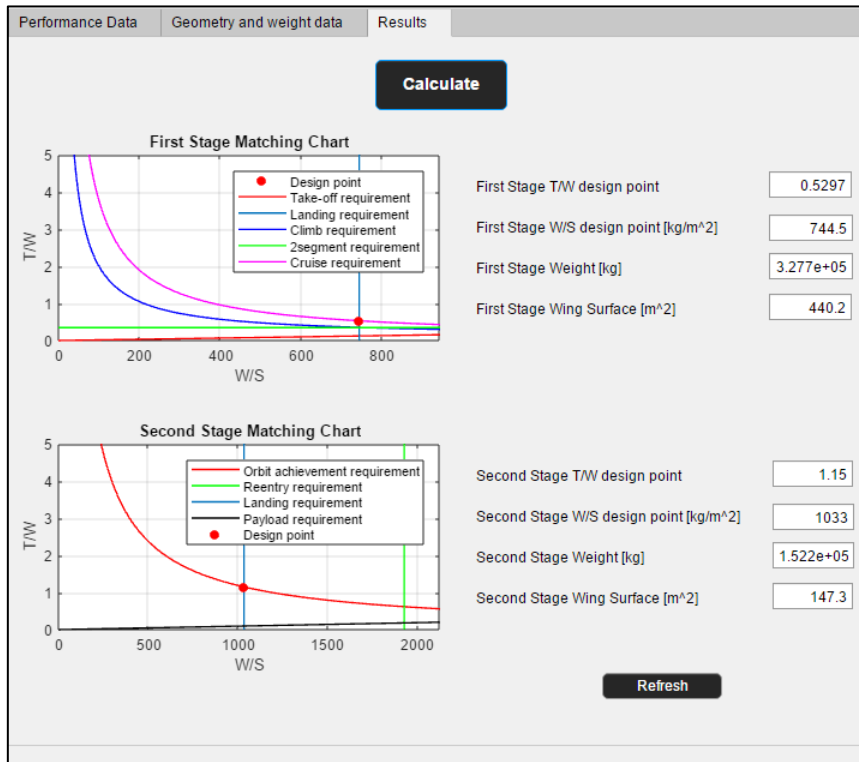
First stage and second stage performance data:

Performance Data	Geometry and weight data	Results	
First Stage			
Maximum mach	<input type="text" value="7"/>	Landing maximum lift coefficient	<input type="text" value="2.2"/>
Take-off distance [m]	<input type="text" value="1900"/>	Climb mach	<input type="text" value="0.5"/>
Take-off airport altitude [m]	<input type="text" value="200"/>	Climb angle [°]	<input type="text" value="5"/>
Take-off maximum lift coefficient	<input type="text" value="2"/>	Cruise mach	<input type="text" value="0.7"/>
Landing distance [m]	<input type="text" value="1500"/>	Oswald factor	<input type="text" value="0.9"/>
Landing airport altitude [m]	<input type="text" value="200"/>	Aspect ratio	<input type="text" value="9"/>
Second Stage			
Payload weight [kg]	<input type="text" value="9000"/>		
Landing distance [m]	<input type="text" value="1500"/>	Ascent angle [°]	<input type="text" value="20"/>
Landing airport altitude [m]	<input type="text" value="200"/>	Target orbit altitude [m]	<input type="text" value="2.5e+05"/>
Landing maximum lift coefficient	<input type="text" value="2"/>	Deorbit start altitude [m]	<input type="text" value="1.2e+05"/>

First and second stage weight and geometry data:

Performance Data	Geometry and weight data	Results	
First stage			
First stage type: <input type="text" value="Supersonic First stage"/>			
Geometry: <input type="text" value="Ellipse"/>			
Major semi-axis [m]	<input type="text" value="14"/>	Minor semi-axis [m]	<input type="text" value="2"/>
		Wing sweep angle [°]	<input type="text" value="70"/>
Fuselage Length [m]	<input type="text" value="0"/>	K furnishing system	<input type="text" value="0"/>
K composite	<input type="text" value="0"/>	Number of engines	<input type="text" value="0"/>
K delta fuselage	<input type="text" value="0"/>	Engine weight [kg]	<input type="text" value="0"/>
K flight control system	<input type="text" value="0"/>	K installation	<input type="text" value="0"/>
K hydraulic system	<input type="text" value="0"/>	K gear	<input type="text" value="0"/>
K fuel system	<input type="text" value="0"/>	K tail	<input type="text" value="0"/>
K environmental control system	<input type="text" value="0"/>	Number of passengers	<input type="text" value="0"/>
K avionic system	<input type="text" value="0"/>	Single passenger weight [kg]	<input type="text" value="0"/>
K engine system	<input type="text" value="0"/>	K secondary fuel	<input type="text" value="0"/>
Second stage			
Geometry: <input type="text" value="Ellipse"/>			
Major semi-axis [m]	<input type="text" value="8"/>	Minor semi-axis [m]	<input type="text" value="1.5"/>
		Wing sweep angle [°]	<input type="text" value="80"/>

Here below are the results:



It is easily visible that for the first stage the design space is delimited by the cruise and the landing requirement while the second stage design space bordered by the orbit-achievement and the re-entry requirement, moreover the first stage's weight and is almost the double of the value of the second stage while the wing surface is the triple.

Conclusion

In the previous pages all the effort to reach the initial target are described, in order to study the development of the conceptual design of a TSTO, the goal was the definition of a database for the calculation of the main Guess Data to start the statistical analysis and the determination of the method to execute a matching chart analysis to calculate the best design point for this category of vehicle given some preliminary data. The model used for this thesis was the Sanger, where the first stage acts as a 'carrier vehicle' and then a winged second stage is used to deploy in orbit the payload.

Even if the main topic was the TSTO with a high speed first stage propelled by an airbreathing engine, for a more complete and a comparative analysis also a subsonic first stage and a rocket first stage were analysed. At the end of this analysis a Graphical User Interface was defined to help the user to find the values of interest.

The results of the statistical analysis are useful to give the order of magnitude of the main values needed to start the conceptual analysis, the main point of the latter is the definition of a design point, and this is done by means of a matching chart analysis.

To achieve this target, in the thesis the methodologies to run the analysis are reported, this has been done starting from flight mechanics considerations, the study of propulsive systems characteristics and the analysis of the mission profile, from the latter the main requirements that the vehicle has to fulfil are specified.

From a sensitivity analysis the main parameters that influences the outcomes of the requirements calculations are identified, the user can act on them to modify the project and the curves as consequences. Even for this point a Graphical User Interface was defined to make the user aware of which are the most stringent requirements.

In conclusion this work can be considered as an excellent starting point to deepen the analysis in the future, in particular the main aerodynamics coefficient, that have been supposed in this thesis on the base of the similar vehicles, can be evaluated in a analytical and more precise way, to reach more reliable results. Moreover, due to the lack of a great amount of similar vehicle that accomplish precisely the same mission studied in this thesis, the database can be enriched as some new applications will born.

This page has been intentionally left blank

Ringraziamenti

A valle della trattazione, desidero dedicare alcune righe a tutte le persone che mi hanno accompagnato nel percorso universitario e che hanno contribuito alla realizzazione della tesi di laurea.

Grazie alla professoressa Nicole Viola, alla professoressa Roberta Fusaro e al professor Davide Ferretto per avermi supportato negli aspetti tecnici e per avermi mostrato grande disponibilità quando ne avevo bisogno.

Grazie alla mia famiglia, ai miei genitori che mi hanno dato la possibilità di intraprendere gli studi e per aver appoggiato le mie scelte, grazie a mio fratello che ogni giorno dimostra la sua fiducia in me, che nota la mia fatica ed apprezza i miei sforzi quotidiani.

Grazie ai miei amici di sempre, presenza costante nelle mie giornate, con i quali ho condiviso tantissime esperienze ed altrettante spero ancora di dividerne.

Grazie ai compagni e amici di università senza i quali questi anni non sarebbero stati gli stessi, e con cui ho potuto festeggiare e gioire per il raggiungimento di ogni piccolo traguardo.

Bibliography

- [1] Irwin E. Alber, *Aerospace Engineering in the Back on an Envelope*, Springer, Praxis Publishing
- [2] Paul Czysz, Jean Vandekerckhove, *Transatmospheric Launcher Sizing, Chapter 16*, Parks College, Saint Louis University, St.Louis, Missouri, VDK System, Brussel, Belgium
- [3] Milton O.Thompson, Joseph Weil, Euclid C. Holleman, *An assessment if lifting reentry flight control requirements during abort, terminal glide and approach and landing situations*, Flight Research Center Edwards, California, USA
- [4] Dieter Jacob, Gottfried Sachs, Siegfried Wagner, *Basic Research and Technologies for Two-Stage-to-Orbit Vehicles*, Deutsche Forschungsgemeinschaft
- [5] Davide Ferretto, Roberta Fusaro, Nicola Viola, *A conceptual design methodology for complex high-speed vehicles*, Politecnico di Torino
- [6] Claus Weiland, *Aerodynamic Data of Space Vehicles*, Springer
- [7] Gabriele Vittori, *Analisi delle prestazioni degli statoreattori (ramjet e scramjet)*, Politecnico di Torino 2018
- [8] Joseph M. Hank, Captain, USAF, *Comparative analysis of two-stage-to-orbit rocket and airbreathing reusable launch vehicles for military applications*, Air Force Institute of Technology
- [9] Mark D. Ardena, *Structural Analysis of Hypersonic aircraft*, Office of Advanced Research and Technology Advanced Concepts and Mission Division Moffett Field
- [10] Roberta Fusaro, *Comparative analysis if new configurations of new aircraft aimed at competitiveness, environmental compatibility and safety*, Politecnico di Torino, 2017
- [11] Marc A. Brock, Captain, USAF, *Performance study of Two-Stage-to-Orbit reusable launch vehicle propulsion alternatives*, Air Force Institute of Technology

- [12] James K. Nilsen, 1st Lieutenant, USAF, *Performance study of staging variables on Two-Stage-to-Orbit reusable launch vehicles*, Air Force Institute of Technology
- [13] D. Ferretto, R. Fusaro, N. Viola, *A conceptual design tool to support high-speed vehicle design*, Politecnico di Torino, Italy
- [14] Raymer, Daniel, *Aircraft design: a conceptual approach*, American Institute of Aeronautics and Astronautics, Inc., 2012.